National Library of Canada
Acquisitions and Bibliographic Services Branch
395 Wellington Street
Ottawa, Ontario
K1A 0N4

Bibliothèque nationale du Canada
Direction des acquisitions et des services bibliographiques
395, rue Wellington
Ottawa (Ontario)
K1A 0N4

Your file Votre référence

Our file Notre référence

NOTICE

The quality of this microform is heavily dependent upon the quality of the original thesis submitted for microfilming. Every effort has been made to ensure the highest quality of reproduction possible.

If pages are missing, contact the university which granted the degree.

Some pages may have indistinct print especially if the original pages were typed with a poor typewriter ribbon or if the university sent us an inferior photocopy.

AVIS

La qualité de cette microforme dépend grandement de la qualité de la thèse soumise au microfilmage. Nous avons tout fait pour assurer une qualité supérieure de reproduction.

S'il manque des pages, veuillez communiquer avec l'université qui a conféré le grade.

La qualité d'impression de certaines pages peut laisser à désirer, surtout si les pages originales ont été dactylographiées à l'aide d'un ruban usé ou si l'université nous a fait parvenir une photocopie de qualité inférieure.

Canada

Determining the Molecular Basis of the Mutation Underlying the Mouse Neural Tube Closure Mutant, *Splotch*.

By

Douglas J. Epstein

Department of Biology

McGill University

Montréal, Québec, Canada.

May, 1993.

A Thesis submitted to the Faculty of Graduate Studies and Research in partial fulfillment of the requirements for the degree of Doctor of Philosophy

ISBN 0-315-91747-4

Canada

Abstract

Splotch (*Sp*) is a semidominant mouse mutant which maps to the proximal portion of chromosome 1 and is phenotypically expressed as a pleiotropic defect during neurogenesis, resulting in spina bifida, exencephaly and dysgenesis of neural crest cell derivatives. To identify the aberrant gene underlying the defects observed in the *Sp* mouse mutant we initiated a positional cloning strategy. Our preliminary efforts were directed at establishing the boundaries of a deleted chromosomal segment found in the Sp^r allele, using nine gene probes that were assigned to that region of chromosome 1. Four of these genes,*Vil*, *Des*, *Inha*, and *Akp-3*, spanning a genetic distance of approximately 15 cM, were found to map within the Sp^r deletion. In order to further delineate the subchromosomal location of the *Sp* gene, the proximal segment of mouse chromosome 1 was saturated with microclones isolated from a library of microdissected genomic fragments generated from this region. An additional eight markers were found to map within the confines of the Sp^r deletion.

During the course of this work a member of the paired box gene family, *Pax-3*, was described as a candidate for *Sp*. The striking similarity between the tissue distribution of *Pax-3* mRNA in normal developing embryos, and the neural structures affected in *Sp* mice, together with the chromosome 1 location of *Pax-3* led us to examine whether *Pax-3* was mutated in three alleles at this locus Sp^r, Sp^{2H} and *Sp*. The entire *Pax-3* gene was determined to be deleted in the Sp^r allele. Analysis of genomic DNA and cDNA clones constructed from RNA isolated from Sp^{2H}/Sp^{2H} embryos identified a deletion of 32 nucleotides within the paired type homeobox and is predicted to produce a truncated protein as a result of a newly created termination codon at the deletion breakpoint. The original *Sp* allele was also characterized and found to contain an A to T transversion at position -2 in the third intron of *Pax-3* which abrogates the normal splicing of this intron due to the loss of its natural 3' splice acceptor. Taken together, these studies indicate that the severe defect in neural tube formation detected in *Sp* and its allelic variants is linked to the inactivation of the paired box gene *Pax-3*, and provides direct genetic evidence of a key role for *Pax-3* in normal neural development.

Résumé

Le *locus Splotch* (*Sp*), situé sur la partie proximale du chromosome 1 de la souris, est lié à des mutations semi-dominantes qui entrainent un phénotype pléiotropique lors de la neurogénèse. On observe chez les souris *Sp* une malformation de l'axe neural avec exencéphalie, *spina bifida* et malformation des structures dérivées des cellules de la crête neurale. Nous avons initié l'approche du clonage positionnel afin d'identifier le gène mutant associé au phénotype observé chez les souris *Sp*. Notre premier objectif était d'établir les limites du segment chromosomique délété chez le variant allélique Sp^r, en utilisant neuf marqueurs génétiques préalablement localisés dans la même région du chromosome 1. Quatre de ces marqueurs, provenant des gènes de la villine, la desmine, la sous-unité α de l'inhibine et la phosphatase alkaline placentale, et couvrant une distance génétique de 15 cM, ont été localisés à l'intérieur de la région délétée chez Sp^r. Pour mieux cerner le *locus Sp* quant à sa localisation subchromosomique, nous avons saturé la région proximale du chromosome 1 de marqueurs génétiques, provenant d'une librairie préparée à partir d'un fragment d'ADN obtenu par microdissection de la même région du chromosome 1. Huit de ces marqueurs ont été localisés dans la région délétée chez Sp^r.

Au cours de ce travail, *Pax-3*, un membre de la famille de gènes '*paired box*', s'est révélé être un candidat pour le *locus Sp*. La similitude entre les tissus affectés chez *Sp* et les tissus où l'ARN messager du gène *Pax-3* est exprimé chez les embryons normaux, de même que la localisation du gène *Pax-3* sur le chromosome 1, nous ont incité à tester si ce gène était altéré chez *Sp* et les deux variants alléliques, Sp^r et Sp^{2H}. Nous avons d'abord déterminé que le gène *Pax-3* était entièrement délété chez le variant Sp^r. Par la suite, l'analyse de clones d'ADN génomique et d'ADNc du gène *Pax-3* produits à partir de l'ARN isolé d'embryons homozygotes Sp^{2H}/Sp^{2H}, a permis d'identifier une délétion de 32 nucléotides à l'intérieur du domaine homéo de type 'paired', entraînant la formation d'une protéine tronquée, privée de sa partie COOH-terminale. Finalement, une transversion d'un A pour un T à la position -2 du troisième intron de *Pax-3* a été décelée chez les souris *Sp*. Cette transversion cause une anomalie au niveau de l'épissage normal du gène, causée par la perte du site accepteur d'épissage à l'extrémité 3' de l'intron 3.

L'ensemble de ces résultats démontre que la malformation de l'axe neural observée chez les souris *Splotch* est liée à l'inactivation du gène 'paired box' *Pax-3* et établit de manière évidente que ce gène a un rôle déterminant lors du développement normal du tube neural.

Table of Contents

	Page
Abstract	i
Résumé	ii
Table of Contents	iv
List of Figures	vii
List of Tables	x
List of Abbreviations	xi
Acknowledgements	xii
Preface	xiv
Objectives of the Presented Work	xvi
Chapter 1 Literature Review	1
1. The genetic control of human neural tube defects	2
1.1. Introduction	2
1.2. Epidemiological studies	4
1.2a. Sex ratios	8
1.2b. Twin studies	9
1.3. Studies of consanguinous matings	9
1.4. Familial aggregation studies	11
2. Mouse models of human neural tube closure defects	16
2.1. Introduction	16
2.2. Midbrain exencephaly	20
2.3. Hindbrain exencephaly and lumbosacral spina bifida	23
2.4. Lumbosacral spina bifida	29
2.5. Craniorachischisis	30
2.6. Genetic modes of action	31
2.7. Of *Pdgfra*, *Gli3* and other genes	32
3. The *paired* gene set of Drosophila	34
Chapter 2 Molecular chracterization of a deletion encompassing the *splotch* mutation on mouse chromosome 1	42
Abstract	43
Introduction	44

Page

Materials and methods 46
Mice 46
Probes 46
Southern hybridization 46
Densitometric analysis 47

Results and Discussion 48

Acknowledgements 51

References 52

Tables and Figures 57

Chapter 3 ***splotch*** **(Sp^{2H}), a mutation affecting development of the mouse neural tube, shows a deletion within the paired homeodomain of *Pax-3*** 60

Abstract 61

Introduction 62

Results 64

Discussion 68

Experimental procedures 73
Mice 73
Construction and isolation of cDNAs 73
PCR amplification of genomic DNA 74
Southern hybridization 75

Acknowledgements 76

References 77

Figures 83

Page

Chapter 4 **A mutation within intron 3 of the *Pax*-3 gene produces aberrantly spliced mRNA transcripts in the *splotch* (*Sp*) mouse mutant** 88

Abstract 89

Introduction 90

Materials and methods 92
Mice 92
Preparation and isolation of cDNAs 92
PCR amplification of genomic DNA 92

Results 94

Discussion 97

References 101

Acknowledgements 104

Figures 105

Chapter 5 **Characterization of a region-specific library of microclones in the vicinity of the *Bcg* and *splotch* loci on mouse chromosome 1** 109

Abstract 110

Introduction 111

Materials and methods 113
Mice 113
Microdissection and microcloning 113
Isolation of microclone inserts 113
Southern hybridization 114
Statistical analysis 115

Results 116
Description of library 116
Interval mapping of microclones 116

Discussion 118

Page

Acknowledgements 121

References 122

Tables and Figures 126

Chapter 6 General Discussion 131

References 147

Claims to originality 172

List of Figures

Chapter 1		Page
Figure 1	Schematic representation of the pattern of anterior neural tube closure in wildtype and mutant mouse embryos.	19
Chapter 2		
Figure 1	Southern blot analysis of *MspI* digested DNA from a Sp^r heterozygote and its wildtype littermate.	58
Figure 2	Genetic distances (in cM ± SE) of eight loci spanning the chromosomal segment deleted in the Sp^r mouse mutant.	59
Chapter 3		
Figure 1a	Chromosomal assignment of *Pax 3* in relation to 8 other loci spanning the proximal portion of mouse chromosome 1.	83
Figure 1b	Haplotype analysis of 9 loci on mouse chromosome 1 in interspecific (*Mus spretus* x C57BL/6J)F1 x C57BL/6J hybrids.	84
Figure 2	Southern blots of *Taq I* digested genomic DNA from *Sp/Sp*; Sp^{2H}/Sp^{2H}; $Sp^r/+$; C3H/HeJ; and 101/OR mice hybridized with *Pax 3* cDNA subfragments.	85
Figure 3	Analysis of *Pax-3* cDNAs from Sp^{2H}/Sp^{2H} and C3H/HeJ embryos.	86
Figure 4	Homozygous Sp^{2H}/Sp^{2H} and wildtype littermate embryos at day 14 of gestation.	87

Chapter 4

		Page
Figure 1	Analysis of *Pax* 3 cDNA from wildtype and *Sp/Sp* embryos.	105
Figure 2	Sequence analysis of wildtype and aberrant *Pax* 3 cDNAs from *Sp/Sp* embryos.	106
Figure 3	Sequence analysis of intron 3 of the *Pax* 3 gene from wild type and *Sp/Sp* genomic DNA.	107
Figure 4	Schematic representation of normal and aberrant splicing of the *Pax* 3 gene in wildtype and *Sp/Sp* mice.	108

Chapter 5

Figure 1	Haplotype analysis of 252 (C57BL/6J x *Mus spretus*) F1 x C57BL/6J backcross progeny for 7 loci on chromosome 1.	129
Figure 2	Interval mapping of 26 microclones on mouse chromosome 1.	130

Chapter 6

Figure 1	Compilation of PAX3 mutations in individuals with WSI, II, and III and the mouse mutant Sp^d.	138
Figure 2	Diagrammatic representation of *Pax* gene expression in a transverse section of a day 11 embryonic mouse neural tube.	143

List of Tables

		Page
Chapter 2		
Table 1	Chromosomal map positions of eight loci conserved between mouse chromosome 1 and human chromosome 2q.	57
Chapter 5		
Table 1	Properties of the 1C2-C5 library.	126
Table 2	List of markers used to define eight chromosome 1 intervals.	127
Table 3	List of DNA restriction fragment length polymorphisms identified by each of the chromosome 1 specific microclones.	128

List of Abbreviations

Axd	Axial defects
Bn	Bent tail
Cd	Crooked
cm	cranioschisis
ct	curly tail
Lp	Loop tail
Ph	Patch
Rf	Rib fusion
Sp	Splotch
Sp^d	Splotch delayed
Sp^r	Splotch retarded
T(2;4)1Sn	Snell's translocation
T^c/t^w	t-complex
vl	vacuolated lens
xn	exencephaly
Xt	extra toes

Acknowledgements

During the past four years I have been in a privileged predicament in being supervised by three excellent scientists. I am indebted to Dr. Michel Vekemans for having layed down the initial ground work of this project and for having the tremendous insight into the approaches taken from which a number of individuals have benefitted. Dr. Daphne Trasler has generously provided an enormity of time in relaying to me her expert knowledge of early mouse development for which I am extremely grateful. Finally, I cannot begin to express my utmost appreciation to Dr. Philippe Gros for providing me with the opportunity to work in his laboratory. The scrupulous manner in which Philippe conducts his science and runs his lab will undoubtedly benefit me for years to come.

As for my fellow labmates, I could not have envisioned a better group of individuals with whom to pursue science. Silvia 'Sita' Vidal, Danielle 'Marshmallo' Malo and Pierre 'Pee' Lepage, have taught me a great deal about science and life in general and I can only consider them great people to share knee-holes with. I am indebted (literally) to Storman Normand Groulx and Maxi France Talbot for all their help during the past four years. Thanks for the free coffee France and the sports section Norm (Les Canadiens, all the way!). Kyle 'Mr. Strato-King's-X' Vogan and Alan 'Octapeptide' Underhill, the new Paxers on the block, thanks for bringing in new dimensions to the Pax story. I would like to especially thank Pamster Brinkley for having Slimon, Greg 'the knife' Govoni for moving me to Boston, and Ing Swe for marrying Alan, otherwise he never would have made it out of London. As for the MDR gang, Hanna Maya Hanna, Lulu and Arthur Beaudet, Ellen 'Buschminster' Buschman, Rajan 'the Rajman' Dhir, Dave 'Far Side Fanatic' Tang-Wai, Stephan 'Shtephie' Ruetz, and Minnie 'ta gueule' Garnier, thanks for introducing me to the fascinating phenomenon of multidrug resistance.

Having been registered in the Department of Biology, I would like to acknowledge the entire Department of Biochemistry for their kindly acceptance of an outsider, as well as for allowing me to play on the Pipetman softball and hockey teams.

Finally, I would like to extend my gratitude to my personal support crew consisting of family and friends. Thanks to Leslie and Murray for feeding me on Thursday nights, Bev and Jack for their generous hospitality during my trips to Toronto, Richard and Lucie for their constant encouragement, Tori and Evan for showing interest in mice, Lorne for being a great friend, Bari for not typing my thesis, and lastly my mother for her unconditional support throughout my life.

Preface

In compliance with the Faculty of Graduate Studies and Research, the following excerpt from the "Guidelines Concerning Thesis Preparation" is cited below:

"The candidate has the option, subject to the approval of their department, of including as part of the thesis the text, or duplicated published text, of an original paper or papers. Manuscript-style theses must still conform to all other requirements explained in the Guidelines Concerning Thesis Preparation. Additional material (procedural and design data as well as descriptions of equipment) must be provided in sufficient detail (eg. in appendices) to allow clear and precise judgement to be made of the importance and originality of the research reported. The thesis should be more than a mere collection of manuscripts published or to be published. It must include a general abstract, a full introduction and literature review and a final overall conclusion. Connecting texts which provide logical bridges between different manuscripts are usually desirable in the interest of cohesion. It is acceptable for theses to include, as chapters, authentic copies of papers already published, provided these are duplicated clearly and bound as an integral part of the thesis. In such instances, connecting texts are mandatory and supplementary explanatory material is always necessary. Photographs or other materials which do not duplicate well must be included in their original form.

While the inclusion of manuscripts co-authored by the candidate and others is acceptable, the candidate is required to make an explicit statement in the thesis of who contributed to such work and to what extent, and supervisors must attest to the accuracy of the claims at the Ph.D. Oral Defense. Since the task of the Examiners is made more difficult in these cases, it is in the candidate's interest to make the responsibilities of authors perfectly clear."

The work described in Chapters 2, 3 and 4 of this thesis has been published in the following journals:

Chapter 2. Epstein D. J., Malo, D., Vekemans, M., and Gros, P. (1991a). Molecular characterization of a deletion encompassing the *splotch* mutation on mouse chromosome 1. Genomics *10*, 89-93.

Chapter 3. Epstein, D. J., Vekemans, M., and Gros, P. (1991b). *Splotch* (Sp^{2H}), a mutation affecting development of the mouse neural tube, shows a deletion within the paired homeodomain of *Pax-3*. Cell 67, 767-774.

Chapter 4. Epstein, D.J., Vogan, K.J., Trasler, D.G., and Gros, P. (1993). A mutation within intron 3 of the *Pax-3* gene produces aberrantly spliced mRNA transcripts in the splotch (*Sp*) mouse mutant. Proc. Natl. Acad. Sci. USA 90, 532-536.

The work described in Chapter 5 has been provisionally accepted for publication in Genomics, in a revised format.

The work performed for each of these publications is entirely my own with the following exceptions:

Chapter 2: D. Malo in our laboratory provided the mapping data for several of the probes used.

Chapter 4: K. Vogan assisted with some of the sequencing reactions.

Chapter 5: A. Weith generated the microdissected library. N. Bardeesy, S. Vidal, and D. Malo, each participated in the mapping of the microclones.

Objectives of the Presented Work

Neural tube defects in human populations have a considerably high incidence with respect to other genetic defects, yet little is known about their etiology. Although heritable and environmental factors have both been implicated in the cause of these defects, the actual genes and environmental agents have remained virtually elusive. To gain insight into the pathogenicity of neural tube defects and to better our understanding of the neurulation process in general, we have initiated a positional cloning strategy to identify the genetic determinants which when mutated give rise to neural tube defects.

As a result of the heterogeneous and multifactorial nature of human neural tube defects and the difficulty in mapping such complex traits in human pedigrees, we decided to utilize the large number of single gene mouse models of human neural tube closure defects to fulfill our task. Once the particular mouse gene is cloned we will exploit the high degree of homology between the genomes of mice and humans to clone the corresponding human gene. We will then be in a position to determine whether mutations in the human homologue result in a comparable phenotype to that of the mouse mutant.

To inaugurate our strategy, we embarked on a positional cloning approach to identify the molecular basis underlying the defects observed in the *splotch* (*Sp*) mouse mutant. Armed with a large interstitial deletion on mouse chromosome 1 encompassing several genetic loci including *Sp*, a region specific library of microdissected clones spanning this chromosomal segment and a panel of intraspecific backcross animals segregating the *Sp* phenotype (in collaboration with F. Mancino and D.G. Trasler, Department of Biology, McGill University) we set out to define a minimal candidate interval within which the *Sp* gene would be contained. Once a reasonably small genetic and physical interval flanking the *Sp* locus is delineated, this candidate region could then be screened for transcribed sequences. The likelihood of these transcripts being equivalent to the *Sp* gene product would then be assessed by 1) comparing their individual expression patterns with the tissues affected in homozygous *Sp* embryos and 2) examining the integrity of the candidate transcripts in the various *Sp* alleles.

Chapter 1

Literature Review

1. The genetic control of human neural tube defects

1.1. Introduction

Congenital malformations of the neural tube, known collectively as neural tube defects (NTDs), comprise some of the most common forms of defects observed at birth (Bergsma 1979). NTDs are the second most common cause of perinatal death (the first being heart defects) in the United Kingdom, accounting for approximately 15% of perinatal mortalities (Office of Population Census and Surveys, 1985). The prevalence at which NTDs are recognized, although varying geographically and racially, is 1 in 1000 live births (Edmonds and James 1990).

Clinically, NTDs are classified according to the location of the lesion in the neural tube, the mechanism by which the defect arises, and the stage of development at which it occurs. These distinctions are important because they relate directly to the cause of the defect. In order to categorize an NTD according to these criteria it is important to briefly outline the normal process by which the primordium of the central nervous system is formed. This process, known as neurulation, occurs during the third and fourth weeks of embryogenesis and is divided into two stages, primary and secondary neurulation (Muller and O'Rahilly 1987). Primary neurulation is initiated upon the induction of the embryonic ectoderm by the underlying notochord and paraxial mesoderm to form the neural plate which runs along the anteroposterior axis of the developing embryo. The edges of the neural plate, the neural folds, begin to elevate until their apices are apposed. Fusion of the neural folds then occurs along the dorsal midline. Cranio-caudal variations in this process gives rise to the complex formation of the brain and spinal cord. Secondary neurulation results in the canalisation through a group of tightly packed mesenchymal cells to form the neural tube at the caudal extremity of the embryo (Copp *et al.*, 1990).

Defects arising during the process of primary neurulation often result in open neural tubes. A congenital fissure of both the skull and spinal cord results in craniorachischisis. When the anterior neural tube in the region of the brain fails to close, degeneration of the exposed nervous tissue ensues and results, in the case of anencephaly, in the absence of the cranial vault. An open lesion anywhere along the spinal axis in which there is

protrusion through the defect of a cystic swelling involving the meninges (meningocele) spinal cord (myelocele) or both (meningomyelocele) is generally known as spina bifida cystica. If these lesions occur at or above the level of the posterior neuropore, coinciding with the second sacral vertebra, (the final point of closure along the neural tube) then they are considered primary neurulation defects (Lemire 1988). If they occur below the level of the posterior neuropore then they are considered secondary neurulation defects. It is essential to distinguish between the two as the mechanisms of origin are entirely different and therefore, may be causally distinct. On the other hand, the disruption of certain cellular events common to both processes may explain why both types of lesions are sometimes found segregating in families or even in the same individual (Campbell *et al.*, 1986). Defects which are thought to occur after the closure of the neural tube such as: spina bifida occulta, iniencephaly, encephalocele, and hydrocephaly, are also often considered causally distinct from those NTDs that arise before closure (Lemire 1988).

Presently, no single factor may be deemed responsible for the majority of NTDs, however, both genetic and environmental components have been implicated (for a review see Campbell *et al.*, 1986; Copp *et al.*, 1990). A generally accepted hypothesis stipulates that malformations of the neural tube occur when an embryo's underlying genetic and environmental risk factors surpass a tolerable threshold, known as the multifactorial threshold model (Carter 1976). However, in some instances single mutant genes segregating in Mendelian fashion may be enough to predispose the embryo to insult, for examples of such refer to McKusick (1990) (182940, 206500, 301410, and references therein). A single teratogen, acting at the gene or protein level, may also suffice as a cause in the mal-development of the embryo (Copp 1990). These represent only a few of a variety of models that have been proposed to account for the high incidence of NTDs. Others which have been proposed such as chromosomal anomalies (Byrne and Warburton 1986), although frequent in spontaneous abortions, constitute only a small proportion (≈1%) of NTDs at birth, while other models implicating components in maternal cytoplasm (Nance 1969) and uterine interactions (Carter 1974) are not well supported.

The ultimate aims in identifying the responsible agents causing NTDs are twofold. First, it should allow for the design of a means to prevent the malformations from occurring. At present, embryos with NTDs are effectively recognized *in utero* by ultrasonography, by screening pregnant mothers for elevated levels of maternal serum alpha-fetal protein, or both (Wald and Cuckle 1977; Brock 1983). Parents are then offered the option of selectively terminating an affected pregnancy. A far more preferable scenario would be the outright prevention of the NTD. True prevention relies on identifying the gene(s) which contribute significantly to the embryo's liability for the NTD. Once these genes have been isolated, parents may undergo genetic screening to identify those individuals at risk of conceiving an embryo with an NTD. Potential therapies involving gene product replacement may then be carried out before or at the time of conception. Second, the identification of mutant genes which cause NTDs will provide a better understanding of the molecular and cellular events required for the normal process of neurulation to occur. Identification of these genes will provide a direct means to investigate the effects of potential teratogenic agents on their function.

The purpose of this review is to provide the reader with an overview of the evidence from a large number of studies supporting a genetic contribution in the formation of an NTD. The primary indications that genetic factors do indeed play a role in the formation of NTDs come from: 1) epidemiological studies 2) studies of consanguinous matings and 3) familial aggregation studies. Each of these topics will be addressed in turn.

1.2. Epidemiological studies

Epidemiological methods of studying the causation of malformations in general and NTDs in particular focus on two aspects, environmental and genetic factors which may predispose the embryo to a defect (Carter 1974; Campbell 1986). Epidemiological studies are divided into four components (Leck 1972). Initially, descriptive studies are performed to determine the frequency of a defect in different groups of children at a particular time. Correlative studies are then performed to determine if the varying prevalences between two groups can be associated with the exposure to a

potentially causal factor. Geneticists would conduct these studies by investigating whether the defect segregates in families (suggestive of a genetic etiology), while environmental epidemiologists would look to see if affected individuals were exposed to a common factor such as a drug, as in the case of babies born with phocomelia when exposed to thalidomide. Analytic studies would be carried out next to test the hypothesis formulated by the correlative studies. Geneticists would perform linkage analysis to see if the defect segregates with genetic markers on a particular chromosome, while environmental epidemiologists would examine the histories of the individuals involved, for instance, was the proportion of phocomelic children whose mothers took thalidomide unusually high. The fourth and final study utilizes the experimental process to determine whether the causal agent, gene or drug, can be manipulated to make the defect less widespread. The geneticist could genetically screen couples at risk of conceiving a child with the defect and offer a preventative treatment for those fetuses at risk, whereas, the environmental epidemiologist would, in the case of phocomelia, simply refrain from prescribing thalidomide to pregnant women.

A large number of epidemiological studies have been conducted according to the aforementioned method in order to identify the environmental and genetic agents thought to play a causal role in the formation of an NTD. Unfortunately, as was previously mentioned by Leck (1972) and which continues to hold true today, few of these studies have succeeded past the descriptive and correlative stages of analysis. The prevalence of NTDs at birth has been extensively investigated in a large number of populations (Stevenson 1966). They have been shown to vary geographically (Leck 1974), temporally (Elwood and Elwood 1980), racially (Carter 1974), and seasonally (Leck 1974). Children with NTDs have been found to be more prevalent in young and older first time mothers (Carter and Evans 1973a), in families of lower social class (as measured by the father's occupation) (Carter 1974), and in mothers exposed to environmental heat stress (Milunsky 1992). The consumption of a variety of foods including, blighted potatoes, canned cooked meats (containing nitrites and nitrates) canned peas, tea, and ice-cream have all been correlated with the presence of NTDs at birth (Carter 1974). It cannot be overstated that correlations do not provide evidence of a causal role,

nonetheless, there does appear to be growing support for the idea that maternal diet is an important factor in preventing NTDs, especially in light of the vitamin supplementation trials which in some studies showed a reduction in the number of cases of NTDs in mothers given vitamin supplements compared to controls (Smithells *et al.*, 1983; Mulinaire *et al.*, 1988; Milunsky *et al.*, 1989; MRC Vitamin Research Group 1991).

The epidemiological studies that were set forth to identify the environmental factors contributing towards the etiology of NTDs in different populations may not have succeeded in recognizing specific causal factors, however, the studies did generate important data concerning the birth frequencies of NTDs in distinct populations. For instance, ethnic differences have been reported in the birth frequency of NTDs (Carter 1974). The prevalence of NTDs (anencephaly and spina bifida) per 1000 births was found to be as high as 8.8 in the Irish, 7.6 in the English from South Wales, and 7.1 from a number of primarily Sikh cities in northern India, compared to the significantly lower rates of 1.0 for black populations in Lagos, United States, West Indies or Britain and 0.9 for Japanese in Hiroshima and Nagasaki (Chung et al., 1968; Carter 1974; Verma 1978). Although one cannot distinguish between the genetic and environmental reasons for these differences, some support for at least a partial genetic component comes from examining the birth frequencies of NTDs in the various populations after migration. For example, the low birth frequency of NTDs in West African blacks remained low even after they moved to an area where the prevalence was particularly high (Carter 1974). The reasons for these differences appear to be genetic rather than cultural in origin because the low birth frequency in blacks has persisted in several different geographic locales some of which African blacks migrated to over three hundred years ago, a considerable amount of time for dietary and other cultural habits to adapt to the new habitat (Carter 1974).

Additional evidence supportive of genetic factors being implicated in the cause of NTDs comes from population studies which detected high rates of NTDs in Sikh populations from several geographic regions. The majority of the world's Sikh population inhabits the Punjab province of India. The birth frequency of NTDs in Sikhs was shown to be considerably higher than that for Hindus from the same geographic region (Stevenson *et al.*, 1966; Verma 1978). A consistently high rate has been shown to persist when

Sikhs emigrate to areas of low prevalence, namely Singapore and Canada (Searle 1959; Baird 1983). Furthermore, siblings of Sikh probands having an NTD had a higher occurrence of hydrocephalus without spina bifida (6%) compared to sibs of non-Sikh probands (0.15%) (Hall *et al.*, 1988). These findings prompted Hall *et al* (1988) to suggest that a Mendelian disorder may be segregating among Sikhs expressed as either a primary NTD or as isolated hydrocephalus. The Sikh religion grew out from Hinduism approximately 500 years ago. It is therefore conceivable, that a mutant gene originating in a "founder Sikh" gave rise to the high incidence of NTDs found specifically in the Sikh community. Strict laws preventing the marriage between Hindus and Sikhs may explain the lower prevalence of NTDs in Hindus (Hall et al., 1988). Informative pedigrees from the Sikh population should be useful for linkage analyses in order to map the responsible gene(s) to a particular chromosome.

A worldwide decline in the prevalence of NTDs over the past two decades has been documented (Seller, 1987a). This decline cannot be fully explained by prenatal diagnosis and improved maternal diets. However, now that the rates have dropped considerably and somewhat plateaued (at least in the United States at one NTD birth per thousand) this may be suggestive that the primary causal agents in the environment have been removed and what has remained is the underlying genetic predisposition. Although this theory remains virtually untested, complex segregation analyses on different populations may provide some evidence in support of this view. Some of these studies have already been done and will be discussed below.

Roberts and Lloyd (1973) proposed an alternative explanation for why there are differences in the rates of NTDs between populations. They suggested that these findings were the result of a differential ability in women from different populations to selectively terminate an affected fetus. This hypothesis is not unfounded for it has been shown that the survival of trisomic fetuses in mice is strain dependent (Vekemans and Trasler 1987; Epstein and Vekemans 1990). Byrne and Warburton (1986) tested this hypothesis by examining the rate of NTDs in spontaneous abortions from populations displaying low, intermediate, or high prevalences of NTDs at birth. Their finding of a positive correlation between rates of NTDs in spontaneous abortions and rates of NTDs at birth

suggested that the population differences in NTDs were not due to differential fetal loss but most likely due to differences in their incidence during embryogenesis (Byrne and Warburton, 1986).

1.2a. Sex Ratios

An overall preponderance of females with NTDs have been identified (Carter 1976; Seller 1987b; and Mariman and Hamel 1992). However, when the NTDs are categorized according to the position of the lesion the sex ratio (M:F) is 0.66 for anencephaly, 0.42 for "upper" spina bifidas (lesions involving the thorax), and 3.0 for "lower" spina bifidas (lesions involving only lumbar/sacral regions) (Seller 1987b). Recalling that open NTDs occurring above the second sacral vertebra are indicative of primary neurulation defects and those arising below are the result of defects in secondary neurulation (see introduction), one may conclude that defects in primary neurulation are more prominent in females and that defects in secondary neurulation are more prominent in males. Given that gonadal differentiation occurs after neurulation during embryogenesis (Goldbard and Warner 1982), the most obvious explanation for the above findings, involvement of sex specific gene products, must be excluded (Mariman and Hamel, 1992). Still, differential rates in early mouse development have been observed between the sexes. For instance, male mice reach the blastocyst stage before females (Tsunoda *et al.*, 1985) and male embryos are known to have on average three more pairs of somites than do females at the onset of neurulation (Seller and Perkins-Cole 1987). Moreover, a female bias has been reported in homozygous curly-tail mouse embryos displaying an NTD (Embury *et al.*, 1979). Based on these observations Seller (1987b), proposed that if female embryos are developmentally delayed, compared to males, they would be more susceptible to defects in neural tube closure (primary neurulation defects). Seller (1987b) also reasoned that males would be more susceptible to lower lesions of the neural tube (canalization or secondary neurulation defects) because they would be inclined to "over-canalize" as a result of their faster rates of development. The only way differential rates of growth between males and females can explain the sex ratio differences in NTDs would be if a regional rather than

general growth difference was exhibited between the sexes. Thus far, no such regional variation in neurulation between the sexes has been reported. In offering an alternate hypothesis for the overall female predominance of fetuses with NTDs, Mariman and Hamel (1992) proposed that mechanisms influencing the level of expression of certain genes on the X chromosome may be involved. Their hypothesis is supported by the finding that variability in gene dosage resulting from anomalous X inactivation has been reported as a cause for some NTDs (James 1988).

1.2b. Twin studies

Typically, twin studies are a geneticist's ultimate tool for determining the heritability of a particular disease. The more significant the genetic contribution is to the underlying cause of the disease, the greater the concordance should be between affected and unaffected sibs in monozygotic versus dizygotic twins. Studies of twins affected with neural tube defects have been plagued with inconclusive data. A particularly low incidence of twins with meningomyelocele has made it difficult to collect large sample sizes which are needed for proper analysis. Furthermore, early fetal loss of affected twins is greater than for normal twins, thus explaining why fewer twin cases are observed (Elwood and Elwood 1980). Nevertheless, in the limited number of studies that were performed, concordance rates of NTDs in twins was determined to be 2-4% overall (Campbell *et al.*, 1986) with like sex concordance slightly higher at 4.5% (Windham and Sever 1982). These concordance rates are lower than most genetic diseases including those that are multifactorial in nature (Carter 1976). These studies are therefore suggestive that environmental influences may also significantly contribute in the etiology of NTDs.

1.3. Studies of Consanguinous matings

The frequency of malformations in children from consanguinous matings was investigated worldwide (Stevenson *et al.*, 1966). It was determined that in two cities, Alexandria and Bombay, related parents, by

any degree, more often had children with NTDs than unrelated parents. In Alexandria, consanguinous matings constituted 30% of all matings and were responsible for more than 50% of all births with an NTD. The rates of NTDs (per 1000 births) in the offspring of parents whose relations were first cousins or closer was 14.2 (30/2109) in Alexandria and 4.1 (16/3875) in Bombay, which was significantly higher when compared to the rates of NTDs in nonconsanguinous matings in these two cities, 5.7 (37/6431) and 3.8 (135/35620) respectively. When the relationship between parents was less than first cousins, a higher rate of births with NTDs was still reported in related compared to unrelated couples.

As is often brought up in studies of consanguinity, a failure to account for the socioeconomic status of the parents can lead to an overestimation of the effects of inbreeding (Bittles *et al.*, 1991). Stevenson *et al* (1966) concede that some of their results may be confounded by these variables but not to the point of making them insignificant. It can be surmised that their findings are indeed supportive of a genetic basis in the formation of an NTD. On their own, the data suggest that an individual's chance of being afflicted with an NTD is significantly increased when transmission of the deleterious gene or genes is identical by descent. This is further supported by the fact that the greater the degree of consanguinity the more prevalent the defects are at birth (Stevenson *et al.*, 1966).

One shortcoming worth mentioning, concerning the report by Stevenson *et al* (1966), was that no extensive family data was collected. Information on the status of sibs would have enabled them or others to calculate segregation ratios in order to determine the possible mode of inheritance, or at least the relative contribution to the phenotype by major genes. Furthermore, consanguinous families are often associated with relatively large pedigrees (Bittles *et al.*, 1991) and therefore, would have been an excellent resource for linkage analysis.

Several pedigrees have been reported over the years in which recurrent anencephaly had been observed in progeny of consanguinous matings (Polman 1951; Carter *et al.*, 1968; Fuhrman *et al.*, 1971; Farag *et al.*, 1986). Because of these frequent observations, Penrose (1957), went so far as to say that autosomal recessive forms of anencephaly existed. Carter (1968) astutely pointed out that this was unlikely because the proportion of

affected sibs in first-cousin marriages does not approach the typical segregation ratio of one in four for autosomal recessively inherited diseases.

Shaffer *et al* (1990), compared the segregation ratios from 24 consanguinous families (containing at least one child with anencephaly) with that of 294 presumably nonconsanguinous families. The estimated segregation ratios for the non-sporadic cases in both populations suggested that a major genetic locus was involved. A recessive mode of inheritance was proposed as the method of transmission for some of the consanguinous families, with a recurrence risk that may be as high as 25%. However, one serious limitation of this study was that the consanguinous families were not ascertained through a population based study, where the chances are higher that the segregating gene will be of common origin, but were collected from the literature and are therefore, of a variety of origins.

1.4. Familial aggregation studies

Crucial to the understanding of the genetic involvement in the etiology of NTDs is the determination of their rates of recurrence in families. The importance of this is two-fold. First, the existence of a familial recurrence for NTDs is not only confirmatory of a genetic etiology, but the extent of the familial recurrence is indicative of the number of genes involved in causing the malformation. For instance, a recurrence rate of 25% in sibs (with equal numbers of affected males and females) for a particular type of NTD would suggest that the defect is being inherited in an autosomal recessive fashion, with little or no environmental influence. This information is of utmost importance when counselling parents with an affected child about the risk that a subsequent child will have of developing an NTD. Second, establishing the rate of familial recurrence is important for gene mapping studies. The mode of inheritance is an important variable in the determination of linkage to genetic markers.

In three large family studies from the United Kingdom it was observed that when one child was affected with an NTD, 5% of his or her sibs would also be affected (Carter 1974). The risk to sibs was determined to be 7-15 times that of the general population (depending on the city from where the study was conducted). Similar risks were reported in a Rhode

Island study (Yen and MacMahon 1968). Interestingly, one study has reported that children of mildly afflicted parents have a 3-4% chance of being affected with an NTD (Carter 1974). Carter (1976) also determined that the risk to third degree relatives (cousins) was two-fold that of the general population.

A common genetic mechanism used to explain these findings is the multifactorial threshold model (Yen and MacMahon 1968; Carter 1974, 1976; Leck 1972). The multifactorial threshold model stipulates that the threshold beyond which there is a risk of malformation is determined by both polygenic and environmental factors (Fraser 1976). First degree relatives (either sibs or children) of index cases (having 50% of their genes in common) have a greater chance of crossing the threshold than do members of the general population. Similarly, second and third degree relatives of index cases have a greater liability than do members of the general population, but because they have a smaller proportion of genes in common with the index case they are at a lower risk of developing the malformation than both the index case and first degree relatives. These patterns were consistent with what was observed in the family studies on NTDs and have also been observed for other common malformations including cleft lip, talipes equinovarus and pyloric stenosis (Carter 1976).

Another genetic mechanism put forth on the basis of family studies postulates that NTDs are inherited as a single gene disorder with a marked reduction in penetrance (Penrose 1957). Support for this idea comes from the segregation analysis performed on 298 families (with at least one case of NTDs) from France (Demenais *et al.*, 1982). Results from this study conclude that the familial aggregation of NTDs may result from the inheritance of a monogenic component with a large influence of environmental factors, some of which may be common to sibs. Other segregation analyses, performed on large English and Polish data sets, could not resolve between a single locus and polygenic models, to explain the familial aggregation of NTDs (Lalouel *et al.*, 1979; Pietrzyk 1980).

Other examples suggesting that NTDs can be transmitted as single genes have been reported in the literature. For instance, Fineman *et al* (1982) observed an increased frequency of spina bifida occulta in four families with multiple cases of spina bifida cystica, suggesting that spina bifida cystica and spina bifida occulta may be different phenotypic

expressions of the same gene. They surmised that the two disorders may be due to an autosomal dominant gene with a penetrance of 75%. Fellous *et al* (1982) reported on a five generation family with sacral malformations including complete sacral agenesis, spina bifida aperta, and spina bifida occulta. A fully penetrant major dominant gene was postulated to be the cause of the sacral agenesis, however mendelian transmission was rejected when the cases of spina bifida were included as affected cases. Possible explanations for these findings included, genetic heterogeneity, a dominant major gene transmitted in excess by heterozygotes (segregation distortion) (Fellous et al., 1982), or what seems most feasible, ascertainment bias (Opitz and Gilbert 1982).

Yet another mode of transmission of NTDs has been detected, albeit rarely, that of X-linked inheritance. A total of four kindreds have been reported in the literature in which the segregation of the NTD (anencephaly, and/or spina bifida), from mother to son, is indicative of X-linked recessive inheritance (Toriello *et al.*, 1980; Baraitser and Burn 1984; Toriello 1984; Jensson *et al.*, 1988). Unfortunately, once again, no linkage studies with X-linked probes were performed to confirm these findings.

When determining the familial recurrence rates of NTDs it is important to distinguish between the syndromic and non-syndromic forms. The causes of NTDs when in combination with other malformations (syndromic) must differ from those of isolated NTDs (non-syndromic). For example, the autosomal recessive Meckel syndrome includes in its phenotypic description, a sloping forehead, exencephalocele, polydactyly and polycistic kidneys (McKusick 1990). The unknown gene which when mutated causes these phenotypes must either be expressed in a variety of developing organ systems or is expressed in a primordial cell or tissue type common to the affected structures. Alternatively, the NTD may simply be secondary in nature to the primary defect. It is likely that the gene responsible for the Meckel syndrome is not specific to the process of neurulation and therefore, should not be included in the same category as those malformations which are restricted to the neural tube. Similarly, the NTDs resulting from gross chromosomal abnormalities (large deletions, trisomies, duplications, and triploidies) are probably due to disruptions of a variety of developmental systems not necessarily specific to neurulation. Moreover, syndromic forms of NTDs constitute only a small proportion of

all NTDs, estimated to be less than 10% (Holmes *et al.*, 1976). NTDs resulting from chromosomal abnormalities on the other hand, are extremely prevalent in early spontaneous abortions, representing almost 80% of NTDs found at the embryonic stage, but are rarely found at birth (Byrne and Warburton 1986).

The massive epidemiological and familial aggregation studies performed over the past few decades have accumulated large amounts of data revealing the importance of both genetic and environmental components in the etiology of NTDs. It is quite clear from these studies that there is no single gene or teratogen that causes the majority of malformations affecting the neural tube, but that many variant genes acting either independently or in unison with various environmental agents are the likely causes. Holmes *et al* (1976) pointed out very clearly the heterogeneous nature of neural tube defects. The authors predict from their studies that 90% of the NTDs at birth are multifactorial in nature with the remaining 10% being caused by single genes, as part of a syndrome, chromosomal abnormality or non-genetic entities. Holmes *et al* (1976) also rightly brought forth the argument that the genetic counselling of families at risk should not be governed by the 5% recurrence risk that was determined for all NTDs. It is quite clear that different families have varied risks of having a child affected with an NTD. For these reasons, other counselling strategies must be put forth. These strategies, which should apply to both genetic counselling and prenatal diagnosis rely on the identification and characterization of the genes involved in causing the NTDs.

Having firmly established that genes do play a role in the cause of NTDs, the focus must now turn on the identification and characterization of them. Thirteen years have passed since the landmark paper by Botstein et al (1980) described the use of restriction fragment length polymorphisms (RFLPs) in the mapping of genetic markers to disease genes of interest. At the time, perhaps only a handful of genetic markers were available to follow the segregation of the RFLP with the presence or absence of the disease phenotype, making it very difficult to localize a disease gene to a particular chromosome. We are presently in the midst of a new era, that of the human genome project, the initiative of which is to map, clone, and ultimately sequence the entire human genome. Over 3000 genetic markers

in the form of sequence tagged sites (STSs) covering 100% of the human genome are readily available (Todd 1992). These STSs must now be put to use to map the genes segregating in families that cause NTDs. This strategy is presently being employed for other multifactorial traits including type 1 diabetes. This complex trait is being dissected, at the genetic level, by the mapping in mice of nine unlinked loci contributing to immune destruction of the insulin producing beta-cells (Todd 1992). Similar progress must be realized with respect to the study of NTDs. Only when the mapping and eventual cloning of the genes causing NTDs is accomplished can screening strategies be initiated to identify couples at risk of conceiving a child with an NTD. Upon the identification of high risk couples, gene product replacement or other preventative measures can then be taken. Furthermore, the identification of these genes will help unravel the curious environmental interactions thought to occur during neural development.

2. Mouse models of human neural tube closure defects

2.1. Introduction

The morphogenetic events responsible for the development of the vertebrate neural tube occur through coordinated interactions between cells and molecules resulting in cellular shape changes, cellular migrations, and complex cellular communications with both neighboring cells and the extracellular matrix (reviewed in Schoenwolf and Smith 1990). To gain understanding of the complex pattern of developmental events which lead to the formation of the nervous system, and how errors in this developmental process may lead to malformations of the neural tube, it is important to study the process of neurulation in a controlled experimental system. Human embryos would be the ideal source for study, however, for obvious ethical reasons this is not possible. Furthermore, as mentioned in the previous section, human neurulation occurs early in embryogenesis, at a time when most women do not even know that they are pregnant, thus making non-invasive methods to examine the developing embryo difficult. On the other hand, for a number of advantageous reasons, the laboratory mouse has proven to be an excellent model system for the study of both normal and aberrant processes of neurulation. Firstly, all developmental stages in the mouse embryo are accessible for analysis (Hogan *et al.*, 1986). Secondly, the genetic homology between humans and mice is such that if a gene is involved in a particular developmental process in one species, then it would be expected to be involved in the same developmental process in the other species. Thirdly, there exist a large number of single gene mouse mutants which disturb the normal process of neurulation (Lyon and Searle 1989). The identification of these genes will allow for the isolation of their human homologues, and the assessment of whether or not the genes in question may cause similar phenotypes in both organisms (Winter 1988). Finally, the potential for environmental factors to produce NTDs can be tested in the mouse, however, caution must be applied in the interpretation of these results because what may be teratogenic to one organism may not necessarily be teratogenic to another (Copp *et al.*, 1990).

The availability of a large number of neurulation mutants in the mouse has provided a means for investigating the pathogenesis of a variety

of different NTDs. The variation, both genetic and phenotypic, in the types of mouse NTD mutants compares quite well with what has been observed in humans. For instance, there are mouse mutants whose neural tube malformation results from mutations in either single (*Axd*, *Bn*, *Cd*, *crn*, *ct*, *Lp*, *Ph*, *Rf*, *Sp*, T^c/t^{w5}, *vl*, *xn*, *Xt*) or multiple (*SELH*) loci, as well as from chromosomal aberrations (Trisomies 12 and 14, T(2;4)1Sn) (reviewed in Copp *et al.*, 1990)(see List of Abbreviations for nomenclature of mouse mutants). There are mutants in the mouse whose phenotypic expression is restricted to a component specifically associated with the process of neurulation (*Axd*, *Bn*, *crn*, *ct*, *SELH*, *Sp*, *vl*, *xn*) as well as to other organs and systems (*Cd*, *Ph*, *Rf*). With respect to the level of the lesion, there are mouse mutants that result in spina bifida alone-including tail flexion defects (*Axd*,T^c/t^{w5}, *vl*), exencephaly alone (*Cd*, *crn*, *SELH*, Ts 12 and 14), spina bifida and exencephaly (*Bn*, *ct*, *Sp*, T(2;4)1Sn) and craniorachischisis (*Lp*, *Rf*). All of these examples of NTDs in the mouse have previously been described for humans (Opitz and Gilbert 1982; see previous section) and should thus represent valid models of human NTDs.

The failure of the neural tube to close within the defined developmental period is a predominant feature observed in the majority of mouse NTD mutants. This failure may result from either a defect in one of the driving forces behind neural fold closure, or a defect in an associated system which is required, but not sufficient, for neurulation to proceed (Copp *et al.*, 1990). To understand the mechanism by which an NTD may arise it is important to understand the normal manner by which the neural tube closes (a brief description of primary and secondary neurulation can be found in the previous section). This understanding includes the forces involved in raising the neural folds and the actual process of initiating, continuing and completing the closure.

The origin of the forces which drive the formation of the neural plate, shaping and bending of its lateral edges, culminating in the closure of the neural groove, remain relatively uncertain. Efforts to comprehend these forces are further complicated by the differences between regions (cephalic versus spinal) in which neurulation occurs (Waterman 1976; Geelan and Langman 1979; Bush *et al.*, 1990). Nevertheless, several cellular mechanisms, both intrinsic and extrinsic to the neuroepithelial folds, have been postulated to explain the forces behind neurulation

(reviewed in O'Shea 1987; Schoenwolf and Smith 1990). The intrinsic forces are thought to act primarily through changes in neuroepithelial cell shape (Sadler 1982; Schoenwolf and Smith 1990). Microfilament bundles have been identified at the apical ends of neuroepithelial cells (Morris-Kay and Tuckett 1985). By virtue of their contractile ability these microfilament bundles are thought to be involved in the apical constriction of neuroepithelial cells which presumably alters their morphology in the neural plate from column-like (flat) to wedge-like (bent), thus aiding in the raising of the neural folds (Schoenwolf and Smith 1990). Differential cell proliferation and increases in intercellular adhesion are also thought to play roles in the curvature of the neural plate (O'Shea 1987). The postulated extrinsic forces, include a role for the underlying mesenchyme in providing support to the neuroepithelium as its lateral folds rise, as well as the process of axial elongation, which is presumed to cause the neural plate to collapse dorsally (becoming concave) resulting in the elevation of the neural folds (Jacobson and Gordon 1976).

Once the neural folds have risen and are closely apposed, neural tube closure commences (Kaufman *et al.*, 1979). The initiation of neural tube closure involves the fusion of the neural folds along the dorsal mid-line at four independent sites along the rostro-caudal axis, at various stages of embryonic development (Kaufman *et al.*, 1979; MacDonald *et al.*, 1989). Continuation of closure (which is comparable to the action of a zipper, Copp *et al.*, 1990) then proceeds either uni or bidirectionally depending on the particular initiation site. Neural tube closure terminates at three points, deemed neuropores, along the rostro-caudal axis. Initiation of closure is first established in the cervical region (at the level of the third somite, Sakai 1990) and proceeds both caudally towards the posterior neuropore and rostrally to the posterior end of the rhombencephalon (Figure 1a). The second point of closure occurs at the level of the posterior prosencephalon and proceeds bidirectionally. Closure two terminates caudally at the hindbrain neuropore and rostrally at the forebrain neuropore. Closure three initiates at the ventral most aspect of the prosencephalon and proceeds caudally until it meets closure two at the site of the forebrain neuropore. The fourth and final site of closure occurs at the level of the

Figure 1

Schematic representation of the pattern of anterior neural tube closure in wildtype and mutant mouse embryos. The numbers identify the sites (in order) where neural tube closure is initiated. The dotted lines with arrows indicate the direction in which closure proceeds from the initial site of fusion. a) Closure pattern in normal embryos. b) Pattern in *SELH/Bc* embryos that are able to complete closure. c) Pattern in SELH/Bc mice that fail to complete closure. d) Pattern of closure in Trisomy 12 embryos. e) Pattern of closure in Trisomy 14 embryos. P, prosencephalon; M, mesencephalon; R, rhombencephalon; ANP, anterior neuropore (Modified from MacDonald *et al.*, 1989).

A) Normal closure

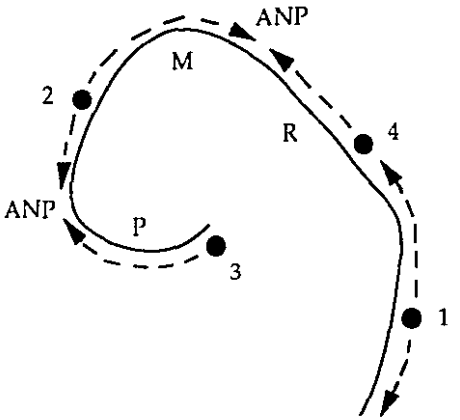

B) SELH closure

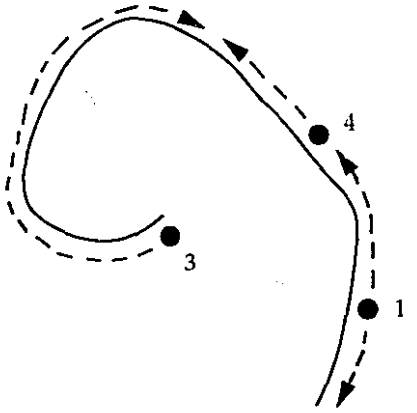

C) SELH exencephaly

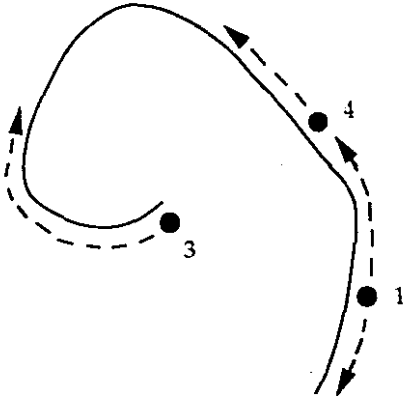

E) Trisomy 12

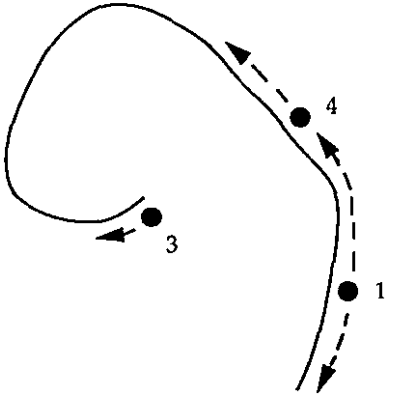

D) Trisomy 14

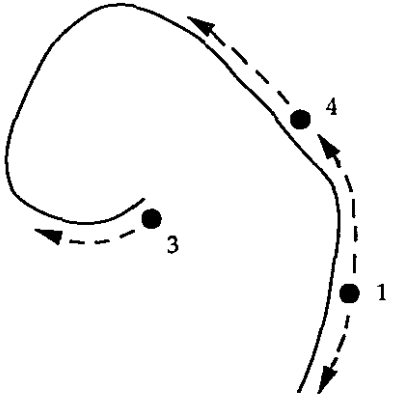

rhombencephalon and proceeds rostrally until it meets closure two at the hindbrain neuropore. Well after the closure of both anterior neuropores, closure one, which had proceeded caudally, culminates in the closure of the posterior neuropore.

Interference with any of the forces involved in neurulation may invoke a delay and if prolonged, a failure in the closure of the neural tube. Moreover, the localization and nature of the defect may be indicative of which neurulation event was faulty (Copp *et al.*, 1990). For instance, midbrain exencephaly (*SELH*, Trisomy 12 and 14, *xn*) results from a failure to initiate neural fold closure at the midbrain/forebrain boundary (closure 2, Figure 1a) (MacDonald *et al.*, 1989). Hindbrain exencephaly (*Sp*), on the other hand, is probably due to a failure in the continuation of closure four (Figure 1a) in the posterior portion of the rhombencephalon (Auerbach 1954). Spinal defects, which, in the mouse, always occur in the lumbosacral region of the neural tube (*Axd*, *Bn*, *ct*, *Sp*, *vl*) result from a failure in the completion of neural tube closure at the posterior neuropore (Copp *et al.*, 1990). And finally, craniorachischisis, as found in the *Lp* and *Rf* mouse mutants, occurs due to a failure in the elevation of the neural folds in both spinal and cephalic portions of the neural tube (Wilson and Wyatt 1992; Theiler and Stevens 1960). Specific examples of mouse mutants from each of these categories will now be described.

2.2. Midbrain exencephaly

Perhaps the most convincing example of a midbrain exencephaly resulting from the failure to initiate neural tube closure is depicted by the *SELH* mouse mutant (MacDonald *et al.*, 1989). The penetrance of midbrain exencephaly in homozygous *SELH* embryos is 17%, however, almost all the homozygous mutant embryos display abnormalities in the pattern by which their anterior neural tube closes. The genetic liability for this defect was determined to be under the control of two or three loci (Juriloff *et al.*, 1989).

As previously mentioned, neural tube closure occurs according to a well defined sequence of events. This morphological pattern of neural tube closure was compared between homozygous *SELH* and wildtype embryos at

various stages of neurulation using scanning electron microscopy (SEM) (MacDonald *et al.*, 1989). It was shown that the primary defect in the homozygous *SELH* mouse was in its inability to initiate neural tube closure in the region of the posterior prosencephalon (closure 2, Figure 1b,c). Rather than initiating closure of the cephalic neural folds at site two, the *SELH* mutants omitted this stage and initiated cephalic neural tube closure at the ventral most aspect of the prosencephalon (closure 3). Observations at slightly later stages of development revealed that the majority of the *SELH* homozygous embryos were able to close the entire cephalic portion of their neural tube by this alternative method (Figure 1b), however, in some instances (17% of embryos) closure by this process produced exencephaly resulting from a prolonged delay in neural tube closure (Figure 1c).

Two important questions remain to be answered concerning the defects observed in the *SELH* mutant embryos. First, what is the cellular mechanism underlying this defect. Second, why are only 17% of the embryos affected when it was found that almost all the heterozygous male and female parental lines possessed the ability to transmit the phenotype to their progeny (Juriloff *et al.*, 1989). In answer to the former question, histological studies revealed that the mesenchymal tissue underlying the open midbrain neural folds was collapsed, and the surface ectoderm at this site was rippled in appearance. The distorted morphology of these cell types was not sufficient to offer an explanation as to why or how the midbrain closure is prevented from occurring, however, the question is still under investigation (Juriloff *et al.*, 1989).

In answer to the second question, the authors put forth the idea that a qualitative difference exists in the mechanisms by which wildtype and mutant *SELH* embryos close their neural tube, and that this qualitative trait is clearly heritable in *SELH* mutant mice (use of site 3 instead of site 2 to close the cephalic neural tube). However, the authors propose that the reason why only 17% of the homozygous *SELH* embryos go on to develop midbrain exencephaly, given the variant way that they close their neural tube, is the result of quantitative differences. These quantitative differences within the population of homozygous embryos may be portrayed by varying degrees of delay in the closure of the neural tube or varying degrees to which the neural folds collapse. Presumably, these quantitative traits are

under the control of epigenetic or stochastic events (MacDonald et al., 1989).

Additional support for the claim that midbrain exencephaly may be due to a failure in the initiation of neural tube closure stems from the examination of mouse embryos trisomic for chromosome 12 or 14. Exencephaly is observed in 100% of trisomy 12 embryos and 50% of trisomy 14 embryos, however, the severity of the lesion differs between these two trisomies. SEM and transmitting electron microscopic (TEM) analyses revealed that the entire cranial neural tube rostral to the otic pits fails to close in trisomy 12 embryos, whereas, in trisomy 14 embryos only the forebrain and midbrain are affected (Figure 1 d,e)(Putz and Morris-Kay 1981; Morris-Kay and Putz 1986). These studies further revealed that apposition of the neural folds at the forebrain/midbrain junction failed to occur in both trisomic embryos, however, neural fold closure did proceed, albeit late, in the hindbrain and ventral forebrain regions (Morris-Kay and Putz 1986). These examples of midbrain exencephaly appear once again to result from a failure of the neural folds to initiate closure at site two.

The cellular mechanisms underlying the defect in the trisomic embryos are more evident than they were for the *SELH* embryos. Abnormalities in tissue structure were apparent early in neurogenesis, with the most striking feature being a general reduction in the number of cranial mesenchymal cells, particularly those in contact with the overlying neuroepithelial basement membrane (Morris-Kay and Putz 1986). Additional abnormalities in the trisomic embryos include a delay in the normal appearance of the apical microfilament bundles in the pre-exencephalic regions of the neuroepithelium, however, this finding was considered secondary in nature (Morris-Kay and Putz 1986).

A direct consequence of the reduction in the mesodermal cell population in the trisomic embryos was the finding of a deficiency of glycosaminoglycans (GAGs) in both the extracellular matrix (ECM) of the mesoderm and the neuroepithelial basement membrane (Morris-Kay and Putz, 1986). This finding in itself was not surprising because it had previously been shown that the source of neuroectodermal basement membrane GAGs (hyaluronate, chondroitin sulphates and heparan sulphate) is the underlying mesenchyme (Solursh and Morriss 1977). The relevance of the GAG deficiency is realized by reviewing earlier studies

which showed that depleting chondroitin sulphate proteoglycan (CSPG) levels in rat embryo cultures leads to a failure in the initiation of closure in the cephalic, but not spinal, portion of the neural tube (Morris-Kay and Crutch 1982). CSPG is known to decrease the adhesiveness of cells to fibronectin and collagen substrates in vitro (Knox and Wells 1979; Perris and Johansson 1987). What remains to be determined in these trisomic embryos is whether the primary defect responsible for the reduction in cranial mesoderm is specific to the overexpression of particular genes on chromosomes 12 or 14, or a general phenomenon resulting from the aneuploid state.

2.3. Hindbrain exencephaly and lumbosacral spina bifida

The phenotype of the *Sp* mouse mutant can be described as pleiotropic with developmental perturbations in neural tube closure, neural crest cell (NCC) derived structures, and limb musculature (Auerbach 1954; Moase and Trasler 1992; Franz *et al.*, 1993). The most striking of these defects was originally described by Auerbach (1954) who observed, in 56% of homozygous *Sp* embryos, a failure in the closure of the neural folds in the region of the hindbrain resulting in exencephaly. The same mice were also seen to have posterior defects in their neural tube, ranging from a bend in the tail, to a complete failure in the closure of the posterior neuropore resulting in spina bifida (Auerbach 1954). Further morphologic analysis revealed that the entire neural tube manifested some degree of abnormality, being wavy instead of linear in spinal regions, as well as appearing collapsed at irregular intervals throughout the cranio-caudal axis (Auerbach 1954).

Yet another feature of the abnormal neural tube, in the area of the open neural folds, was the presence of an extensive overgrowth of neural tissue on either side of the dorsal midline (Auerbach 1954). The proliferation of neuroepithelium in the regions of the hindbrain and lumbosacral neuropores became more pronounced as development proceeded and was offered as an explanation for why the neural tube failed to close in these areas (Auerbach 1954). However, no differences in the mitotic indices were detected when comparing neuroepithelial cells from gestational day 9 (prior to neural tube closure) homozygous *Sp* and

wildtype neural tubes (Kapron-Bras and Trasler 1988). In fact, a delay in the cell-cycle of cephalic neuroepithelial cells was reported (Wilson 1974). It is apparent therefore, that the neuroepithelial overgrowth was secondary to the failure in closure of the *Sp* neural tube (Hsu and Van Dyke 1948; Moase and Trasler 1992). Other secondary features stemming from the neural overgrowth which were observed in the *Sp* mutant included distortions in various structures of the brain (Auerbach 1954; O'Shea *et al.*,1987) including the otic vesicle (Deol 1966).

In an effort to explain the cause of the primary defect in *Sp* animals Dempsey and Trasler (1983) examined early morphological differences between homozygous *Sp* and wildtype embryos. They detected a significant increase in the length of both anterior and posterior neuropores in the mutant population. Based on these observations, it was proposed that the hindbrain exencephaly and spina bifida detected in homozygous *Sp* mutants resulted from a delay in the closure of both anterior and posterior neuropores (Dempsey and Trasler 1983). Examining the pattern of normal neural tube closure as depicted in Figure 1a, the aberrations in the *Sp* mouse appear to result from a failure to either continue or complete closure extending rostrally from site four and caudally from site one.

To gain insight into the precise cellular mechanism which causes the delay in neural tube closure in the *Sp* mutant, much attention has focussed on the neural crest. Neural crest cells (NCCs) originate from the transition zone of the neuroepithelium and at specific times during neurulation emigrate from dorsal positions along almost the entire length of the neural tube (Geelan and Langman 1979). Fate mapping studies have shown that NCCs participate in the morphogenesis of a variety of structures of the peripheral nervous system (sensory and autonomic neurons, glia, and Schwann cells) heart (truncus and aortico-pulmonary septa), mesodermally derived craniofacial structures, as well as various paraendocrine and melanocyte cell types (Le Douarin 1982; Kirby *et al.*, 1983; Phillips *et al.*, 1987; Hall 1988). The majority of these NCC derived structures and cell types have been shown to be reduced or completely absent in *Sp* and two of its alleles, Sp^{d} and Sp^{1H} (Auerbach 1954; Moase and Trasler 1989; Franz 1989, 1990). In fact, the characteristic white spots (commonly referred to as splotches, hence the name of the mutant) usually seen on the abdomen, tail, and feet of *Sp* heterozygotes is the semi-dominant

feature of this mutant which results from a deficiency in NCC derived melanocytes populating these areas (Auerbach 1954).

Since neurulation and NCC emigration are related in a temporal and spatial fashion and given that these two processes are disrupted in the *Sp* mutant, it is conceivable that their developmental pathways are interdependent. NCC emigration from midbrain and hindbrain regions is known to precede cephalic neural tube closure (Nichols 1981). Furthermore, the timing of the NCC release corresponds with the subsequent bending of the apices of the neural folds (Morriss and New 1979). It was therefore postulated that delaying or preventing NCC emigration may actually cause the hindbrain exencephaly observed in the *Sp* mutant (Copp *et al.*, 1990). This postulation is less likely to explain the caudal defects observed in *Sp* because NCC emigration occurs after the posterior neuropore has closed (Schoenwolf and Nichols 1984). Moreover, in rare instances *Sp* heterozygotes display neural tube defects without abnormalities in NCC derived structures (Franz 1992). Also, *Sp* homozygotes have occasionally been reported with NCC derived deficiencies in the absence of neural tube defects (Moase and Trasler 1992). It would seem therefore, that the primary defect of the *Sp* mutant is not specific to NCC release *per se* but is probably related to an abnormality that is common to both neural tube closure and NCC emigration.

Efforts to identify the cellular process common to both neural tube closure and NCC emigration which when disrupted causes the *Sp* phenotype, initially centered on determining whether the primary defect was intrinsic or extrinsic to the neural tube. Ultrastructural analysis of the neuroepithelium by TEM revealed a significant increase in the number of gap junctional vesicles in early day 9 *Sp* homozygotes compared to wildtype controls, particularly in regions of the neural tube which subsequently failed to close (Wilson and Finta 1979). Gap junctional vesicles have been associated with a reduction in cellular contact (Espey and Stutts 1972; Albertini et al., 1975; Murray et al., 1978) reflecting a loss in cellular communication which could presumably result in a failure in neural tube closure (Wilson and Finta 1979). The increase in gap junctional vesicles however, were restricted to regions of the neural tube which failed to close, whereas, NCC emigration occurs along almost the entire length of the neural tube. It is therefore, unlikely that the restricted nature of the

location of the gap junctional vesicles is causal of the defects but perhaps represents a secondary response to the initial defect. Furthermore, the increase in gap junctional vesicles was not confirmed in homozygous Sp^d embryos (Yang and Trasler 1991).

Other TEM and SEM analyses have shown that the neuroepithelium from homozygous *Sp* and Sp^d embryos is highly disorganized (Morris and O'Shea 1983; O'Shea and Liu 1987; Yang and Trasler 1991). Typically, neuroepithelial cells from hindbrain sections of wildtype day 10 neural tubes are wedge-like in shape, arranged radially, tightly packed, and extend cellular projections into both luminal and basal surfaces (Morris and O'Shea 1983). However, the same cells from homozygous *Sp* embryos appeared disoriented in that they did not display the usual radial configuration, had cell processes that were projected laterally, and were separated by large amounts of extracellular space (Morris and O'Shea 1983). It was presumed that the cellular disorganization depicted in homozygous *Sp* embryos stemmed from a defect in the neuroepithelial basal lamina which normally helps orientate cells of the neuroepithelium in addition to providing structural support (Morris and O'Shea 1983). A similarly disorganized neuroepithelium was observed in the posterior neuropore region of homozygous Sp^d embryos with spina bifida (O'Shea and Liu 1987; Yang and Trasler 1991). A reduction in notochordal area, mesodermal and neuroepithelial cell number, as well as an increase in neuroepithelial intercellular space, in Sp^d compared to wildtype embryos was also observed (Yang and Trasler 1991). In addition, the normally smooth basal lamina was found to be highly irregular and often wavy in form (O'Shea and Liu 1987). It was not concluded whether an abnormal distribution of ECM components (fibronectin, laminin, CSPG, and HSPG) was the cause or consequence of these findings (O'Shea and Liu 1987).

Up to this point, descriptions of the abnormal tissues of homozygous *Sp* and Sp^d embryos have been widely documented but the origin of the defects in neural tube closure and NCC derived structures have remained elusive. Two important studies which shed some light on this issue have pointed towards the neuroepithelium as the primary tissue affected by the *Sp* mutant gene product. The first of these studies set out to determine why the NCCs did not contribute to the development of their predefined structures (Kapron-Bras and Trasler 1988). Auerbach (1954), showed that

there were no melanocytes in the skin of *Sp* homozygotes and that there was a considerable reduction in the size and number of the spinal ganglia. What remained to be determined was whether these NCC defects were the result of an ECM environment nonconducive for the required migration, differentiation, and proliferation of these cells, or whether the NCCs were able to secure their release from the neural tube given that they had been formed at all. In Kapron-Bras and Trasler's (1988) examination of the neuroepithelium from *Sp* homozygotes, they noted that the extracellular space which normally forms between the neuroepithelium and the surrounding ectoderm failed to appear prior to the normal time of NCC migration. This space was previously shown to be required for the NCCs to migrate into after they are released from the neural tube (Newgreen and Gibbons 1982). A marked reduction in the number of NCCs being released from the neural tube of *Sp* homozygotes compared to wildtype controls was detected (Kapron-Bras and Trasler 1988).

In order to determine whether the reduction in the number of migrating NCCs from homozygous *Sp* neural tubes was a property of the ECM (extrinsic) or the neuroepithelium (intrinsic), Moase and Trasler (1990) tested the ability of NCCs to migrate from caudal portions of neural tubes excised from day 9 homozygous *Sp* and Sp^d embryos when explanted to either gelatin coated tissue culture dishes or 3-D matrix gels consisting of ECM components. A 24 hour delay in the release of NCCs from both *Sp* and Sp^d neural tube explants compared to wildtype controls, as measured by the rate of outgrowth and the number of NCCs released, was detected when the explants were cultured on gelatin coated tissue culture dishes. The delay, although significant for both alleles, was more pronounced in the *Sp* compared to Sp^d cultures. After 72 hours, this delay was no longer apparent. Interestingly, the 24 hour delay in NCC emigration persisted when the *Sp* and Sp^d mutant explants were cultured in 3-dimensional basement membrane matrigels suggesting that the neuroepithelium and not the ECM is the tissue expressing the primary defect. The authors concluded that because the migrating NCCs from both mutant alleles appeared normal in morphology, the defects in NCC derived structures seen in *Sp*, and to a lesser extent in Sp^d, result from a delay in the migration of these cells from the neural tube (Moase and Trasler 1990). Presumably, this delay

interferes with the precise developmental pathway that these cells must follow.

In an attempt to understand how the *Sp* gene product mediates its action on the neuroepithelium, the distribution of a candidate protein, N-CAM, was investigated (Moase and Trasler 1991). Cell adhesion molecules in general, and N-CAM in particular, are involved in cellular interactions during development including neurogenesis (Linnemann and Bock 1989). *N-CAM* is expressed in the neuroepithelium and mesoderm during neurulation and is tightly regulated at the time of NCC emigration, being absent in migrating NCCs and reappearing in specific NCC derivatives (Edelman 1986). To examine whether N-CAM was aberrantly modulated during neurulation in *Sp* embryos immunohistochemical studies using a polyclonal N-CAM antibody were carried out (Moase and Trasler 1991). N-CAM was found to be more abundant in the neuroepithelium of homozygous day 9 *Sp* embryos compared to controls, but not so in earlier *Sp* embryos. Furthermore, in addition to the 180 kd and 140 kd N-CAM species normally present at day 9 of gestation, a 200 kd protein was identified (this time with a monoclonal N-CAM antibody) on a Western blot containing protein extracts from homozygous *Sp* embryos (Moase and Trasler 1991).

The authors concluded that the above findings are suggestive of qualitative rather than quantitative differences in the N-CAM expression profile (even though quantitation of *N-CAM* RNA remains to be assessed). It was thought that the increase in immunofluorescence detected in the *Sp* embryos was the result of using a polyclonal N-CAM antibody which recognizes the polysialic acid epitope (Moase and Trasler 1991). Furthermore, the authors speculate that the higher molecular weight N-CAM protein seen in *Sp* embryos may result from an increase in its sialylation, which interestingly enough, has been associated with a decrease in N-CAM adhesiveness (Rutishauser et al., 1988; Rutishauser and Jessell 1988). This interpretation awaits proper confirmation through the treatment of the *Sp* protein extracts with neuraminidase in order to determine whether the 200 kd N-CAM protein can be reduced in size (through the cleavage of its sialic acid residues).

A reduction in the adhesive properties of N-CAM could explain the disorganized nature of the neuroepithelium in *Sp* mutants. In turn, a disorganized neuroepithelium could explain the prevention of NCC

migration from a *Sp* neural tube and why their neural folds fail to close. It is conceivable then, that the *Sp* gene product may regulate, whether transcriptionally or through some post-translational modification such as the addition of sialic acid residues, the N-CAM gene product or protein. The speculations on the role that N-CAM may have in disrupting neurogenesis in the *Sp* mouse mutant are clearly premature, however, identification of the *Sp* gene product will allow for a critical evaluation of the putative interactions between *Sp* and *N-CAM*.

2.4. Lumbosacral spina bifida

The *vl* and *ct* mouse mutants are comparable to *Sp* in that the lumbosacral spina bifida observed in homozygous forms of these mutant strains results from a delay in the closure of the posterior neuropore (Copp 1985; Wilson and Wyatt 1988a), albeit through entirely different mechanisms (Wilson and Wyatt 1988b; Brook *et al.*, 1991). Unlike the homozygous *ct* mutant which displays a penetrance of 60% (20% open neural folds, 40% tail flexion defects) (Copp *et al.*, 1990), all homozygous *vl* mutants, upon close inspection, show abnormal defects of the caudal neural tube (Wilson and Wyatt 1986). The range of defects seen in *vl* embryos is also highly variable. Gross abnormalities of the caudal neural tube are easily detected and usually include widely flared neural folds at the posterior neuropore, whereas, more subtle defects consisting of a dorsally expanded neural lumen with a closed but distorted roof plate can only be detected by SEM or TEM analysis (Wilson and Wyatt 1988b).

The pathogenesis of the defects observed in the caudal neural tube of the *vl* mouse mutant appear to stem from an inability of the neural folds to initiate or maintain fusion (Wilson and Wyatt 1988b). Typically, at the actual site of neural fold closure, lamellopodia and filopodia from transitional zone cells (presumptive NCCs) of the apposed neural folds extend across the neural lumen and interdigitate to initiate contact (Copp *et al.*, 1990). These lamellopodia and filopodia must be coated with a carbohydrate component (probably GAGs) in order for convergence and fusion of the neural folds to occur (Lee *et al.*, 1976; Sadler 1978). In homozygous *vl* embryos the distribution of this surface coat was similar to

that of wildtype controls (Wilson and Wyatt 1988b). However, the transitional zone cells from homozygous *vl* embryos formed an erratic knot of disorganized cells in caudal portions of the newly fused neural tube (Wilson and Wyatt 1988b). Furthermore, an abundance of large blebs, possibly representing decaying transitional zone cells, were identified along the entire length of the posterior neuropore in *vl* embryos which subsequently go on to develop lumbosacral spina bifida (Wilson and Wyatt 1988a). These findings, in addition to the fact that some homozygous *vl* mice show white abdominal spots similar to those seen in *Sp* heterozygotes, have pointed to the presumptive neural crest (transitional zone) as the cell type expressing the primary defect. It remains to be determined whether the abnormalities of the putative NCCs in *vl* mutants act in a cell autonomous or non-autonomous fashion.

The pathogenic mechanism underlying the caudal defects in neural tube closure observed in the *ct* mouse mutant is perhaps the best understood of all the neurulation mutants. Through a variety of well designed experiments it has been shown that a reduction in the rate of proliferation of the notochord and gut endoderm can cause ventral curvature of the caudal portion of the embryo (Copp *et al.*, 1988; Brook *et al.*, 1991). Consequently, the ventral curvature opposes the forces which bring the neural folds together preventing their closure. It was further determined that the greater the amount of ventral curvature, the larger the size of the posterior neuropore, hence producing a more severe lumbosacral spina bifida (Brook *et al.*, 1991). Preventing the ventral curvature experimentally, by implanting a human eyelash into the lumen of the hindgut as a means of providing structural support, reduces the size of the posterior neuropore and thus, the severity of the ensuing defect (Brook *et al.*, 1991). The cause of the reduced proliferation of the notochord and gut endoderm in the homozygous *ct* embryo remains to be determined.

2.5. Craniorachischisis

Mice heterozygous for the *Lp* mutation exhibit loops or kinks in their tail, while homozygous *Lp* mutants have wide open neural folds throughout their entire cranio-caudal axis with the exception of a closed

area rostral to the myelencephalon (Strong and Hollander 1949). Abnormalities in neurulation are noticed early in homozygous *Lp* embryos, as indicated by disturbances in the growth of the gut endoderm, notochord, somites, and neuroepithelium (Smith and Stein 1962). It has been proposed that axial elongation is required in the overall development of the embryo and in particular, acts as an important force in neurulation (Copp *et al.*, 1990). Jacobson and Gordon (1976), suggest that axial elongation creates a buckling force that may aid in the rolling up of the neural folds into a tube. The observations by Wilson and Wyatt (1992) that the process of elevation and convergence of the spinal neural folds in homozygous *Lp* embryos compared to wildtype controls is defective in early phases of neurulation supports these views.

2.6. Genetic modes of action

The genetic mechanisms by which the mutant genes produce their phenotypes differ among the various mouse mutants. With respect to NTDs, the mode of inheritance is usually recessive, however, heterozygous *Axd* and *Sp* animals develop NTDs with a frequency of 1% (Essien *et al.*, 1990) and 9% (Moase and Trasler 1992) respectively, depending on their genetic background. Several of the mutant genes (*Lp*, *Ph*, *Sp*, *Xt*) exert their effects in a semi-dominant mode of action. A reduction by one half, of the wildtype gene, in these mutants produces a less severe phenotype (curly tail in *Lp*, white belly spots in *Ph*, *Sp*, and sometimes *Xt*, as well as extra digits in *Xt*) than when both copies of the wildtype gene are missing. This indicates that the *Lp*, *Ph*, *Sp*, and *Xt* mutant loci are strictly regulated in a dose-dependent manner. Furthermore, Copp *et al* (1990) suggest that as a result of their fully penetrant effects in the homozygous state these semi-dominant mutant loci represent loss-of-function or null alleles. Interestingly, this speculation put forth by Copp *et al* (1990), has recently been substantiated with the identification of significant deletions in candidate genes for three out of four of the aforementioned semi-dominant loci (see below). Other mutant loci whose NTDs are not fully penetrant (*Bn*, *ct*, *SELH*, *xn*) are presumably dependent on other epigenetic factors

(MacDonald *et al.*, 1989) for the expression of their phenotypes, or alternatively, have residual gene function (Copp *et al.*, 1990).

2.7. Of *Pdgfra*, *Gli3* and other genes

Mouse neurulation mutants have contributed much information towards an understanding of the cellular events which, when disrupted, result in a failure in neural tube closure. Unfortunately, no matter how thorough the examination of these mutants has been, the underlying genes responsible for the various phenotypes have remained elusive. For this reason, alternate strategies of identifying the molecular components contributing to both normal and aberrant neurulation events have been undertaken. Recently, a candidate gene approach, which relies on the co-localization of a mutant locus and a candidate gene (based on various criteria) to the same chromosomal position, successfully identified the genes coding for platelet-derived growth factor receptor α-subunit (*Pdgfra*) and *Gli3*, which when disrupted are responsible for the phenotypes observed in the *Ph* and *Xt* mouse mutants, respectively (Stephenson *et al.*, 1990; Hui and Joyner 1993; Schimmang *et al.*, 1992). Both of these semi-dominant mutants have pleiotropic phenotypes which include exencephaly (Johnson 1967; Gruneberg and Truslove 1960).

Homozygous *Ph* mutants display a variety of morphological abnormalities involving neural crest derived structures which include, craniofacial and heart defects, exencephaly, as well as the presence of fluid filled blebs along a wavy spinal cord (Gruneberg and Truslove 1960). Heterozygous *Ph* mice show a spotting pattern similar to what has been described for the *Sp* mouse. It is thus apparent that the *Ph* mutant involves abnormalities in the migration or differentiation of NCCs. The NCCs from homozygous *Ph* mutants are capable of securing their release from the neuroepithelium, however, due to an abnormal extracellular matrix environment, they are unable to migrate to their predefined destinations (Morrison-Graham and Weston 1989). The recent findings that *Ph* and *Pdgfra* map to the same region on mouse chromosome 5, that *Pdgfra* is entirely deleted in the *Ph* mutant, and that *Pdgf* is important in the production of matrix constituents including hyaluronan have made *Pdgfra*

an excellent candidate for the *Ph* locus (Stephenson *et al.*, 1990; Heldin 1992).

The homozygous *Xt* (*Xt*^{J}) mouse mutant is characterized by the formation of extra digits. Moreover, a wide range of abnormalities affecting the development of the limb, craniofacial structures, and the central nervous system including exencephaly, have been described (Johnson 1967). Heterozygous *Xt* mice display less severe limb abnormalities and occasionally, white ventral spotting (Johnson 1967). The candidacy of the *Gli3* gene for the *Xt* locus is supported by the finding that this gene is altered in a phenotypically similar human condition entitled Greig cephalopolysyndactyly syndrome (GCPS) (Vortkamp *et al.*, 1991) which maps to a chromosomal segment conserved between human (7p13) and mouse (13). The comparable expression pattern of *Gli3* with the tissues disrupted in homozygous *Xt* embryos (Schimmang *et al.*, 1992; Hui and Joyner 1993), the co-localization of GCPS and *Xt* to homologous map positions (Winter and Huson 1988), as well as the identification of a large intragenic deletion in the *Gli3* gene of *Xt* mice (Hui and Joyner 1993), have further supported the idea that *Gli3* and *Xt* are allelic.

The molecular mechanism by which *Gli3* causes the phenotypic features detected in GCPS and *Xt* has not been unravelled. Sequence homology and tissue expression profiles (Ruppert *et al.*, 1988, 1990; Schimmang *et al.*, 1992) support the idea that *Gli3* is a transcription factor regulating some aspect of limb and craniofacial morphogenesis. Furthermore, the observation that exencephaly in *Xt* mice may be caused by an overgrowth of neural tissue, thus preventing closure of the neural tube, suggests that *Gli3* may regulate the proliferative capacity of the neuroepithelium. Formal testing of this hypothesis has yet to be performed.

Several of the other mouse neurulation mutants have been assigned to specific chromosomal positions. Although candidate genes cannot be expected to "pop up" for each of them, the refinement of gene cloning strategies should facilitate their identification by alternative means. Positional cloning strategies, although labor intensive, have been successful in the identification of several mouse and many human disease genes (Reith and Bernstein 1991; Collins 1992; Bultman *et al.*, 1992; Vidal *et al.*, 1993). Similar success should come about in attempts to clone the various mouse neurulation mutants using comparable strategies.

3. The *paired* gene set of Drosophila

It will become evident in forthcoming chapters of this thesis that the paired box containing family of transcriptional regulators, commonly referred to as *Pax* genes, play an important role in mammalian development. To provide a foundation for these studies a brief review of the paired box containing genes of Drosophila follows.

In Drosophila, the entire body plan is established by the blastoderm stage of embryogenesis (Akam 1987; Ingham 1988). Through a cascade of interactions between transcriptional regulators, the metameric nature characteristic of insect bodies is defined, with each body segment containing the required information to differentiate into a particular structure (Ingham 1988). Many of the genes participating in embryonic pattern formation in Drosophila have been identified on the basis of their mutant phenotypes (Nüsslein-Volhard and Wieschaus 1980). For instance, maternal effect mutations have allowed for the identification of four genes whose products are required to define polarity in the early embryo (St Johnston and Nüsslein-Volhard 1992). This maternal information is then interpreted by a hierarchy of zygotically expressed gap, pair-rule, segment polarity, and homeotic genes in order to sub-divide the embryo into repeating segments with assigned identities (Ingham 1988; Ingham and Martinez Arias 1992; McGinnis and Krumlauf 1992). Each of the classes of segmentation genes has been categorized according to the spatial organization of its mutant phenotype (Nüsslein-Volhard and Wieschaus 1980). The gap genes are so named because mutations disrupting their function cause large deletions or gaps in the number of segments making up the final body plan. The pair-rule mutants result in deletions of homologous regions from every other segment, while the segment polarity mutants result in deletions of homologous portions from every segment. Finally, the homeotic genes are so named because their mutant phenotypes display the transformation of one segment type into another (Lewis 1978; Bender *et al.*, 1983; Kaufman *et al.*, 1990).

The cloning and subsequent sequencing of a variety of these developmentally important genes has identified several functional domains which show a high degree of conservation between genes of the same and distantly related species, suggesting that these domains may share similar

modes of function in developmental processes common to many organisms (McGinnis *et al.*, 1984; Scott and Weiner 1984; Scott and O'Farell, 1986; Frigerio *et al.*, 1986; Bopp *et al.*, 1989). The prototypic gene segment showing a high degree of conservation across a large number of species is the 180 bp homeobox (reviewed by Scott *et al.*, 1989). The homeobox has been identified in most classes of Drosophila segmentation genes, and is best known for its presence in all of the true homeotic selector (segment identity) genes of the *Antennapedia* (*Antp*) and *bithorax* complexes (Bender *et al.*, 1983; Kaufman *et al.*, 1990). A variety of *in vitro* and *in vivo* studies have shown that the homeodomain containing proteins act as sequence-specific DNA-binding proteins which function as activators and/or repressors of transcription (for a review see Gehring 1992). Structural analyses of the *Antp* and *engrailed* (*en*) homeodomain DNA complexes by nuclear magnetic resonance spectroscopy (Otting *et al.*, 1990) and X-ray crystallography (Kissinger *et al.*, 1990), respectively, have identified a helix-turn-helix motif similar to that which mediates DNA binding by many prokaryotic proteins (Laughon and Scott 1984). DNA binding specificity was shown to be conferred, at least in part, by the ninth amino acid of the recognition helix (the second of the helices in the helix-turn-helix motif) (Treisman *et al.*, 1989). Mutational analysis of several mammalian homeobox containing genes has revealed that like their Drosophila counterparts, these genes play a significant role in the specification of positional information along the anteroposterior body axis (reviewed by McGinnis and Krumlauf 1992). Moreover, the mechanisms by which the homeobox containing genes control development appears to be evolutionarily conserved (McGinnis and Krumlauf 1992).

Another group of genes which has emerged as being important in Drosophila segmentation is the paired-box containing gene family. Paired-box containing genes have so far been identified in pair-rule and segment polarity classes of segmentation genes (Bopp *et al.*, 1986, 1989). The archetypal paired box containing gene, *paired* (*prd*), was originally defined by its mutant phenotype. The *prd* mutant, an embryonic lethal, has deletions of analogous portions of segments at a two segment periodicity, characteristic of other pair-rule mutants (*even-skipped* and *runt*) and results in the formation of only half the normal number of segments (Nüsslein-Volhard and Wieschaus 1980).

A positional cloning strategy was used to identify the *prd* gene (Kilchherr *et al.*, 1986), the sequencing of which revealed several interesting motifs (Frigerio *et al.*, 1986). Subsequent screening of genomic and cDNA libraries using probes overlapping several of these motifs identified the *prd* gene set, a group of genes with structurally homologous segments with related functions (Frigerio *et al.*, 1986; Bopp *et al.*, 1986; Baumgartner *et al.*, 1987; Bopp *et al.*, 1989). The DNA sequence common to all five members of the *prd* gene set, the paired box, encodes the 128 amino acid paired domain. A second DNA segment, the paired-type homeobox, was identified in three of five *prd* gene set members (*prd*, *gsb-BH4*, *gsb-BH9*). Interestingly, the paired-type repeat (his-pro)n, initially identified at the carboxy terminus of prd, was not present in other paired domain containing proteins but was found in bicoid, a maternal effect protein whose homeodomain is distantly related (38% amino acid identity) to the paired-type homeodomain (Frigerio *et al.*, 1986).

The presence of a paired-type homeodomain in three of the five Drosophila *prd* gene set members, in addition to the nuclear localization of pox meso and pox neuro (two tissue specific members of the *prd* gene set), suggested that these genes may function as transcriptional regulators (Frigerio *et al.*, 1986; Bopp *et al.*, 1989). *In vitro* DNA binding studies showed that the prd protein was able to recognize more than one DNA sequence and that this DNA binding activity was not solely mediated by the paired-type homeodomain (Treisman *et al.*, 1989). In fact, a DNA sequence from the *even-skipped* (*eve*) promoter, e5, previously identified as a binding site for prd (Hoey and Levine 1988) was shown to be composed of two juxtaposed sites which accommodate the independent binding by both the paired-type homeodomain and the paired domain (Treisman *et al.*, 1991). Notably, a second site in the *eve* promoter, e4, necessitates cooperativity between the two domains in order for binding to occur, suggesting that these domains, in addition to their independent binding capabilities, may act synergistically (Treisman *et al.*, 1991).

Secondary structure predictions suggest that the paired domain contains at least three α-helices, with helices two and three potentially forming a helix-turn-helix motif (Burri *et al.*, 1989). In comparing the putative helix-turn-helix motif of the paired domain with that of the homeodomain, several interesting features were noted. Within the paired

domain, class specific amino acids were located in the first α-helix of the helix-turn-helix motif, while the second α-helix of this motif was found to be conserved (Burri *et al.*, 1989). This arrangement is in contrast to that of the homeodomain, where the first α-helix of the helix-turn-helix motif is the one that is conserved, while the second serves as the DNA recognition helix. Surprisingly, it is the first α-helix of the paired domain which shows the highest degree of homology to the first α-helix of the helix-turn-helix motif of the homeodomain, with up to seven conserved amino acid residues (Bopp *et al.*, 1989).

Exactly how the paired domain mediates its DNA binding properties and whether or not it does so in a similar fashion to that of the homeodomain was investigated by Treisman *et al* (1991). They showed that deleting the third α-helix (second helix of the predicted helix-turn-helix motif) or disrupting the second α-helix (first helix of the predicted helix-turn-helix motif) of the paired domain was not sufficient to abrogate its DNA binding properties. On the other hand, disrupting the first α-helix was sufficient to prevent the paired domain from binding DNA. From these studies, it is apparent that the paired domain and homeodomain bind DNA by completely different means. The determination of the actual structure of the paired domain and how it contacts DNA will necessitate further analysis by NMR-spectroscopy or X-ray crystallography.

Although the functional relevance of the *prd* gene set has yet to be fully elucidated, its members have been organized into structural classes with the premise that structurally related proteins will share common functions. The two criteria used to categorize members of the *prd* gene set were whether a particular structural domain was present and how similar these domains were between individual proteins (Bopp *et al.*, 1989). As previously stated, *prd*, *gsb-BH4*, and *gsb-BH9* each contain a paired-type homeodomain in addition to a paired domain and for this reason, make up the *prd-gsb* class of the *prd* gene set. The homeodomains of these three genes are very similar (85-92% amino acid identity) but differ significantly from other classes of homeodomain containing genes (prd-antp, 37% amino acid identity; prd-bcd, 38% amino acid identity), particularly at residues important in sequence specific recognition (prd has a ser at position 9 of its recognition helix while antp and bcd homeodomains contain glu and lys at this position, respectively)(Treisman *et al.*, 1989). A high degree of amino

acid conservation also exists for the prd-gsb class when comparing their paired domains. In examining the first 74 amino acids of the paired domain, which includes the first α-helix contained in a single exon, 92-97% of the amino acids are conserved among the three genes, whereas 79-85% amino acid identity exists over the entire paired domain (Bopp *et al.*, 1989).

The *pox-meso* and *pox-neuro* genes, which do not contain homeodomains, possess paired domains which deviate at a number of amino acid positions (non-conservative substitutions) from each other and from the paired domains of the prd-gsb class. Pox-meso and pox-neuro display 76% identity for the first 74 amino acids of the paired domain and only 66% amino acid identity over the entire paired domain (Bopp *et al.*, 1989). Similar values were observed when comparing the pox-meso and pox-neuro proteins with the prd-gsb class suggesting that the pox proteins each belong to a separate class.

The premise that the structurally homologous domains shared between members of the *prd* gene set is indicative of a functional link between them (Bopp *et al.*, 1989) is supported by examining the expression profiles of these genes in both wildtype and mutant embryos. In the case of *prd*, a pair-rule gene, its transcripts are expressed during late syncitial blastoderm in a pattern of seven evenly spaced bands reflecting a double-segment periodicity (Kilchherr *et al.*, 1986). During cellularization of the blastoderm, *prd* expression is changed to a pattern of 14 regularly spaced bands indicative of single-segment repeats (Kilchherr *et al.*, 1986). The mutant phenotype observed in *prd*$^-$ embryos, the reduction in segment number by one-half, is consistent with the loss of the most intense *prd* expressing cells at the syncitial blastoderm stage (Nüsslein-Volhard and Wieschaus 1980; Kilchherr *et al.*, 1986).

The two *gooseberry* loci, *gsb-BSH9* and *gsb-BSH4*, as members of the segment-polarity class of segmentation genes, are expressed in subsets of cells from every segment. Both *gsb* transcripts show peak levels of expression shortly after that of *prd*. *Gsb-BSH9* transcripts are located in the posterior ventrolateral region of each primordial segment in cells which later give rise to a variety of tissues including mesoderm, ectoderm, and neurectoderm (Baumgartner *et al.*, 1987). *Gsb-BH4*, on the other hand, is limited in its expression to neuroectodermal lineages which give rise to individual neurons during neuronal differentiation (Baumgartner *et al.*,

1987). The *gsb*$^{-}$ mutant has posterior portions of segments deleted which are replaced by mirror-image duplications of the remaining anterior portions of these segments (Nüsslein-Volhard and Wieschaus 1980). The wildtype expression pattern of *gsb-BH9* appears to most closely match the segments deleted in the *gsb*$^{-}$ mutant suggesting that they are allelic (Baumgartner *et al.*, 1987).

The *pox meso* and *pox neuro* transcripts also appear in a segmentally repeated pattern during the late stage of germ band elongation (Bopp et al., 1989). Transcripts of *pox meso* are observed posterior to the parasegmental grooves in the posterior half of each segment and are restricted to the mesodermal germ layer (Bopp *et al.*, 1989). *Pox neuro* transcripts appear in neural precursors of the peripheral and central nervous systems in each segment (Bopp *et al.*, 1989) and are responsible for the specification of the poly-innervated external sense organs (Baumbly-Chaudière *et al.*, 1992; Nottebohm *et al.*, 1992). Unfortunately, mutant screens have not been successful in identifying phenotypes correlating to mutations in either *pox meso* or *pox neuro*.

Consistent with the view that members of the *prd* gene set are not only related structurally but also functionally was the finding that all five members are expressed in a segmented fashion along the anteroposterior axis. Further comparison of the expression profiles of the various *prd* gene members identified a subset of cells in the posterior half of each segment which express *prd*, *gsb-BSH9* and *pox meso* transcripts (Bopp *et al.*, 1989). Based on these observations it was proposed that *prd*, *gsb-BSH9* and *pox meso* act along a common pathway to refine the positional information passed on to them by the other segmentation genes (Bopp *et al.*, 1989).

As previously stated, Drosophila segmentation is achieved through a hierarchical system of gene regulation whereby positional information is relayed from the maternal coordinate genes to the gap, pair-rule and segment polarity genes in a fashion which progressively subdivides the embryo into individual segments (Ingham 1988). The pair-rule genes, such as *prd*, are intermediaries in this cascade and are responsible for conveying positional information received from the zygotically expressed gap genes to the segment polarity genes. Within the pair-rule class of segmentation genes a hierarchical system of gene regulation is also achieved. The primary pair-rule genes, *runt* and *hairy*, which are themselves regulated by

gap genes (*hunchback*, *Krüppel* and *knirps*) act to regulate the expression of the secondary pair-rule genes *even-skipped*, *fushi tarazu*, *odd-paired*, and *odd-skipped* (Ingham 1988). Through combinatorial mechanisms of positive and negative regulation these secondary pair-rule genes act to modulate the expression of *prd*, a tertiary pair-rule gene (Baumgartner and Noll 1991). Recent evidence suggests that the products of the gap genes themselves are required to activate early *prd* expression (Gutjahr *et al.*, 1993). Because *prd* is at the bottom of the regulatory hierarchy among pair-rule genes, in addition to the fact that the *prd* pattern of expression changes from a two segment repeat (typical of pair-rule genes) to a single segment repeat (typical of segment polarity genes), it was felt that *prd* directly mediates the transition of positional information from the pair-rule to the segment-polarity genes (Baumgartner and Noll 1991). Evidence supporting this view comes from the analysis of the expression patterns of various segment-polarity genes in *prd*$^-$ mutants (Bopp *et al.*, 1989).

In examining the expression profiles of the two *gsb* genes, *gsb-BH4* and *gsb-BH9*, in *prd*$^-$ mutants it was found that the transcripts of each of these genes were activated only in every other segment as compared to the single segmental repeat typically observed for these gene transcripts in wildtype embryos (Bopp *et al.*, 1989). It was therefore surmised that prd protein is required for the proper expression of the *gsb* genes in the posterior half of alternating segments, whereas other pair-rule genes are most likely responsible for the *gsb* genes' expression in the other segments. *Pox meso* gene expression was shown to be altered in *prd*$^-$ embryos in a similar fashion (Bopp *et al.*, 1989). Whether *prd* regulates *pox-meso* directly or through an intermediate such as *gsb-BH9* remains to be proven. In addition to the regulation of *prd* gene set members by *prd*, the segment-polarity gene *engrailed* (*en*) also appears to be misexpressed in *prd*$^-$ mutants (Dinardo and O'Farrell 1987). In fact, several studies have shown that *prd* acts in concert with *eve* to activate *en* expression in the anterior portion of odd numbered parasegments (Dinardo and O'Farrell 1987; Morrissey *et al.*, 1991). Whether genes like *en* or other as yet unidentified genes are viable downstream targets of prd necessitates further studies.

As is the case for homeobox containing genes, paired box containing genes are also evolutionarily conserved. Paired box containing genes have been identified in the genomes of such diverse organisms as nematode,

Drosophila, zebrafish, quail, frog, mouse, and human (Gruss and Walther 1992). The importance of this gene family is shown not only by the conservation of their gene sequences but also by the observation that like the Drosophila genes, mutations in several of the mammalian *Pax* genes disturb the pattern of embryonic development (reviewed in Gruss and Walther 1992). The significance of mutations in members of the *Pax* gene family in general, and *Pax-3* in particular, will be addressed in the forthcoming chapters of this thesis.

Chapter 2

Molecular Characterization of a Deletion Encompassing the *Splotch* Mutation on Mouse Chromosome 1.

Abstract

We have used a set of markers newly assigned to the proximal portion of mouse chromosome 1 to characterize the chromosomal segment deleted in the splotch-retarded (Sp^r) mouse mutant. Among nine markers tested in the heterozygote $Sp^r/+$ mouse, we have identified four genes: *Vil*, *Des*, *Inha*, and *Akp-3* which map within the Sp^r deletion. The closest distal marker to the deletion is the *Acrg* gene, with the distal deletion breakpoint mapping within the 0.8 cM segment separating *Akp-3* and *Acrg*. The most proximal gene to the Sp^r deletion is *Tpl*. The proximal deletion breakpoint maps within the 0.8 cM segment separating *Tpl* and *Vil*. The minimum size of the Sp^r deletion would therefore be limited to 14 cM, the genetic distance between *Vil* and *Akp-3*. The maximum size of the Sp^r deletion is estimated to be 16 cM, the genetic distance between *Tpl* and *Acrg*.

Introduction

Neural tube defects are one of the most common congenital malformations, occurring in 1-3/1000 livebirths (Bergsma, 1979). Multiple factors, genetic and environmental, have been implicated in the etiology of both spina bifida and anencephaly, underlying the causal heterogeneity of these disorders (Bergsma, 1979). At present, the genetic components involved in the cause of neural tube defects in man remain unknown. Evidence for the segregation of major genes associated with familial anencephaly have been proposed (Shaffer *et al.*, 1990; Jenson *et al.*, 1988; and Toriello *et al.*, 1980) but none have yet been mapped.

One strategy to map single gene defects that cause developmental malformations in man is to identify similar defects in other genetically well defined mammals, such as the laboratory mouse. This strategy allows for comparative gene mapping to be carried out. For instance, if a single gene mouse mutant responsible for a particular defect is mapped to a chromosomal segment conserved between mouse and man, then molecular analysis of the corresponding target region can be performed to determine if a human equivalent to the mouse gene exists (Winter, 1988).

A candidate mutant gene for this study is splotch (*Sp*), and its allelic variants, splotch-delayed (Sp^d), and splotch-retarded (Sp^r). The *Sp* alleles are all autosomal dominant/semidominant mutants which display a pattern of increasing developmental disruption in the order of Sp^d, *Sp*, and the most severe allele, Sp^r. The homozygous Sp^d mutant is characterized by spina bifida and dysgenesis of neural crest cell derivatives including spinal ganglia (Moase and Trasler, 1990). They can survive until day 16 of gestation depending on their genetic background. The characteristic features of the homozygous *Sp* mutant include exencephaly, meningocele, and spina bifida (Auerbach, 1954), as well as dysgenesis of neural crest cell derived spinal ganglia and pigment cells of the skin. It survives until approximately day 13 of gestation. Unlike the *Sp* and Sp^d mutants which arose spontaneously (Dickie, 1964), the Sp^r mutant studied here was created by X-ray mutagenesis, is characterized by a cytogenetically detectable deletion of band C4 on chromosome 1, and animals homozygous for Sp^r die before implantation. Animals heterozygous for any of the three alleles at the *Sp* locus display white spotting of the belly, tail, and feet possibly due to the

absence of melanocyte migration to these regions (Auerbach, 1954). In addition the Sp^r heterozygote undergoes a persistent growth retardation throughout its adult life.

The *Sp* locus has been assigned to band C4 of mouse chromosome 1 (Evans *et al.*, 1988) within an approximated 32 cM evolutionarily conserved linkage group corresponding to the distal region of human chromosome 2q (Schurr *et al.*, 1990; Searle *et al.*, 1989). Our preliminary efforts in the attempt to isolate the gene responsible for the *Sp* mutation have been directed at the molecular characterization of the cytogenetically detectable deletion associated with the Sp^r mutant.

Materials and Methods

Mice

The Sp^T heterozygote was obtained from the MRC Radiobiology Unit, Chilton (Harwell), England. The original mouse was recovered among the progeny of a 3H1 (C3H/HeH x 101/H) F1 female given 6 Gy X-irradiation. The heterozygote is presently being inbred onto a C3H/HeJ background by brother-sister mating.

Probes

The *Len2*, *Fn*, *Akp-3*, and *Acrg* gene probes have previously been described (Schurr *et al.*, 1989). The *Tpl* probe used was a 0.4 kb EcoR1 mouse cDNA clone obtained from Dr. N. Hecht. The *Vil* probe used was a 1.4 kb BamH1/BglII mouse genomic clone. The *Des* probe used was a 2.2 kb BamHI mouse genomic clone. The *Inha* probe used was a 1.4 kb mouse genomic clone. The genomic *Vil*, *Des*, and *Inha* probes contained part of the coding segments of the gene and were all isolated in our laboratory after chromosome walking in a cosmid genomic library initially screened with the human *Des* (Li *et al.*, 1989), *Vil* (Rousseau-Merck *et al.*, 1988), and *Inha* (Barton *et al.*, 1989) cloned probes. The *Sag* probe was a 0.5 kb BamHI/BamHI genomic mouse clone (Ngo *et al.*, 1990). The 1.2 kb EcoR1 cDNA fragment of the rat *Na, K-ATPase* β_2 subunit which maps to chromosome 11 (Malo *et al.*, 1990) was used as an internal hybridization standard. The DNA inserts of cloned probes were gel purified and labelled to high specific activity ($5x10^8$ cpm/μg DNA) with $\alpha[^{32}P]$-dATP using the random primer labelling technique and the Klenow fragment of *E. coli* DNA polymerase I (Feinberg and Vogelstein, 1984).

Southern Hybridization

High molecular weight genomic DNA was isolated from spleens and kidneys of heterozygous $Sp^T/+$ and wildtype (+/+) littermate mice according to a standard protocol (Sambrook *et al.*, 1989). Genomic DNA was digested to completion with a ten-fold excess (10 Units/μg DNA) of restriction endonucleases according to the conditions suggested by the supplier (Pharmacia, Bethesda Research Laboratories). Five micrograms of

restricted genomic DNA were electrophoresed in 1% agarose gels containing TAE (40mM Tris-acetate, 20mM sodium acetate, and 20mM EDTA, pH 7.6) and transferred by capillary blotting onto nylon membranes (Hybond-N, Amersham). To ensure that each lane was equally loaded, prior to electrophoresis, the restricted DNA was quantified by fluorometric analysis using a DNA specific fluorescent dye (Hoechst 33258). The membranes were prehybridized for 16 hours and then hybridized with [^{32}P]-radiolabelled DNA probes for 16 hours at 60°C (human probes) or 65°C (rodent probes) in 6xSSC, 0.5% SDS, 5x Denhardt's solution, and 0.4 mg/ml sonicated denatured salmon sperm DNA. The membranes were washed at room temperature, first in 2xSSC, 0.1% SDS for 20 minutes, then in 0.5xSSC, 0.1% SDS for a further twenty minutes. The final wash was in 0.1xSSC, 0.1% SDS at 65°C for rodent probes, and 60°C for human probes. The membranes were exposed to XAR-film (Kodak) at -80°C with an intensifying screen for 16-72 hours.

Densitometric analysis

The gene copy number detected by individual probes for each lane was determined by quantifying the hybridization signals with a laser densitometer (LKB/Pharmacia). Corrections for the amounts of DNA loaded on the gel and transferred to the hybridization membranes were done for each lane by quantifying the hybridization signal of a control single copy probe.

Results and Discussion

The creation of a mouse mutant allelic to splotch (Sp^r) by X-ray mutagenesis and the subsequent identification of a cytogenetically detectable deletion in this mutant has localized the *Sp* gene to band C4 on mouse chromosome 1 (Evans *et al.*, 1988). In order to further delineate the subchromosomal location of the *Sp* gene, we have established the boundaries of the deleted chromosomal segment from the heterozygous mutant $Sp^r/+$, using nine cloned probes that we have recently assigned to that region of chromosome 1 (Malo *et al.*, 1990; Schurr *et al.*, 1989). These loci form part of a linkage group which has been evolutionarily conserved between the proximal portion of mouse chromosome 1 and the distal region of human chromosome 2q (Schurr *et al.*, 1990) (Table 1).

To determine which of the gene probes map within the Sp^r deletion, Southern blots of genomic DNA from the $Sp^r/+$ and wildtype littermates (+/+) were sequentially hybridized with the aforementioned gene probes (Figure 1). Each DNA sample was prepared in quadruplicate. Furthermore, each of the probes tested was hybridized to at least two Southern blots containing DNA samples restricted with different enzymes. In this analysis, internal hybridization standards that map to other chromosomes were used to control for possible variation in DNA concentrations per lane. Relative intensities of the hybridization signals (one copy versus two per diploid genome) were determined by densitometric analysis.

Results presented in Figure 1, demonstrate that the *Vil*, *Des*, *Inha*, and *Akp-3* genes are present at only one copy/genome in the $Sp^r/+$ mouse compared to two copies/genome in the +/+ littermate. The *Vil*, *Des*, *Inha*, and *Akp-3* genes must therefore map within the Sp^r deletion. These four genes can now be physically assigned to band C4 of chromosome 1. On the other hand, the *Len2*, *Tp1*, *Fn*, *Acrg*, and *Sag* genes show the control gene copy number in the $Sp^r/+$ mouse and therefore, map outside the deletion.

The proposed gene order on mouse chromosome 1, as determined by linkage analysis, is the following: *Len2-Fn-Tp1-Vil-Des-Inha-Akp3-Acrg-Sag* (Schurr *et al.*, 1990; Malo *et al.*, 1990). Thus, the *Len2*, *Tp1*, and *Fn* genes map proximal to the Sp^r deletion (Figure 2). The proximal breakpoint of the deletion maps within the 0.8 cM segment separating *Tp1* and *Vil*. The

Acrg and *Sag* genes map distal to the deletion (Figure 2). The distal breakpoint of the deletion maps within the 0.8 cM fragment which separates the *Akp-3* and *Acrg* genes. The minimum size of the Sp^r deletion is limited to 14 cM, the genetic distance between *Vil* and *Akp-3*. The maximum size of the Sp^r deletion can be approximated at 16 cM, the genetic distance between *Tpl* and *Acrg*.

It is of particular interest that within the syntenic group of loci, conserved between the proximal portion of mouse chromosome 1 and the distal region of human chromosome 2q, of which part is deleted in the $Sp^r/+$ mouse, there are seven genes which code for structural proteins. These loci, *Col3a1*, *Myl*, *Len2*, *Fn*, *Vil*, *Des*, and *Col6a3* contribute to the composition of the cytoskeleton and extracellular matrix (ECM) of cells of various tissues. The participation of cytoskeletal and ECM proteins in neural fold elevation and closure has been well documented (for review see O'Shea, 1986). In particular, Kapron-Bras and Trasler (1988) have noticed a reduction in the ECM filled space surrounding the neural tube of homozygous *Sp* mutants. Interestingly, at least two of the genes which map within the Sp^r deletion, *Vil* and *Des*, encode for proteins that contain actin-binding core sequences which are thought to be implicated in controlling cell shape, adherence to extracellular substrates, and migration. The *Vil* and *Des* genes are not known however, to be expressed during neural tube development, nor are they or any of the other genes tested in this report, found to be deleted or rearranged in the *Sp* or Sp^d heterozygotes (unpublished results).

Recently, Foy *et al* (1990) have demonstrated that the placental alkaline phosphatase locus on human chromosome 2q37 segregates with the Waardenburg Syndrome Type 1 (*WS1*). *WS1* is a dominant condition and is characterized by dystopia canthorum, pigmentary disturbances, and sensorineural deafness. Furthermore, Ishikiriyama *et al* (1989) identified a child with WS1 and a *de novo* inversion of 2q35-37. These findings, in addition to our report confirming the assignment of the *Akp-3* gene to band C4 of mouse chromosome 1, would strongly suggest that the WS1 locus is contained within the linkage group conserved between mouse chromosome 1 and human chromosome 2q. As a result of the homologous mapping of *Sp* and *WS1*, and the apparent similarities in the two phenotypes, it is tempting to speculate that *WS1* could be a human counterpart to the mouse *Sp* mutation. Further characterization of the region, in both species, by

multipoint linkage testing and long range physical mapping will be necessary to confirm this hypothesis.

Acknowledgements

The authors wish to thank Drs. R. Hynes, J.L. Guenet, L.C. Tsui, M. Breitman, L.P. Merlie, P. Henthorn, D. Paulin, T. Shinohara, R. Levenson, N. Hecht, and A.J. Mason for their generous contribution of hybridization probes. The authors would also like to thank Dr. K. Morgan for his assistance in the statistical analysis of the data. This work was supported by grants to M.V. and P.G. from the Medical Research Council (MRC) of Canada. P.G. is a recipient of a scientist award from "Fonds de recherche en Santé du Québec" (FRSQ). D.M. is supported by a fellowship from MRC and D.E. by a scholarship from the "Fonds de recherche en Santé du Québec" (FRSQ).

References

1. Auerbach, R. (1954). Analysis of the developmental effects of a lethal mutation in the house mouse. J. Exp. Zool. **127**:305-329.

2. Barton, D.E., Yang-Feng, T.L., Mason, A.J., Seeburg. P.H., and Francke, U. (1989). Mapping of genes for inhibin subunits, α, $ß_A$, and $ß_B$ on human and mouse chromosomes and studies of jsd mice. Genomics 5:91-99.

3. Beechey, C.V., and Searle, A. (1986). Mutations at the *Sp* locus. Mouse News Letter **75**: .

4. Bergsma, D. (1979). "Birth defects compendium" second edition. Alan R. Liss, Inc. Ney York.

5. Cohen-Haguenauer, O., Barton, P.J.R., Merlie, J.P., Van Cong, N., Masset, M., De Tand, M.F., and Frezal, J. (1987). Localization of the human acetyl choline receptor gamma subunit gene to 2q32-qter. Cytogenet. Cell Genet. **46**:595-598.

6. Danciger, M., Kozak, C.A., Tsuda, M., Shinohara, T., and Farber, D.B. (1989). The gene for Retinal S-Antigen (43-kDa Protein) maps to the centromeric portion of mouse chromosome 1 near *Idh-1*. Genomics **5**:378-381.

7. Dickie, M.M. (1964). New splotch alleles in the mouse. J. Hered. **55**:97-101.

8. Evans, E.P., Burtenshaw, M., Beechey, C.V., and Searle, A. (1988). A splotch locus deletion visible by giemsa banding. Mouse News Letter **81**:66.

9. Feinberg, A.P., and Vogelstein, B. (1984). A technique for radiolabelling DNA restriction endonuclease fragments to high specific activity. Anal. Biochem. **137**:266-267.

10. Foy, C., Newton, V., Wellesley, D., Harris, R., and Read, A.P. (1990). Assignment of the locus for Waardenburg Syndrome type I to human chromosome 2q37 and possible homology to the splotch mouse. Am. J. Hum. Genet. 46:1017- 1023.

11. Griffin, C.A., Smith, M., Henthorn, P.S., Harris, H., Weiss, M.J., Raducha, M., and Emanuel B.S. (1987). Human placental and intestinal alkaline phosphatase genes map to 2q34-37. Am. J. Hum. Genet. 41:1025-1034.

12. Heidaran, M.A., Kozak, C.A., and Kistler, W.S. (1989). Nucleotide sequence of the Stp-1 gene coding for rat spermatid nuclear transition protein 1 (Tp1): homology with protamine P1 and assignment of the mouse Stp-1 gene to chromosome 1. Gene 75:39-46.

13. Heidman, O., Buonanno, A., Geoffray, B., Robert, B., Guenet, .L., Merlie, J.P., and Changeux, J.P. (1986). Chromosomal localization of muscle nicotinic acetyl choline receptor genes in the mouse. Science 234:866-868.

14. Ishikiriyama, S., Tonoki, H., Shibuya, Y., Chin, C., Harado, N., Abe, K., and Niikawa, N. (1989). Waardenburg syndrome type I in a child with de novo inversion (2) (q35q37.3). Am. J. Med. Genet. 33:505-507.

15. Jensson, O., Arnason, A., Gunnarsdottir, H., Petursdottir, I., Fossdal, R., and Hreidarsson, S. (1988). A family showing apparent X-linked inheritance of both anencephaly and spina bifida. J. Med. Genet. 25:227-229.

16. Jhanwar, S.C., Jensen, J.T., Kaebling, M., Chaganti, R.S.K., and Klinger, H.P. (1986). *In situ* localization of human fibronectin (*Fn*) genes to chromosome regions 2p14-p16, 2q34-q36, 11q12.1-q13.5 in germ line cells, but to chromosome 2 sites only in somatic cells. Cytogenet. Cell Genet. 41:47-53.

17. Kapron-Bras, C.M., and Trasler, D.G. (1988). Histological comparison of the effects of the splotch gene and retinoic acid on closure of the mouse neural tube. Teratology 37:389-399.

18. Li, Z., Lilienbaum, A., Butler-Browne, G., and Paulin, D. (1989). Human desmin-coding gene: complete nucleotide sequence, characterization and regulation of expression during myogenesis and development. Gene 78:243-254.

19. Luerssen, H., Mattei, M-G., Schroter, M., Grzeschik, K.-H., Adham, I.M., and Engel, W. (1990). Nucleotide sequence of the gene for human transition protein 1 and its chromosomal localization on chromosome 2. Genomics 8:324-330.

20. Malo, D., Schurr, E., Epstein, D.J., Vekemans, M., Skamene, E., and Gros, P. (1990). The host resistance locus *Bcg* maps within a group of cytoskeleton-associated protein genes which include villin and desmin. Genomics (Submitted).

21. Malo, D., Schurr, E., Levenson, R., and Gros, P. (1990). Assignment of Na, K-ATPase β_2-subunit gene (*Atpb-2*) to mouse chromosome 11. Genomics 6:697-699.

22. Moase, C.E., and Trasler, D.G. (1990). Spinal ganglia reduction in the splotch-delayed mouse neural tube defect mutant. Teratology 40:67-75.

23. Ngo, J.T., Klisak, I., Sparkes, R.S., Mohandas, T., Yamaki, K., Shinohara, T., and Bateman, J.B. (1990). Assignment of the S-Antigen Gene (SAG) to human chromosome 2q24-q37. Genomics 7:84-87.

24. O'Shea, K.S. (1986). Gene and teratogen induced defects of early central nervous system development. Scanning electron microscopy 3:1195-1213.

25. Rousseau-Merck, M.F., Simon-Chazottes, D., Arpin, M., Pringeault, E., Louvard, D., Guenet, J.L., and Berger, R. (1988). Localization of the villin

gene on human chromosome 2q35-37 and on mouse chromosome 1. Hum. Genet. 78:130-133.

26. Sambrook, J., Fritsch, E.F., and Maniatis, T. (1989). Molecular Cloning. A laboratory manual. Cold Spring Harbor Press, Cold Spring Harbor, New York.

27. Shiloh, Y., Donlon, T., Bruns, G., Breitman, M.L., and Tsui, L.C. (1986). Assignment of the human gamma crystallin gene cluster (CRYG) to the long arm of human chromosome 2, region q33-q36. Hum. Genet. 73:17-20.

28. Schurr, E., Skamene, E., Morgan, K., Chu, M., and Gros, P. (1990). Mapping of *Col3a1* and *Col6a3* to proximal murine chromosome 1 identifies conserved linkage of structural protein genes between murine chromosome 1 and human chromosome 2q. Genomics 8:477-486.

29. Schurr E., Skamene, E., Forget, A., and Gros, P. (1989). Linkage analysis of the *Bcg* gene on mouse chromosome 1. Identification of a tightly linked marker. J. Immunol. 142:4507-4513.

30. Searle, A.G., Peters, J., Lyon, M.F., Hall, J.G., Evans, E.P., Edwards, J.H., and Buckle, V.J. (1989). Chromosome maps of mouse and man IV. Ann. Hum. Genet. 53:89-140.

31. Shaffer, L.G., Marazita, M.L., Bodurtha, J., Newlin, A., and Nance, W.E. (1990). Evidence for a major gene in familial anencephaly. Am. J. Med. Genet. 36:97-101.

32. Toriello, H.V., Warren, S.T., and Lindstrom, J.A. (1980). Brief communication: Possible X-linked anencephaly and spina bifida-report of a kindred. Am. J. Med. Genet. 6:119-121.

33. Viegas-Péquignot, E., Lin, L.Z., Dutrillaux, B., Apiou, F., and Paulin, D. (1989). Assignment of human desmin gene to band 2q35 by nonradioactive in situ hybridization. Hum. Genet. 83:33-36.

34. Wilcox, F.H. (1983). Genetics of alkaline phosphatase of the small intestine of the house mouse (*Mus musculus*). Biochem. Genet. 21:641-652.

35. Winter, R.M. (1988). Malformation syndromes: a review of mouse/human homology. J. Med. Genet. 25:480-487.

36. Zneimer, S.M., and Womack, J.E. (1988). Regional localization of the fibronectin and gamma crystallin genes to mouse chromosome 1 by in situ hybridization. Cytogenet. Cell Genet. 48:238-241.

Table 1

Chromosomal map positions of eight loci conserved between mouse chromosome 1 and human chromosome 2q.

Gene	Chromosome Location (Reference*)			
	Mouse		Human	
Len2	1 C2-4	(36)	2q33-36	(27)
Fn	1 C3-4	(36)	2q34-36	(16)
Vil	1 C4	(This report)	2q35-37	(25)
Des	1 C4	"	2q35	(33)
Inha	1 C4	"	2q33-qter	(2)
Akp-3	1 C4	"	2q34-37	(11)
Acrg	1 proximal	(12)	2q32-qter	(5)
Sag	1 proximal	(6)	2q24-37	(23)

* Numbered references pertain to those cited from pages 52 56.

Figure 1

Southern blot analysis of *MspI* digested DNA from a Sp^r heterozygote and its wildtype littermate. The chromosome 1-specific gene probes and the internal hybridization standard (*Atpb-2*) are indicated next to each band. The number beneath each pair of lanes represents the ratio of band intensities (+/+:Sp^r) as determined by laser densitometry.

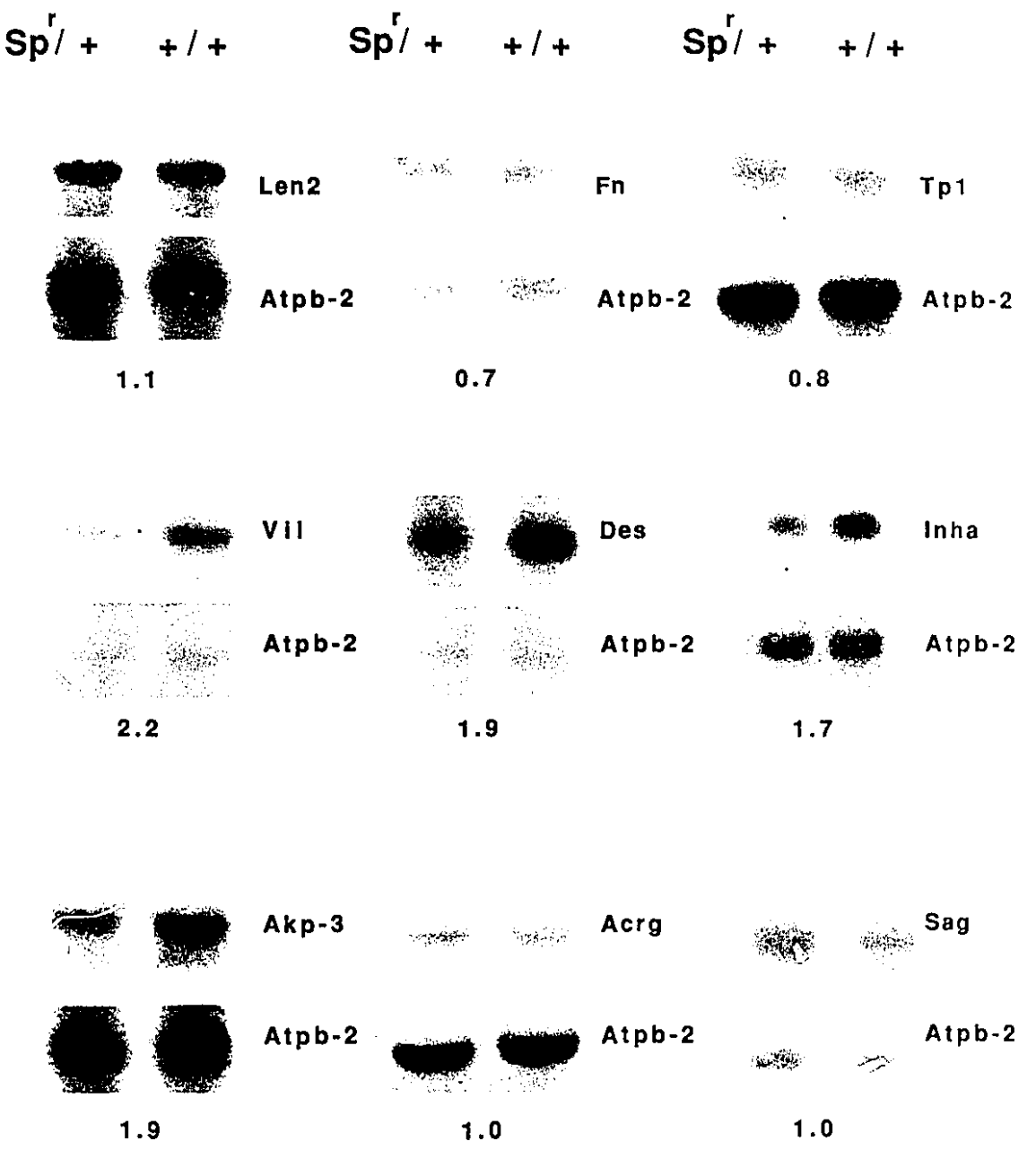
Sp^r/ +
+ / +
Sp^r/ +
+ / +
Sp^r/ +
+ / +
Len2
Atpb-2
1.1
Fn
Atpb-2
0.7
Tp1
Atpb-2
0.8
Vil
Atpb-2
2.2
Des
Atpb-2
1.9
Inha
Atpb-2
1.7
Akp-3
Atpb-2
1.9
Acrg
Atpb-2
1.0
Sag
Atpb-2
1.0

Figure 2

Genetic distances (in cM $\pm$ SE) of eight loci spanning the chromosomal segment deleted in the Sp^r mouse mutant.

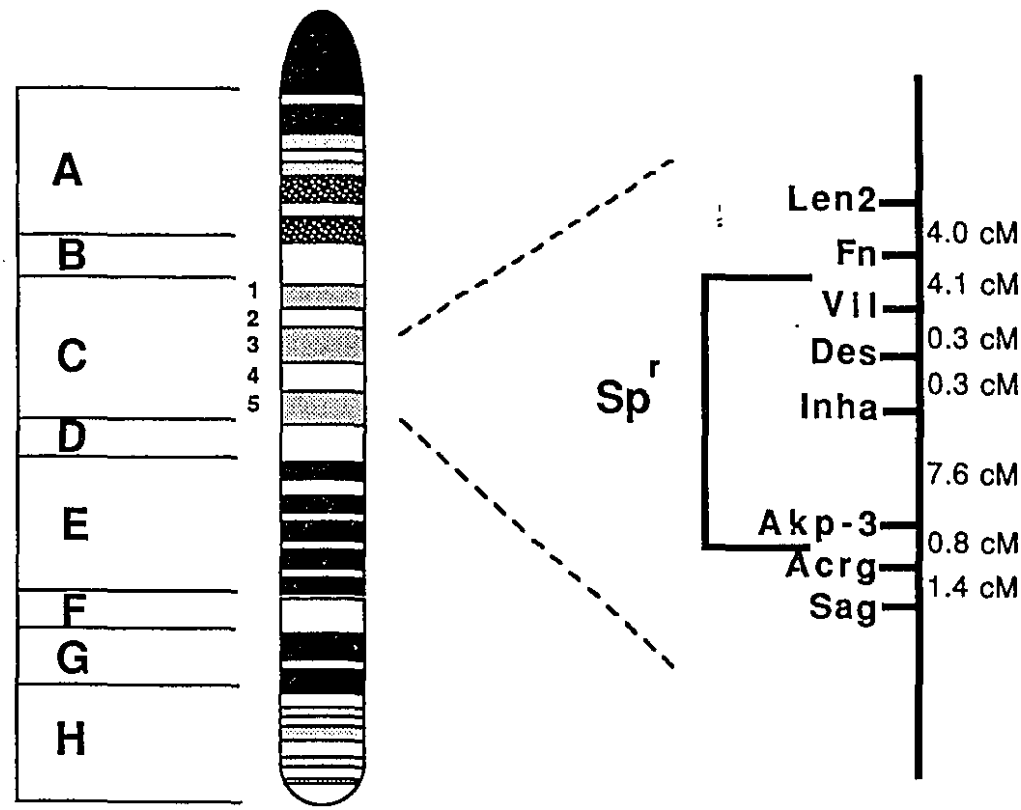
A
B
C
D
E
F
G
H
1
2
3
4
5
Sp r
Len2
Fn
Vil
Des
Inha
Akp-3
Acrg
Sag
4.0 cM
4.1 cM
0.3 cM
0.3 cM
7.6 cM
0.8 cM
1.4 cM

Chapter 3

splotch (Sp^{2H}), a Mutation Affecting Development of the Mouse Neural Tube, Shows a Deletion Within the Paired Homeo Domain of *Pax-3*

Abstract

We have analyzed the molecular basis of the mouse mutation *splotch* (*Sp*) in three alleles at this locus *Sp*, $Sp^{2H}$and Sp^{r}. *Sp* is a semidominant mutation which maps to the proximal part of mouse chromosome 1 and is phenotypically expressed as a pleiotropic defect during neurogenesis, resulting in spina bifida, exencephaly and dysgenesis of neural crest cell derivatives. Using segregation analysis in a panel of interspecific backcross mice, we positioned the paired box gene *Pax-3* within the *Inha* to *Akp3* interval, near or at the *Sp* locus. *Pax-3* was found to be deleted in heterozygous Sp^{r}/+ mice which harbor a large interstitial deletion of the proximal part of mouse chromosome 1. Analysis of genomic DNA and cDNA clones constructed from RNA isolated fromSp^{2H}/Sp^{2H} embryos identified a deletion of 32 nucleotides in the *Pax-3* mRNA transcript and gene of these mice. This deletion maps within the paired homeo domain of the PAX-3 polypeptide, and is predicted to produce a truncated protein as a result of a newly created termination codon at the deletion breakpoint. Our study indicates that the severe defect in neural tube formation detected in the Sp^{2H} mutant is linked to the inactivation of the paired box gene *Pax-3*, and provides direct genetic evidence of a key role for *Pax-3* in normal neural development.

Introduction

The cellular and molecular mechanisms which contribute to the complex process of neurulation in mammals have yet to be fully elucidated. Aberrations in the formation of the vertebrate neural tube result in neural tube defects, such as spina bifida (meningomyelocoele) and anencephaly. Spina bifida and anencephaly are the most common forms of neural tube defects in humans with a combined incidence of 1/1000 live births (Edmonds and James, 1990). Multiple factors, both genetic and environmental (Copp et al., 1990) have been implicated in the etiology of spina bifida and anencephaly, underlying the causal heterogeneity of these disorders. However, theses genetic factors have yet to be identified.

The mouse offers an excellent experimental model for the study of developmental processes such as neurogenesis, because of the accessibility of the developing embryo, the relative abundance of independently derived mutants, and the ease by which one can manipulate both environmental and genetic influences on these developmental processes. In particular, the mouse mutant *splotch* (*Sp*) is an established model for the study of neural tube defects in humans (Copp et al., 1990). *Sp* was initially identified as a spontaneous mutant in a mouse colony (Russell 1947) and since then several other mutants, either spontaneous in the case of splotch-delayed (Sp^d; Dickie 1964), or induced by X irradiation in the case of splotch-retarded (Sp^r), Sp^{1H} and Sp^{2H} (Beechey and Searle, 1986), have been shown by genetic analysis to be allelic to *Sp*. The *Sp* mutant has been classified as a semidominant mutation and has been mapped to the proximal portion of mouse chromosome 1 (Snell et al., 1954; Skow et al., 1988). While the molecular basis of the genetic defect in *Sp* mutants is unknown, the Sp^r allele is characterized by a cytogenetically detectable deletion of chromosome 1, Giemsa band C4 (Evans et al., 1988). We have recently analyzed the deleted chromosome 1 segment in the Sp^r mutant and have established its size as approximately 16 centiMorgans (cM), encompassing the structural genes for villin (*Vil*), desmin (*Des*), inhibin a-subunit (*Inha*), and alkaline phosphatase (*Akp-3*) (Epstein et al., 1991). Phenotypic characteristics of the homozygous mice bearing the *Sp*, Sp^{1H} and Sp^{2H} alleles are very similar and include exencephaly, meningocele, and spina bifida (Auerbach 1954; Beechey and Searle 1986; Franz 1989) as well as

dysgenesis of neural crest cell derived spinal ganglia (Auerbach 1954), Schwann cells (Franz 1990) and structures of the heart (Franz 1989). *Sp*, Sp^{1H} and Sp^{2H} homozygotes survive until approximately day 16 of gestation depending on their genetic background. Sp^{d} homozygotes are similar but only develop spina bifida, and can survive until birth (Dickie 1964), while Sp^{r} homozygotes presumably die prior to implantation. While the respective phenotypes of the different *Sp* alleles may vary with respect to survival time *in utero* and severity of neural tube defect, all heterozygous *Sp* mutants and their allelic variants, are characterized by white spotting of the abdomen, tail, and feet possibly due to the absence of melanocyte migration to these regions (Auerbach 1954).

In the mouse, the *Pax* gene family encodes a group of eight related proteins (Kessel and Gruss, 1990) which share in common a protein domain homologous to that encoded by the Drosophila paired box (Bopp et al., 1986). One member of this family, *Pax-3*, is expressed just prior to neural tube closure along the dorsal part of the neuroepithelium extending from the prosencephalon to the anterior margin of the posterior neuropore (Goulding et al., 1991). In addition, *Pax-3* is expressed in certain neural crest cell derivatives such as the spinal ganglia, dorsal root ganglia, somitic mesoderm and certain cranio-facial neural crest derivatives. The *Pax-3* gene has been mapped to the proximal portion of mouse chromosome 1 between the *tumbler* and *leaden* mutant loci (Goulding et al., 1991) near the structural gene for villin (Olson et al., 1990) within the general area of *Sp*. The striking similarity between the tissue distribution of *Pax-3* mRNA in normal developing embryos, and the neural structures affected in *Sp* mice, together with the chromosome 1 location of *Pax-3* led us to examine whether *Pax-3* was mutated in *Sp*.

Results

Pax-3 has recently been mapped to mouse chromosome 1 and found to co-segregate with *Vil* in a small number of informative backcross progeny (Olson et al., 1990). Since *Vil* is deleted in the Sp^r allele of the *Sp* mutation (Epstein et al., 1991), we determined whether *Pax-3* was also deleted in these mice. Because Sp^r/Sp^r homozygotes die prior to implantation, genomic DNA cannot be easily obtained from them. Therefore, Southern blots of genomic DNA from $Sp^r/+$ heterozygotes and parental controls (C3H/HeJ and 101/OR) were hybridized with a *Pax-3* specific cDNA probe and the intensity of the specific hybridization signals compared to that obtained with a control probe (*Atpb 2*) known to map on chromosome 11 (Malo et al., 1990). The *Pax-3* cDNA probe used for this analysis was a cDNA segment overlapping the amino terminal half of PAX-3 and was obtained by direct cDNA amplification (PCR), using specific oligonucleotides and cellular RNA from embryonal carcinoma P19 cells, known to express *Pax-3* after induction with retinoic acid (Goulding et al., 1991). Relative intensities of the hybridization signals (one copy versus two per diploid genome) were quantified by densitometric analysis. This analysis (Figure 1a) shows that *Pax-3* is present at only one copy/genome in $Sp^r/+$ heterozygotes compared to two copies/genome in the control C3H/HeJ strain, indicating that *Pax-3* is indeed part of the large chromosome 1 segment deleted in the Sp^r allele.

The chromosomal location of *Pax-3* was further established by linkage analysis in an interspecific (*Mus spretus* x C57BL/6J)F1 x C57BL/6J backcross mapping panel with respect to eight other loci previously assigned to the proximal region of mouse chromosome 1 (Schurr et al., 1990; Malo et al., 1991). For this, an 8 kb polymorphic Kpn I *Pax-3* restriction fragment was first identified between *Mus spretus* and C57BL/6J mice (data not shown), and its segregation was followed by Southern blotting analysis in genomic DNA from a total of 253 backcross progeny. The distribution of the various recombinant genotypes in these mice unambiguously positions *Pax-3* within the *Inha* to *Akp-3* interval (Figure 1b), with 13 crossovers identified between *Pax-3* and *Akp-3* and 16 between *Pax-3* and *Inha*. The predicted gene order and intergene distances were calculated as centromere-*Fn-1*-2.0 cM-*Tp-1*-0.8 cM-(*Vil*, *Des*) 0.4 cM-*Inha*-6.3 cM-***Pax-3***- 5.1cM-*Akp-*

3- 0.8cM-*Acrg*-2.0 cM-*Sag* (Figure 1A). The mapping of *Pax-3* to this segment of mouse chromosome 1 is consistent with prior chromosomal assignments of the *Sp* mutation (Skow et al., 1988) and suggests tight linkage between the two loci. Taken together, the finding that *Pax-3* is deleted in the Sp^r mutant and maps near or at the *Sp* locus, prompted us to investigate further the possibility that *Pax-3* and *Sp* may be the same locus.

We reasoned that if such was the case, *Pax-3* may also be deleted, rearranged or otherwise mutated in other alleles at the *Sp* locus. The *Sp* and Sp^{2H} mutants survive long enough *in utero* that genomic DNA and cellular RNA can easily be obtained from homozygous embryos. Genomic DNA from day 14 *Sp/Sp* and Sp^{2H}/Sp^{2H} embryos, as well as adult C3H/HeJ and 101/OR parental strains, were restricted with Taq I and analyzed by Southern blotting for alterations in the *Pax-3* gene, using a *Pax-3* cDNA probe covering the 5' half of the mRNA, from position +84 to +1078 of the reported sequence (Goulding et al., 1991). The *Pax-3* probe detected hybridizing Taq I fragments of size 4.4, 3.1, 2.5, 2.1, 1.5, and 0.6kb in the C3H/HeJ parental strain (Figure 2A, lane 4). The same fragments were detected in the other parent, 101/OR, except for the 3.1kb C3H/HeJ fragment which is polymorphic in 101/OR mice and replaced by a 2.8kb fragment (Figure 2A, lane 5). The pattern of Taq I hybridizing fragments detected by *Pax-3* in DNA from either homozygous day 14 *Sp/Sp* embryos (Figure 2A, lane 1), or heterozygous $Sp^r/+$ adults (Figure 2A, lane 3) was identical to that detected in either the C3H/HeJ or 101/OR parents, suggesting that *Pax-3* is not grossly rearranged in these mice. However, our *Pax-3* probe detected a novel and unique 5kb hybridizing fragment in DNA from homozygous day 14 Sp^{2H}/Sp^{2H} mice (Figure 2A, lane 2), which was absent form either parental strain. A prolonged exposure of the Southern blot (Figure 2A, bottom panel) shows that DNA from Sp^{2H}/Sp^{2H} mice also lacked the 0.6kb *Pax-3* fragment detected in both parents (Figure 2A, bottom panel, compare lane 2 with 4 and 5), consistent with the proposition that at least one Taq I site is specifically altered in the Sp^{2H}/Sp^{2H} mutant. This alteration seems to result from either a point mutation or a small rearrangement, as restriction of genomic DNA with a number of other enzymes failed to reveal differences in hybridization profiles between mutant mice and parental strains (data not shown). It is unlikely that the altered profile of *Pax-3* hybridizing Taq I fragments

detected in Sp^{2H}/Sp^{2H} mice is caused by artifactual or partial digestion by this enzyme since re-hybridizing the same blot with a *Pax-3* probe corresponding to the 3' end of the mRNA (nucleotides +1057 to +1809) generated identical patterns of hybridizing fragments in all mutants and both parental strains (Figure 2B).

To determine if the alteration detected by the *Pax-3* cDNA probe in Taq I digested genomic DNA of Sp^{2H}/Sp^{2H} mice caused changes within the transcribed portion of the gene and/or coding sequence of the PAX-3 polypeptide, we isolated and characterized the corresponding *Pax-3* cDNA clones from both the Sp^{2H}/Sp^{2H} mutant and a normal parent. Total cellular RNA was extracted from Sp^{2H}/Sp^{2H} and C3H/HeJ embryos, and cDNAs overlapping the 5' half of *Pax-3* mRNA were synthesized using a sequence specific oligonucleotide as a primer for reverse transcription (Figure 3A, primer **b**). The *Pax-3* cDNAs were isolated after amplification by PCR, using sequence specific primers (Figure 3A, primers **a** and **b**). The cDNAs isolated from Sp^{2H}/Sp^{2H} and C3H/HeJ RNA were digested with Taq I and analyzed by gel electrophoresis (Figure 3B) . Three Taq I fragments of size 776 bp, 150 bp, and 68 bp corresponding to sizes predicted from the published sequence, were detected in the 994 bp *Pax-3* cDNA subfragment from C3H/HeJ RNA (Figure 3B, lane 2). On the other hand, the corresponding *Pax-3* cDNA subfragment of the Sp^{2H}/Sp^{2H} embryo showed only two Taq I fragments of size 776 bp and 186 bp (Figure 3B, lane 1). These findings confirm that the altered Taq I site detected by Southern analysis in genomic DNA from the Sp^{2H}/Sp^{2H} mutant is also absent from the cDNA, and that its absence is not linked to a simple point mutation but appears to be caused by a deletion of a genomic segment encompassing this Taq I site and approximately 30 nucleotides of transcribed sequence. Further restriction mapping experiments (data not shown) indicated that the missing Taq I site in Sp^{2H}/Sp^{2H} is normally found at position +1010 of the published *Pax-3* sequence (Figure 3A). The *Pax-3* cDNA fragments amplified from C3H/HeJ and the Sp^{2H}/Sp^{2H} mutant were cloned and their nucleotide sequences determined for the region neighboring the proposed deletion (Figure 3A). The deletion in the Sp^{2H}/Sp^{2H} mice was found to be precisely 32 nucleotides in length, and to encompass a segment beginning at alanine 237 and ending at threonine 248 of the PAX-3 polypeptide. This deletion removes part of the highly conserved paired homeo domain of the

protein, interrupts the reading frame of the mRNA and creates a TAG termination codon immediately downstream alanine 237, resulting in a truncated protein lacking its C-terminal half.

To confirm that the deletion in *Pax-3* detected in the Sp^{2H}/Sp^{2H} mutant did not reflect alternative splicing of the *Pax-3* gene, or was caused by an enzymatic artifact of either reverse transcriptase or Taq polymerase used to construct and amplify the cDNAs, we amplified by PCR the genomic DNA segment predicted to span the deletion detected in the cDNAs. For this, genomic DNAs from the Sp^{2H}/Sp^{2H} mutant and parental controls were amplified using two sequence specific primers (primers **b** and **c**, see Figure 3A) located 127 nucleotides apart in the cDNA sequence, and mapping on either side of the deleted segment (Figure 3C) . A 127 bp fragment could be amplified from DNA of both parental controls C3H/HeJ, 101/OR, and the *Sp/Sp* mutant (Figure 3C, lanes 1, 2 and 5 respectively), while a shorter 95 bp fragment was amplified from Sp^{2H}/Sp^{2H} embryonic DNA (Figure 3C, lane 4), and both the 127bp and 95bp fragments were amplified from the DNA of the $Sp^{2H}/+$ heterozygote (Figure 3C, lane 3). Direct DNA sequencing of the 95 bp Sp^{2H} fragment showed that the deletion in the genomic DNA was identical to that detected in the *Pax-3* mRNA.These findings confirm the existence of a small chromosomal deletion of 32 nucleotides in the *Pax-3* gene of these mice.

Discussion

The murine *Pax* gene family encodes a group of eight structurally related polypeptides (*Pax-1-8*; Kessel and Gruss, 1990) which share a sequence homologous domain with the paired (prd) gene product of Drosophila. This common and highly conserved 128 amino acid segment is called the "paired domain", and is found in addition to *prd*, in four other segmentation genes expressed during early Drosophila development *gooseberry-distal* (*gsb-d*), *gooseberry-proximal* (*gsb-p*) (Bopp et al., 1986) *Pox-meso* and *Pox-neuro* (Bopp et al., 1989). In humans, three paired box genes *HuP1*, *HuP2*, and *P29* have so far been identified (Burri et al., 1989). The spatial and temporal expression patterns of the *prd* gene in Drosophila (Morrissey et al., 1991), and the *Pax* genes in the mouse (Deutsch et al., 1988; Dressler et al., 1990; Plachov et al., 1990; Goulding et al., 1991) suggest that they play a regulatory role in establishing the positional identity of cells and tissues along an antero-posterior axis in a variety of developmental processes during embryogenesis. For instance, the *Pax-1* gene is expressed in the ventral sclerotome along the rostrocaudal axis and may contribute to the development of segmented structures of the vertebral column, sternebrae, and thymus (Deutsch et al., 1988). *Pax-2* and *Pax-8* are both expressed along the rostrocaudal axis of the developing neural tube, in addition to the developing excretory system (Nornes et al., 1990; Dressler et al., 1990; Plachov et al., 1990) while *Pax-3* and *Pax-7* share similar expression patterns in the developing neural tube (Jostes et al., 1990; Goulding et al., 1991).

Although the exact mechanism by which members of the *Pax* family exert their regulatory role during development remains to be elucidated, amino acid sequence information and biochemical analyses suggest that they may act at the DNA level by modulating the transcriptional activity of specific target genes. Firstly, polypeptides encoded by Drosophila *Pox meso* and *Pox neuro* genes show a nuclear localization (Bopp et al., 1989). Secondly, the predicted secondary structure of the paired domain overlapping amino acid residues 78-105 shows a helix-turn-helix structural motif (Burri et al., 1989), known to have DNA binding properties (Schleif et al., 1988). Thirdly, the Drosophila genes *prd*, *gsb-d* and *gsb-p*, and the mouse *Pax-3*, *Pax-6*, and *Pax-7* genes encode, in addition to their paired

domain, a paired homeo domain also known to bind DNA (Kissinger et al., 1990). Finally, the capacity of these proteins to bind promoter elements *in vitro* through their paired domains and paired homeo domains has been directly established for three of them (Treisman et al., 1991; Goulding et al., 1991; Chalepakis et al., 1991). These observations support the hypothesis that *Pax* genes encode nuclear trans-acting transcription factors regulating the expression of several target genes, themselves coding for key structural or regulatory proteins implicated in normal development. According to this proposal, inactivating mutations in *Pax* genes would have pleiotropic and possibly deleterious effects on normal embryogenesis. This was indeed shown to be the case for *Pax-1*. A single glycine to serine substitution within the highly conserved paired domain of *Pax-1* is detected in the mouse mutant *undulated* (*un*), which is characterized by vertebral malformations along the entire rostrocaudal axis (Balling et al., 1988). This mutation has recently been shown to alter the DNA binding properties of *Pax-1* in vitro (Chalepakis et al., 1991).

The results presented in our study provide additional genetic evidence supporting this mechanism of action for yet another member of the *Pax* family, *Pax-3*. We find that *splotch* (Sp^{2H}/Sp^{2H}), a mutation affecting the development of the mouse nervous system, has an internal deletion of 32 nucleotides within the *Pax-3* gene. This deletion maps within the boundaries of the paired homeo domain, interrupts the reading frame, and creates a termination codon at the juncture of the deletion breakpoints resulting in a truncated protein lacking a complete paired homeo domain and its entire carboxy terminal half. These results, in addition to the findings that: 1) *Pax-3* and *Sp* share similar or identical map locations; 2) *Pax-3* is deleted in $Sp^{T}/+$ mice; and 3) the temporal and physical distribution of *Pax-3* transcripts in normal developing embryos coincides with that of tissues and cell types affected by the *Sp* mutation, indicate that *Pax-3* and *splotch* are the same genetic locus, and that the *Pax-3* mutation detected in Sp^{2H}/Sp^{2H} mice underlies the neural tube defects detected in these animals. Our inability to detect gross rearrangements in the *Pax-3* gene of embryos from another *Sp* allele (*Sp/Sp*) suggests that the molecular defect in these mice may involve a point mutation, compatible with the spontaneous origin of this *Sp* allele.

Close examination of tissues and specific cell types either affected in Sp^{2H}/Sp^{2H} embryos or showing *Pax-3* expression during normal development may suggest candidate genes for regulation by *Pax-3* during neurogenesis. The phenotypic expression of the *Sp* mutation in homozygous Sp^{2H}/Sp^{2H} mice is pleiotropic and includes exencephaly (cranioschisis), overgrowth of the neural tissue near the posterior neuropore resulting in spina bifida, a tail flexion defect (curly tail), and a general delay in development resulting in a smaller overall size (Figure 4). In addition to the gross anatomical defects portrayed in the various Sp mutants, there are also deficiencies in the neural crest cell derivatives (Auerbach, 1954; Moase and Trasler, 1989). The neural crest cells originate from the neuroepithelium, detach from this tissue at the time of migration and give rise to a variety of differentiated cell types (LeDouarin, 1980). Planar cultures of caudal neural tube explants from day 9 *Sp/Sp* and Sp^{d}/Sp^{d} embryos have revealed a 24 hour delay in the release of the neural crest cells compared to wild type controls (Moase and Trasler, 1990). The neural crest cells that do emigrate appear normal in morphology suggesting that the defect causing their delayed emigration is intrinsic to the neuroepithelium (Moase and Trasler, 1990). It is tempting to speculate that proteins essential to the normal migration of neural crest cells and possibly produced by neuroepithelial cells, such as extracellular matrix proteins and their receptors, or cell adhesion molecules implicated in adhesion to substratum and mobility, may be under the regulatory control of *Pax-3*. *Pax-3* is indeed expressed in cells from the neuroepithelium and in some neural crest cell derivatives (Goulding et al., 1991). One putative candidate for *Pax-3* regulation is the neural cell adhesion molecule, N-CAM. N-CAM shows a pattern of expression similar to PAX-3, that is, high levels in the neural tube before neural crest cell migration, absence in the migrating neural crest cells, and then reappearance in various neural crest cell derivatives (Edelman, 1986; Goulding et al., 1991). Interestingly, the *N-CAM* gene promoter region contains an ATTA motif (Hirsch et al., 1990) known to form part of the DNA recognition sequence of various homeo domain containing proteins, including PAX-3 (Goulding et al., 1991). Moreover, quantitative and qualitative differences in N-CAM expression profiles have been detected by immunological analyses in the neuroepithelium of *Sp/Sp* homozygotes compared to +/+ littermates (Moase and Trasler, 1991).

The chromosomal assignment of *Pax-3* to the proximal portion of mouse chromosome 1 places it within the boundaries of a large evolutionarily conserved linkage group whose human homologous counterpart is found on the long arm of chromosome 2 (2q). This syntenic segment spans approximately 32cM (calculated from recombinational analysis in the mouse; Schurr et al., 1990) and is delineated by two collagen genes, *COL3A1* (2q31-32.3) and *COL6A3* (2q37). Human Waardenburg Syndrome type I (*WS I*, MIM 19530) is an autosomal dominant disorder that has been mapped by linkage analysis in familial cases (Foy et al., 1990; Asher et al., 1991) and by the identification of a specific chromosomal inversion in a sporadic case (Ishikiriyama et al., 1989) to chromosome 2q, band 2q35-37.3. WS I is characterized by dystopia canthorum (lateral displacement of the inner canthi), pigmentary disturbances (heterochromia irides, white forelock) and sensorineural deafness (McKusick, 1990). It is believed that neural crest derived melanocytes responsible for normal pigmentation and implicated in the development of the stria vascularis in the mammalian ear (Steel and Barkway, 1989) may be the cell population phenotypically expressing the WS I defect. As a result of the homologous map positions for WS I in humans and *Sp* in the mouse, in addition to their sharing of some phenotypic features (in particular the pigmentary disturbances) WS I has been suggested to be the human equivalent of the mouse *Sp* mutation (Foy et al., 1990; Asher and Friedman, 1990). The human homolog to mouse *Pax-3* has been proposed to be the *HuP2* gene, based on amino acid sequence homology and common genomic exon/intron organization (Goulding et al., 1991). Although *HuP2* has yet to be mapped in humans, a chromosome 2q localization would make it an attractive candidate gene for WS I.

Although the incidence of WS I in the general population is very low ($1\text{-}2/10^5$, Arias and Mota 1978), neural tube defects, in the form of spina bifida and anencephaly, are some of the more common congenital malformations (combined incidence of 1/1000 live births; Edmonds and James, 1990) in humans. This high frequency has been attributed to both environmental and genetic factors (Copp et al., 1990), the mechanisms of which are not well understood. We would like to suggest that in view of our findings in a mouse model, modulation of *Pax-3* expression or activity

by genetic or environmental factors may contribute to the etiology of spina bifida and/or anencephaly in humans.

Experimental Procedures

Mice

The Sp^{2H} and Sp^{r} mouse mutants were obtained as heterozygotes from the MRC Radiobiology Unit, Chilton (Harwell), England. The original mice were recovered among the progeny of a (C3H/HeH X 101/H) F1 male, in the case of Sp^{2H} and female in the case of Sp^{r}, after exposure to 6 Gy X-irradiation. The *Sp* mouse mutant was kindly provided by Dr. D. Trasler, (Department of Biology, McGill University). The C3H/HeJ inbred mouse strain was obtained from the Jackson Laboratory (Bar Harbor, ME). The 101/OR inbred mouse strain was kindly provided by Dr. E. Rinchik (Oak Ridge National Laboratory, Oak Ridge, TE). Homozygous day 14 *Sp/Sp* and Sp^{2H}/Sp^{2H} embryos were generated by brother/sister mating of the respective heterozygotes. Homozygosity of the embryos was confirmed by the presentation of a neural tube defect (exencephaly, spina bifida, or both). A panel of interspecific backcross hybrids consisting of 253 (C57BL/6J X *Mus spretus*) F1 X C57BL/6J animals was generated by breeding (C57BL/6J X *Mus spretus*) F1 females with C57BL/6J males. Inbred *Mus spretus* (Spain) and C57BL/6J mice were obtained from Dr M. Potter (NIH, Bethesda, MD), and the Jackson Laboratory (Bar Harbor, ME), respectively. Genetic linkage in these backcross mice was determined by segregation analysis. Gene order was deduced by minimizing the number of crossovers between the different loci within the linkage group and the recombination frequencies were calculated as described (Schurr et al., 1990).

Construction and isolation of cDNAs :

For RNA isolation, day 13 C3H/HeJ and day 14 homozygous Sp^{2H}/Sp^{2H} embryos were obtained by cesarian section, quickly frozen on carbonic ice, homogenized with a mortar and pestle, and dissolved in a solution containing 6M guanidinium hydrochloride. RNA was further purified by sequential ethanol precipitations, as previously described (Chirgwin et al., 1981). cDNA synthesis was carried out using as templates either 2 μg of polyadenylated RNA from embryonal carcinoma P19 cells induced to differentiate by treatment with retinoic acid (10^{-7} M, 48 hours), or 5μg of total cellular RNA from day 13 C3H/HeJ and homozygous day 14

Sp^{2H}/Sp^{2H} embryos. Specific *Pax-3* cDNAs were created using either one of two sequence specific oligonucleotide primers (100 ng each), 5'GCTTAAGCATGCCTCCAGTTC3' (position 1809-1789, primer **d**) or 5'CCTCGGTAAGCTTCGCCCTCTG3' (position 1078-1057, primer **b**). The primer/RNA mixture was first incubated 5 mins at 65°C, then cooled to 37°C, followed by addition of enzyme and further incubation at 37°C for 90 mins. The reaction conditions for cDNA synthesis were 0.1M Tris (pH 8.3), 0.01M $MgCl_2$, 0.14M KCl, 0.02M beta-2 mercaptoethanol, 0.001M deoxyribonucleotides triphosphates, 90 U of placental RNAse inhibitor (RNA guard, Pharmacia), and 100 U of MMLV reverse transcriptase (Amersham). cDNAs were purified by phenol/ether extractions, ethanol precipitation, and dissolved in water. *Pax-3* cDNAs were then amplified by the polymerase chain reaction (PCR). Briefly, cDNA amplification was carried out using primer **b** or **d** (3' end) and either one of the two following sequence specific 5' end oligonucleotide primers: 5' GGTTGGGATCCTGACTCAAG 3' (position 84-103, primer **a**), 5' CAGAGGGCGAAGCTTACCGAGG 3' (position 1057-1078, primer **e**). Parameters for PCR amplification were 1 min at 94°C, 1 min at 60°C, and 2 mins at 72°C for thirty cycles, followed by a final extension for 10 mins at 72°C, under experimental conditions suggested by the supplier of Taq polymerase (BIO CAN, Montreal, Canada). The *Pax-3* cDNAs were analyzed by electrophoresis on a 2% agarose, purified, digested simultaneously with Hin DIII (position +1066) and Bam H I (position +89), and cloned in the corresponding sites of the bacterial plasmid pGem7Zf$^+$. Three independent clones carrying *Pax-3* cDNAs from either wild type or Sp^{2H}/Sp^{2H} mutants were obtained and their nucleotide sequence determined by the dideoxy chain termination technique of Sanger (1977), using modified T7 polymerase (Pharmacia).

PCR amplification of genomic DNA

High molecular weight genomic DNA was isolated from day 13 C3H/HeJ and day 14 homozygous Sp^{2H}/Sp^{2H} and *Sp/Sp* embryos according to a standard protocol, using proteinase K treatment and serial phenol and chloroform extractions (Schurr et al., 1990). *Pax-3* genomic DNA fragments overlapping nucleotides +952 to +1078 of the cDNA were isolated from homozygous *Sp/Sp* and Sp^{2H}/Sp^{2H} mutants, as well as

heterozygous $Sp^{2H}/+$, C3H/HeJ, and 101/OR control mice by PCR amplification. Sequence specific oligonucleotide primers b and c (5' CAGCGCAGGAGCAGAACCACCTTC 3', position 952-975) were used as amplimers and the parameters for PCR were 1 min at 94°C, 1 min at 60°C , 1 min at 72°C for twenty-five cycles, followed by a final extension period of 10 min at 72°C. Amplified genomic *Pax-3* fragments were analyzed by electrophoresis on a 10% non-denaturing polyacrylamide gel in TBE buffer (0.09M Tris, 0.09M boric acid, 0.001M EDTA pH 8.0). In some experiments nucleotide sequence of the amplified fragment was determined directly by sequencing the PCR product.

Southern Hybridization

Genomic DNA was digested to completion with a 10-fold excess (10 Units/µg DNA) of restriction endonucleases, according to the conditions suggested by the supplier (Pharmacia). Five micrograms of restricted genomic DNA was electrophoresed in 1% agarose gels containing TAE buffer (40mM Tris-acetate, 20mM sodium acetate, and 20mM EDTA, pH 7.6) and transferred by capillary blotting onto nylon membranes (Hybond-N, Amersham). The membranes were prehybridized for 16h and then hybridized with ^{32}P-radiolabeled DNA probes (specific activity, 5 x 10^8 cpm/ mcg DNA) for 16 h at 42°C in 50% formamide, 5xSSC, 1% SDS, 10% dextran sulfate, 20mM Tris pH 7.5, 1x Denhardt's solution, and 200 µg/ml sonicated denatured salmon sperm DNA. The membranes were washed to a final stringency of 0.1xSSC, 0.5% SDS at 65°C for 30 minutes, and exposed to XAR-film (Kodak) at -80 °C with an intensifying screen for 16-72 h. The *Pax-3* gene copy number detected in the $Sp^r/+$ heterozygote and in the C3H/HeJ parental strain was determined by quantifying the hybridization signals with a laser densitometer (LKB/Pharmacia). Corrections for the amounts of DNA loaded on the gel and transferred to the hybridization membranes were made for each lane by quantifying the hybridization signal of a control single copy cDNA probe encoding the beta 2 subunit of the Na, K^+ ATPase (*Atpb2*).

Acknowledgements

The authors are indebted to Drs D. Trasler (McGill University), and E. Rinchik (Oak Ridge National Laboratories, TE) for the generous gift of *Sp* and 101/OR animals, respectively. The authors also wish to thank Drs M. Featherstone, G. Pelletier, A. Veillette, S. Vidal, P. Lepage, and D. Malo for critical comments on this work. This work was supported by grants to PG and MV from the Medical Research Council of Canada. PG is supported by a career award from the Fonds de la Recherche en Santé du Québec (FRSQ), and DE by a studentship from the FRSQ.

References

Arias, S., and Mota, M. (1978). Current status of the ABO-Waardenburg syndrome type 1 linkage. Cytogenet. Cell Genet. *22*, 291-294.

Asher, J. H. Jr., Morell, R., and Friedman, T. B. (1991). Waardenburg syndrome (WS): The analysis of a single family with a WSI mutation showing linkage to RFLP markers on human chromosome 2q. Am. J. Hum. Genet. *48*, 43-52.

Asher, J. H. Jr., and Friedman, T. B. (1990). Mouse and hamster mutants as models for Waardenburg syndromes in humans. J. Med. Genet. *27*, 618-626.

Auerbach, R. (1954). Analysis of the developmental effects of a lethal mutation in the house mouse. J. Exp. Zool. *127*, 305-329.

Balling, R., Deutsch, U., and Gruss, P. (1988). *undulated*, a mutation affecting the development of the mouse skeleton, has a point mutation in the paired box of *Pax-1*. Cell *55*, 531-555.

Beechey, C. V., and Searle, A. G. (1986). Mutations at the *Sp* locus. Mouse News Letter *75*, 28.

Bopp, D., Burri, M., Baumgartner, S., Frigerio, G., and Noll, M. (1986). Conservation of a large protein domain in the segmentation gene *paired* and in functionally related genes of Drosophila. Cell *47*, 1033-1040.

Bopp, D., Jamet, E., Baumgartner, S., Burri, M., and Noll, M. (1989). Isolation of two tissue-specific *Drosophila* paired box genes, *Pox meso* and *Pox neuro*. EMBO J. 8, 3447-3457.

Burri, M., Tromvoukis, Y., Bopp, D., Frigerio, G., and Noll, M. (1989). Conservation of the paired domain in metazoans and its structure in three isolated human genes. EMBO J. 8, 1183-1190.

Chalepakis, G., Fritsch, R., Fickenscher, H., Deutsch, U., Goulding, M., and Gruss, P. (1991). The molecular basis of the *undulated/Pax-1* mutation. Cell 66, 873-884.

Chirgwin, J. M., Przybyla, A. A., MacDonald, R. J., and Rutter, W. J. (1979). Isolation of biologically active ribonucleic acid from sources enriched in ribonuclease. Biochemistry *18*, 5294-5306.

Copp, A. J., Brook, F. A., Estibeiro, J. P., Shum, A. S. W., and Cockfort, D. L. (1990). The embryonic development of mammalian neural tube defects. Progress in Neurobiology *35*, 363-403.

Deutsch, U., Dressler, G. R., and Gruss, P. (1988). *Pax-1*, A member of a paired box homologous murine gene family, is expressed in segmented structures during development. Cell *53*, 617-625.

Dickie, M. M. (1964). New splotch alleles in the mouse. J. Hered. *55*, 97-101.

Dressler, G. R., Deutsch, U., Chowdhury, K., Nornes, H. O., and Gruss, P. (1990). *Pax2*, a new murine paired-box-containing gene and its expression in the developing excretory system. Development *109*, 787-795.

Edelman, G. M. (1986). Cell adhesion molecules in the regulation of animal form and tissue pattern. Ann. Rev. Cell Biol. *2*, 81-116.

Edmonds L. D., and James, L. M. (1990). Temporal trends in the prevalence of congenital malformations at birth based on the Birth Defects Monitoring Program, United States, 1979-1987. MMWR *39(SS-4)*, 19-23.

Epstein D. J., Malo, D., Vekemans, M., and Gros, P. (1991). Molecular characterization of a deletion encompassing the splotch mutation on mouse chromosome 1. Genomics *10*, 89-93.

Evans, E. P., Burtenshaw, M. D., Beechey, C. V., and Searle, A. G. (1988). A splotch locus deletion visible by Giemsa banding. Mouse News Letter *81*, 66.

Foy, C., Newton, V., Wellesely, D., Harris, R., and Read, A. (1990). Assignment of the locus for Waardenburg syndrome type I to human chromosome 2q37 and possible homology to the splotch mouse. Am. J. Hum. Genet. 46, 1017-1023.

Franz, T. (1989). Persistent truncus arteriosus in the splotch mutant mouse. Anat. Embryol. *180*, 457-464.

Franz, T. (1990). Defective ensheathment of motoric nerves in the splotch mutant mouse. Acta Anat. *138*, 246-253.

Goulding, M. D., Chalepakis, G., Deutsch, U., Erselius, J., and Gruss, P. (1991). Pax-3, a novel murine DNA binding protein expressed during early neurogenesis. EMBO J. *10*, 1135-1147.

Hirsch, M-R., Gaugler, L., Deagostini-Bazin, H., Bally-Cuif, L., and Goridis, C. (1990). Identification of positive and negative regulatory elements governing cell-type-specific expression of the neural cell adhesion molecule gene. Mol. Cell. Biol. *10*, 1959-1968.

Ishikiriyama, S., Tonoki, H., Shibuya, Y., Chin, C., Harado, N., Abe, K., and Niikawa, N. (1989). Waardenburg syndrome type I in a child with de novo inversion (2)(q35q37.3). Am. J. Med. Genet. 33, 505-507.

Jostes, B., Walther, C., and Gruss, P. (1990). The murine paired box gene, Pax-7, is expressed specifically during the development of the nervous and muscular system. Mech. Dev. 33, 27-38.

Kessel, M., and Gruss, P. (1990). Murine developmental control genes. Science
249, 374-379.

Kissinger, C. R., Liu, B., Martin-Blanco, E., Kornberg, T., and Pabo, C. O. (1990) Crystal structure of an engrailed homeodomain-DNA complex at

2.8 Å resolution: A framework for understanding homeodomain-DNA interactions. Cell 63, 579-590.

LeDouarin, N. (1980). Migration and differentiation of neural crest cells. Curr. Top. Dev. Biol. *16*, 31-85.

Malo, D., Schurr, E., Levenson, R., and Gros, P. (1990). Assignment of Na, K-ATPase b2-subunit gene (Atpb-2) to mouse chromosome 11. Genomics 6, 697-699.

Malo, D., Schurr, E., Epstein, D. J., Vekemans, M., Skamene, E., and Gros, P. (1991). The host resistance locus *Bcg* is tightly linked to a group of cytoskeleton-associated protein genes that include villin and desmin. Genomics *10*, 356-364.

McKusick, V., A. (1990). Mendelian inheritance in man, ninth ed. Johns Hopkins University Press, Baltimore, pp 976.

Moase, C. E., and Trasler, D. G. (1989). Spinal ganglia reduction in the splotch-delayed mouse neural tube defect mutant. Teratology *40*, 67-75.

Moase, C. E., and Trasler, D. G. (1990). Delayed neural crest cell emigration from *Sp* and Sp^d mouse neural tube explants. Teratology *42*, 171-182.

Moase, C. E., and Trasler, D. G. (1991). N-CAM alterations in splotch neural tube defect mouse embryos. Development (In press).

Morrissey, D., Askew, D., Raj, L., and Weir, M. (1991). Functional dissection of the *paired* segmentation gene in *Drosophila* embryos. Genes and Dev. 5, 1684-1696.

Nornes, H. O., Dressler, G. R., Knapik, E. W., Deutsch, U., and Gruss, P. (1990). Spatially and temporally restricted expression of *Pax2* during murine neurogenesis. Development *109*, 797-809.

Olson, E., Edmondson, D., Wright, W. E., Lin, V. K., Guenet, J-L., Simon-Chazottes, D., Thompson, L. H., Stallings, R. L., Schroeder, W. T., Duvic, M., Brock, D., Helin, D., and Siciliano, M. J. (1990). Myogenin is in an evolutionarily conserved linkage group on human chromosome 1q31-q41 and unlinked to other mapped muscle regulatory factor genes. Genomics 8, 427-434.

Plachov, D., Chowdhury, K., Walther, C., Simon, D., Guenet, J-L., and Gruss, P. (1990). *Pax8*, a murine paired box gene expressed in the developing excretory system and thyroid gland. Development *110*, 643-651.

Russell, W. L. (1947). Splotch, a new mutation in the house mouse *Mus musculus*. Genetics *32*, 107.

Sanger, F., Nicklen, S., and Coulson, A. R. (1977). DNA sequencing with chain-terminating inhibitors. Proc. Natl. Acad. Sci. USA *74*, 5463-5467.

Schleif, R. (1988). DNA binding by proteins. Science *241*, 1182-1187.

Schurr, E., Skamene, E., Forget, A., Chu, M., and Gros, P. (1990). Mapping of *Col3a1* and *Col6a3* to proximal murine chromosome 1 identifies conserved linkage of structural protein genes between murine chromosome 1 and human chromosome 2q. Genomics *8*, 477-486.

Skow, L. C., Donner, M. E., Huang, S-M., Gardner, J. M., Taylor, B. A., Beamer, W. G., and Lalley, P. A. (1988). Mapping of mouse gamma crystallin genes on chromosome 1. Bioch. Genet. *26*, 557-570.

Snell, G. D., Dickie, M. M., Smith, P., and Kelton, D. E. (1954). Linkage of loop-tail, leaden, splotch, and fuzzy in the mouse. Heredity *8*, 271-273.

Steel, K. P., and Barkway, C. (1989). Another role for melanocytes: their importance for normal stria vascularis development in the mammalian ear. Development *107*, 453-463.

Treisman, J., Harris, E., and Desplan, C. (1991). The paired box encodes a second DNA-binding domain in the paired homeo domain protein. Genes and Dev. 5, 594-604.

Figure 1a

Chromosomal assignment of *Pax-3* in relation to 8 other loci spanning the proximal portion of mouse chromosome 1. Intergene distances (cM) are indicated to the right of the wild type chromosome 1, and the deleted segment in the $Sp^r/+$ heterozygote is shown to the left. Bottom panel shows a Southern blot analysis of genomic DNA from the $Sp^r/+$ heterozygote and the C3H/HeJ parental control digested with Taq I and probed with cDNAs corresponding to *Pax-3* and a control hybridization standard, the beta 2 subunit of the Na, K-ATPase (*Atpb 2*). The number beneath the lanes represents the ratio of hybridization signals (C3H/HeJ: $Sp^r/+$), as determined by laser densitometry.

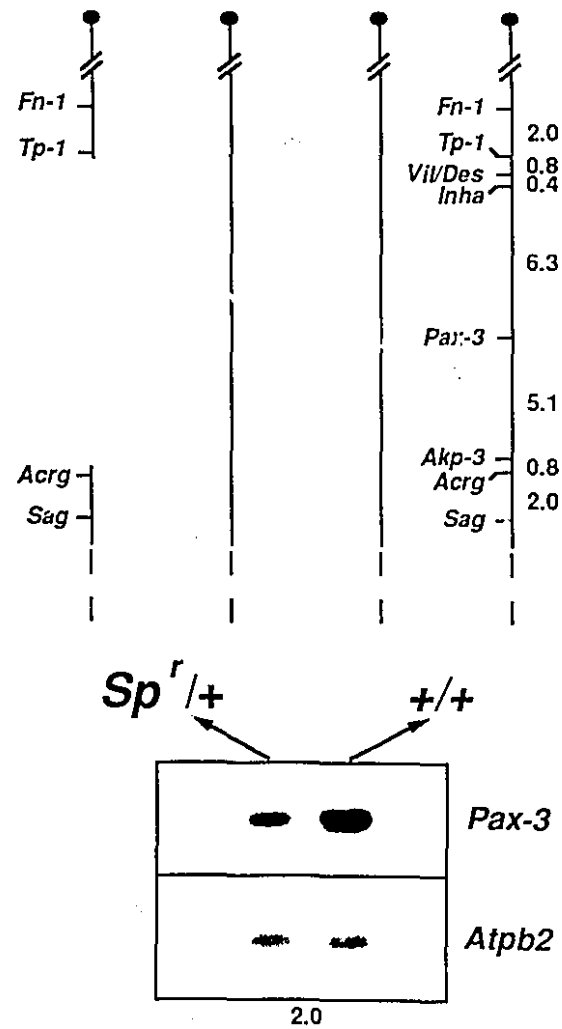
Fn-1
Tp-1
Acrg
Sag
Fn-1
Tp-1
Vil/Des
Inha
Pax-3
Akp-3
Acrg
Sag
2.0
0.8
0.4
6.3
5.1
0.8
2.0
Sp r /+
+/+
Pax-3
Atpb2
2.0

Figure 1b

Haplotype analysis of 9 loci on mouse chromosome 1 in interspecific (*Mus spretus* X C57BL/6J)F1 X C57BL/6J hybrids. Each column represents a chromosomal haplotype for the loci tested. Inheritance of a C57BL/6J allele (open box) or a (*M. spretus* X C57BL/6J)F1 allele (closed box) for the tested loci is indicated. The number of backcross mice for each haplotype is listed at the bottom of each column. Analysis of all loci except for *Pax-3* has been previously reported (Schurr et al., 1989; 1990; Malo et al., 1991).

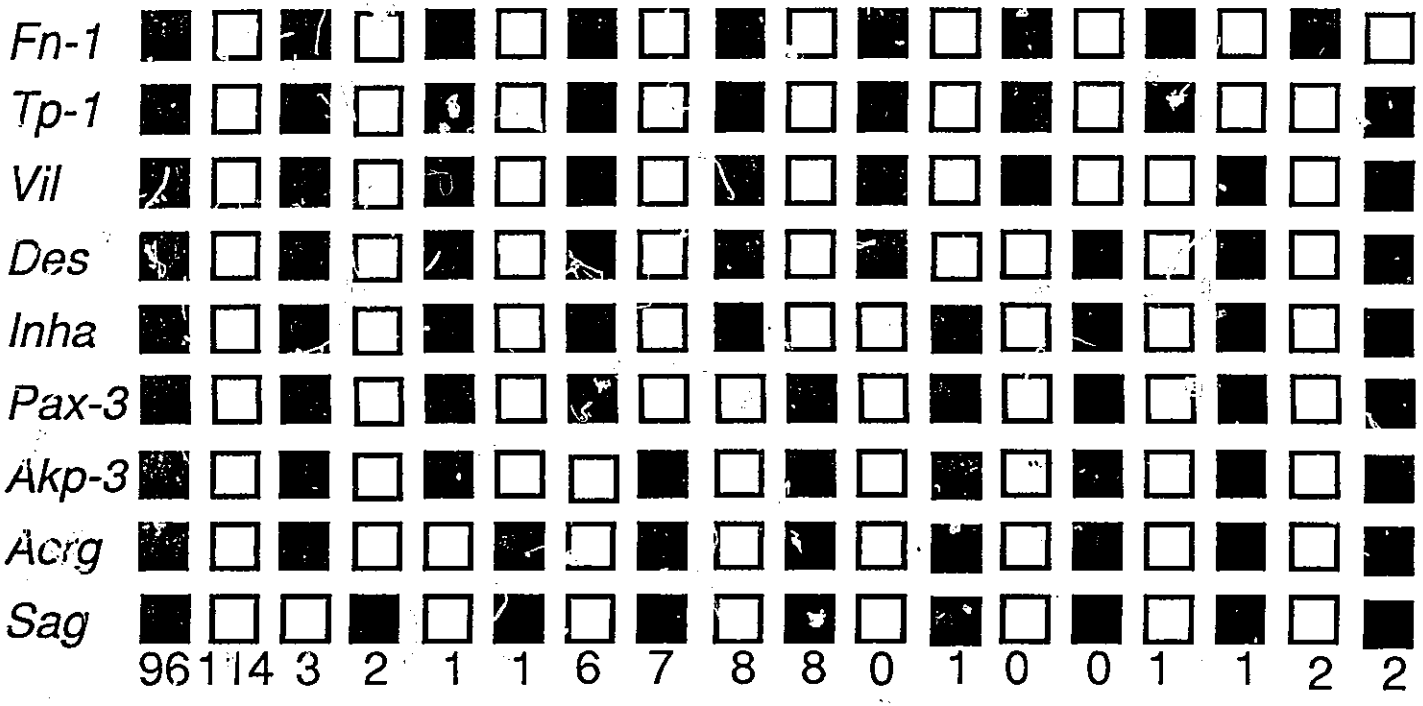
Fn-1
Tp-1
Vil
Des
Inha
Pax-3
Akp-3
Acrg
Sag
96 1 14 3 2 1 1 6 7 8 8 0 1 0 0 1 1 2 2

Figure 2

Southern blots of Taq I digested genomic DNA from *Sp/Sp* (lane 1); Sp^{2H}/Sp^{2H} (lane 2); $Sp^{r}/+$ (lane 3); C3H/HeJ (lane 4); and 101/OR (lane 5) mice hybridized with *Pax-3* cDNA subfragments derived from either the 5' segment (**A**, position +84 to +1078) or the 3' segment (**B**, position +1057 to +1809) of the *Pax-3* mRNA (exposure time, 16hrs). A prolonged exposure (72 hours) of the 0.6 kb *Pax-3* hybridizing band is boxed. Size of hybridizing *Pax-3* fragments are given in kilobase pairs (kb).

A

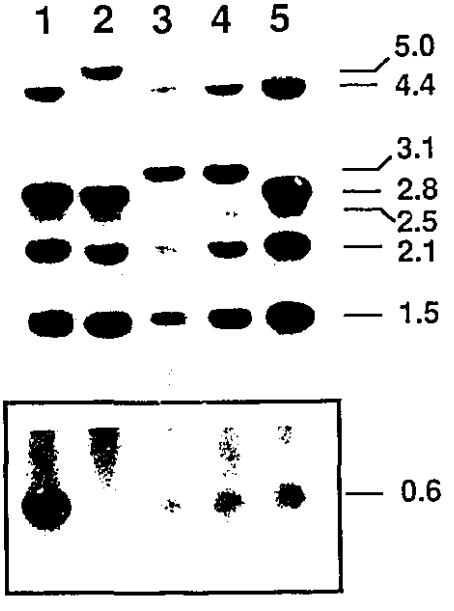

B

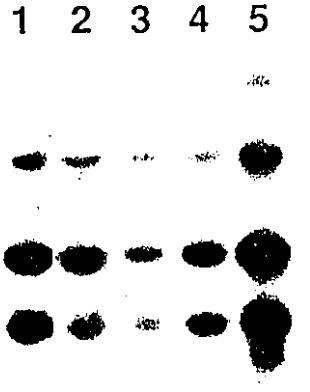

Figure 3

Analysis of *Pax-3* cDNAs from Sp^{2H}/Sp^{2H} and C3H/HeJ embryos.

(A) A partial segment of the *Pax-3* cDNA is shown at the top. Solid line represents the 5' untranslated region. Striped and black boxes represent the paired box and paired homeobox, respectively. Position of primers used for cDNA (a and b) and genomic (b and c) PCR amplification are indicated by lines with arrow heads. The positions of internal Taq I sites (T) are shown, and the deleted Taq I site in the Sp^{2H}/Sp^{2H} mutant is identified ($\dot{T}$). The nucleotide and predicted amino acid sequences surrounding the Taq I restriction site at position +1010, within the paired homeobox, is shown for C3H/HeJ and Sp^{2H}/Sp^{2H} mice. The dashed line within the Sp^{2H}/Sp^{2H} DNA sequence corresponds to the deleted segment and the created TAG termination codon is underlined.

(B) Agarose gel (2% in TBE buffer) electrophoresis of Taq I digested *Pax-3* cDNA (overlapping nucleotides +84 to +1078) amplified from Sp^{2H}/Sp^{2H} (lane 1) and C3H/HeJ (lane 2) RNA. Size of DNA fragments given in base pairs (bp).

(C) Acrylamide gel (10% in TBE buffer) electrophoresis of PCR amplified genomic DNA from C3H/HeJ (lane 1); 101/OR (lane 2); $Sp^{2H}/+$ (lane 3); Sp^{2H}/Sp^{2H} (lane 4); and *Sp/Sp* (lane 5) mice using primers (b and c) overlapping the Taq I site at position +1010 of the *Pax-3* gene. Size of DNA fragments given in base pairs (bp).

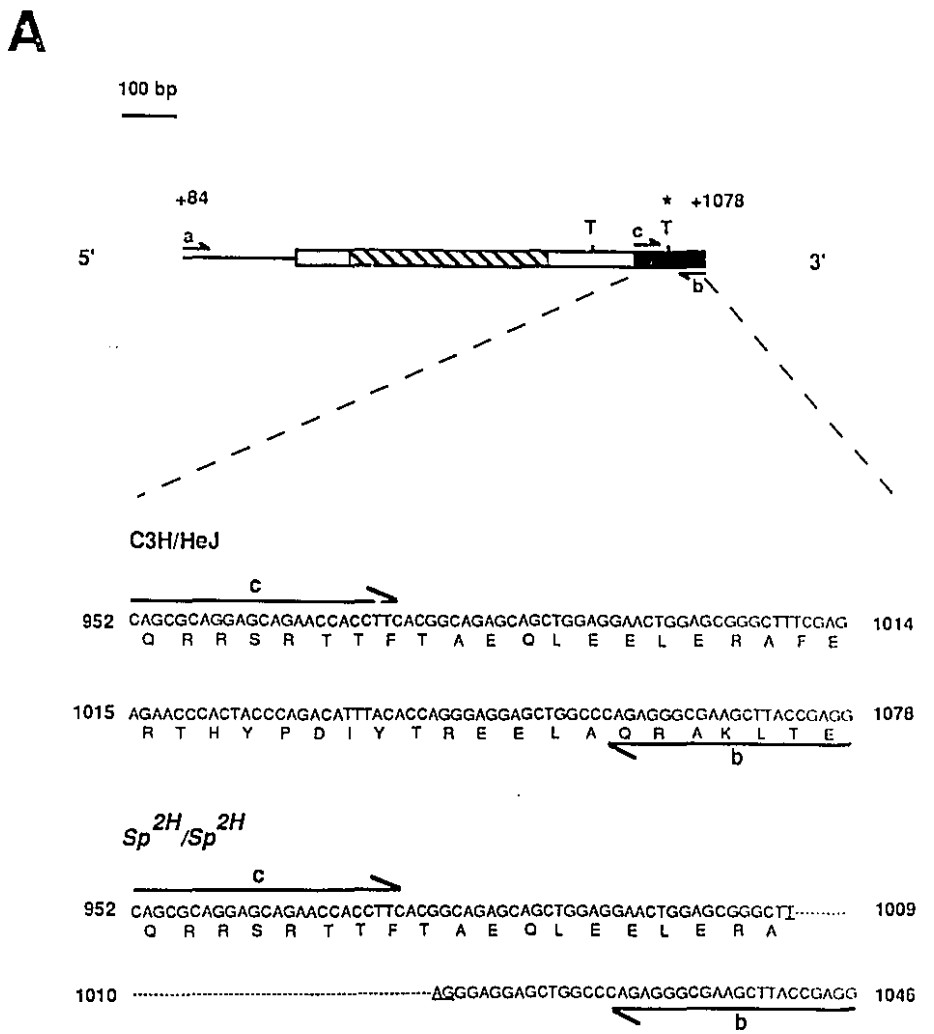
A
100 bp
+84
* +1078
T
c
T
a
5'
3'
b
C3H/HeJ
c
952 CAGCGCAGGAGCAGAACCACCTTCACGGCAGAGCAGCTGGAGGAACTGGAGCGGGCTTTCGAG 1014
Q R R S R T T F T A E Q L E E L E R A F E
1015 AGAACCCACTACCCAGACATTTACACCAGGGAGGAGCTGGCCCAGAGGGCGAAGCTTACCGAGG 1078
R T H Y P D I Y T R E E L A Q R A K L T E
b
Sp2H/Sp2H
c
952 CAGCGCAGGAGCAGAACCACCTTCACGGCAGAGCAGCTGGAGGAACTGGAGCGGGCTI..... 1009
Q R R S R T T F T A E Q L E E L E R A
1010 .....AGGGAGGAGCTGGCCCAGAGGGCGAAGCTTACCGAGG 1046
b
B
1 2
776
186
150
68
C
1 2 3 4 5
127
95

Figure 4

Homozygous Sp^{2H}/Sp^{2H} (**A**), and wildtype littermate (**B**), embryos at day 14 of gestation.

A

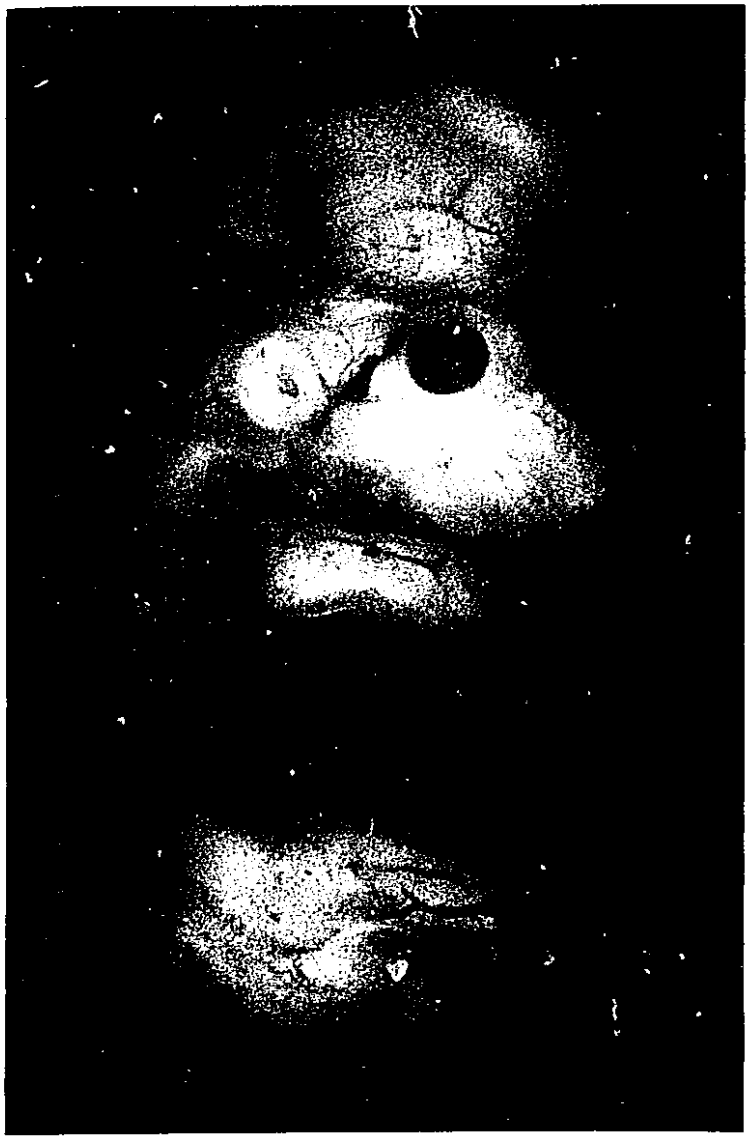

B

Chapter 4

A Mutation Within Intron 3 of the *Pax-3* Gene Produces Aberrantly Spliced mRNA Transcripts in the *splotch* (*Sp*) Mouse Mutant.

Abstract

The *splotch* (*Sp*) mouse mutant displays defects in neural tube closure in the form of exencephaly and spina bifida. Recently, mutations in the *Pax-3* gene have been described in the radiation-induced Sp^{r} and Sp^{2H} alleles. This led us to examine the integrity of the *Pax-3* gene and its cellular mRNA transcript in the original, spontaneously arising, *Sp* allele. A complex mutation in the *Pax-3* gene including an A to T transversion at the invariant 3' AG splice acceptor of intron 3 was identified in the *Sp/Sp* mutant. This genomic mutation abrogates the normal splicing of intron 3, resulting in the generation of four aberrantly spliced mRNA transcripts. Two of these *Pax-3* transcripts make use of cryptic 3' splice sites within the downstream exon, generating small deletions which disrupt the reading frame of the transcripts. A third aberrant splicing event results in the deletion of exon 4, while a fourth retains intron 3. These aberrantly spliced mRNA transcripts are not expected to result in functional Pax-3 proteins, and are thus responsible for the phenotype observed in the *Sp* mouse mutant.

Introduction

Congenital malformations of the neural tube in the form of spina bifida and anencephaly occur at a rate of approximately 1 per 1000 human live births (1). Both environmental and genetic components have been implicated in the cause of these disorders (2), but to date, no single genes have been identified. Mutant strains of mice showing similar phenotypes to these human conditions have been used to study the normal and aberrant cellular events of neurulation (2). Understanding the basis of these mutations at the molecular level should enable the identification of genes and proteins which participate in the complex cascade of events leading to the development of the mammalian neural tube. The *splotch* (*Sp*) mouse mutant has proven to be a valuable model to study defects in neural tube closure (3). *Sp* is a semi-dominant mutation which maps to chromosome 1 and for which several spontaneously arising and radiation-induced alleles have been identified (4,5). This mutation is characterized in the heterozygous state by a white spotting of the abdomen, tail and feet (6), while homozygous *Sp/Sp* embryos display a pleiotropic phenotype whose predominant features include exencephaly, meningomylocele, spina bifida (6), as well as dysgenesis of neural crest cell derived melanocytes, spinal ganglia (6), Schwann cells (7), and structures of the heart (8) .

The *Pax-3* gene is one of eight members of the murine *Pax* gene family which share a homologous region, the paired box, with the *paired* class of *Drosophila* segmentation genes (9,10). The *Pax* gene family encode DNA binding transcription factors whose expression is restricted to discrete regions of the developing mouse embryo (9). *In situ* hybridization experiments show that *Pax-3* is expressed along the entire dorsal portion of the neural tube, as well as in various regions of the brain and neural crest cell derived structures (11). *Pax-3* has been proposed to be involved in establishing positional identity along the dorso-ventral axis of the developing neural tube (11). We have recently determined that *Pax-3* maps to mouse chromosome 1, does not genetically recombine with *Sp* in 125 intraspecific backcross progeny (12) and is included in the large interstitial deletion of chromosome 1 found in the radiation-induced Sp^{r} allele (13). Moreover, we have identified in another radiation-induced *Sp* allele, Sp^{2H}, a small 32 nucleotide deletion in the *Pax-3* gene which interrupts the reading frame of the mRNA, and causes early

termination of translation within the homeodomain of Pax-3 (13). Taken together, these data show that *Pax-3* and *Sp* are allelic, and point at the critical role of *Pax-3* as a transcription factor in neural development. We have now identified and analyzed the molecular basis of the spontaneously arising *Sp* mutant first described by Russell (14).

Materials and methods

Mice

Heterozygous *Sp/+* mutants on a B6C3 (C57BL/6J x C3H/HeJ) background in addition to the C3H/HeJ and C57BL/6J inbred strains were obtained from the Jackson Laboratory (Bar Harbor, ME). Homozygous day 14 *Sp/Sp* embryos were generated by the mating of two *Sp/+* heterozygotes and homozygosity was confirmed at the time of dissection by the presentation of a neural tube defect (spina bifida, exencephaly, or both).

Preparation and Isolation of cDNAs

RNA isolation from day 14 homozygous *Sp/Sp* embryos and first strand cDNA synthesis were carried out as described (13). Amplification of the 5' and 3' halves of the *Pax-3* cDNA was carried out using pairs of sequence-specific oligonucleotide primers. The 5' half was obtained using a combination of primer a (5'-GGTTGGGATCCTGCACTCAAG-3' position 84-103, according to the previously published *Pax-3* cDNA sequence) (11) and primer b (5'-CCTCGGTAAGCTTCGCCCTCTG-3' position 1078-1057), and the 3' half was obtained using a combination of primer c (5'-CAGAGGGCGAAGCTTACCGAGG-3' position 1057-1078) and primer d (5'-GCTTAAGCATGCCTCCAGTTC-3' position 1809-1789). Parameters for PCR amplification were 1 min at 94°C, 2 min at 60°C, and 3 min at 72°C for 30 cycles, under experimental conditions suggested by the supplier of Taq polymerase (BIO CAN, Montreal, Canada). The *Pax-3* cDNAs were analyzed by electrophoresis on a 1.5% agarose gel, purified, and cloned directly into a dT-tailed (15) pBluescript plasmid (Stratagene). For each discrete *Pax-3* cDNA species detected in *Sp/Sp* embryos, four independent clones were isolated and their nucleotide sequences determined by the dideoxy chain termination technique (16).

PCR amplification of genomic DNA

High molecular weight genomic DNA was isolated from day 14 homozygous *Sp/Sp* embryos and from parental C3H/HeJ and C57BL/6J strains as described (17). *Pax-3* genomic DNA fragments overlapping part of exon 3, intron 3, and part of exon 4 were obtained by PCR amplification using cDNA derived oligonucleotide primers e (5'-

CAGAGACAAATTGCTCAAGGACG-3' position 696-718) and f (5'-GCTTCCTTCCTTTCTAGATC position 827-807). Parameters for PCR were 1 min at 94°C, 1 min at 65°C, and 2 min at 72°C for 30 cycles. Amplified genomic *Pax-3* fragments were analyzed by electrophoresis on a 1% agarose gel, purified, and cloned (15). Four independent clones carrying *Pax-3* genomic fragments from control (C3H/HeJ and C57BL/6J) and mutant (*Sp/Sp*) mice were isolated and the nucleotide sequence of the intron/exon boundaries determined (16).

Results

In order to identify the putative alteration in the *Pax-3* gene which underlies the phenotype of the *Sp* mouse mutant, the integrity of *Pax-3* mRNA expressed in *Sp/Sp* homozygous mice was analyzed. For this, RNA from day 14 wildtype (C3H/HeJ) and *Sp/Sp* embryos was used for cDNA synthesis and PCR amplification of the coding region of *Pax-3*. Fragments corresponding to the 5' half (untranslated region, paired box, octapeptide, and part of the homeobox; position +89 to +1078) and the 3' half (part of the homeobox, and C-terminus; position +1057 to +1809) of the *Pax-3* cDNA were independently amplified from wildtype and *Sp/Sp* RNA using sequence specific primers, and the reaction products were analyzed by agarose gel electrophoresis (Fig. 1). Amplification of the 3' portion of *Pax-3* from wildtype and *Sp/Sp* RNA yielded a single fragment of the expected size of 752 bp. While amplification of the 5' portion of *Pax-3* from both wildtype and *Sp/Sp* RNA yielded the expected 994 bp fragment, two additional and novel fragments with an approximated size of 2000 and 860 bp were identified from *Sp/Sp* RNA. These fragments did not appear to result from artifacts of enzymatic reactions (reverse transcription and PCR amplification), since they were reproducibly detected in independent syntheses involving different *Sp/Sp* embryos (data not shown). These results suggested that the 5' portion of the *Pax-3* mRNA may be altered in multiple fashion in *Sp/Sp* mice.

The nature of these observed alterations was further investigated by cloning and determining the nucleotide sequence of the various *Pax-3* cDNA fragments detected in *Sp/Sp* mice (Fig. 2). The sequence of each fragment was determined in at least four independent clones and compared to that of the wildtype *Pax-3* cDNA previously published (11). The sequencing of four clones carrying the 994 bp insert revealed that this fragment was distinct from the wildtype fragment of the same size, and was in fact composed of two sub-populations harboring small overlapping deletions. Three of these clones contained a small deletion of 4 bp between position +749 and +752 (Fig. 2, *Pax-3*Δ4bp) while one showed a 13 bp deletion between position +749 and +761 (Fig. 2, *Pax-3*Δ13bp). The sequencing of six additional clones carrying the 994 bp insert identified only *Pax-3*Δ4bp and *Pax-3*Δ13bp products, with no clones corresponding to the wildtype *Pax-3* sequence. Interestingly, the 5' deletion breakpoint common to *Pax-3*Δ4bp and *Pax-3*Δ13bp corresponds to the

splice junction between intron 3 and exon 4 in the normal *Pax-3* gene. The deletions in *Pax-3*Δ4bp and *Pax-3*Δ13bp disrupt the reading frame of their respective mRNAs and are predicted to lead to early termination of translation due to a TGA termination codon, located 17 and 8 bp downstream of the deletions, respectively (Fig. 2). The resulting truncated Pax-3 polypeptides would lack part of the paired box, the octapeptide sequence, the homeobox and the entire C-terminal half of the protein.

Nucleotide sequence analysis of the 860 bp cDNA fragment also showed the presence of an internal deletion, in this case a 135 nucleotide segment spanning position +749 to +883 (Fig. 2, *Pax-3*ΔE4). This deleted segment corresponds precisely to the fourth exon of the *Pax-3* gene, suggesting that the 860 bp fragment represents an aberrantly spliced mRNA species. The reading frame of the mRNA is preserved in *Pax-3*ΔE4; however, the predicted protein would lack 45 amino acid residues including the terminal portion of the paired box and the octapeptide motif.

Nucleotide sequencing of the novel 2000 bp *Pax-3* fragment identified in *Sp/Sp* cDNA revealed the presence of 1 kb of additional sequences inserted between position +748 and +749 (Fig. 2, *Pax-3*+I3). While partial sequencing of the 5' end of this inserted segment revealed a putative 5' dinucleotide splicing signal (GTACTG...), the 3' end showed a TG instead of the invariant AG dinucleotide typically found at the acceptor splice site in type 1 mammalian introns (18) (Fig. 2). The inserted segment is predicted to alter the amino acid sequence of the Pax-3 protein downstream of Ser^{150}, resulting in early termination of translation due to an in-frame TAG stop codon 143 nucleotides downstream of the insertion site.

The cDNA fragment amplified from the 3' half of the *Pax-3* transcript was also sequenced, with no observed deviations from the published wildtype *Pax-3* sequence. Taken together, the sequencing of *Pax-3* cDNA fragments from *Sp/Sp* mice failed to detect any intact full length wildtype mRNA transcripts, but identified instead four novel mRNA species harboring three deletions and an insertion at position +748. Since this corresponds to the natural site of intron 3 in the *Pax-3* gene (11), these findings were suggestive of sequence alterations in the gene leading to aberrant splicing of this intron.

To directly analyze putative sequence alterations in intron 3 of the *Pax-3* gene in *Sp/Sp* mice, oligonucleotide primers mapping within exon 3 and exon 4 (Fig. 3) were used to amplify by PCR the genomic fragment

overlapping intron 3 from parental (C57BL/6J and C3H/HeJ) and *Sp/Sp* genomic DNAs. In all cases, 1.2 kb fragments containing 130 bp of coding sequences (derived from exons 3 and 4) flanking a 1.1 kb intronic segment were generated (data not shown), cloned and sequenced (Fig. 3). Analysis of the 5' extremity of intron 3 revealed no nucleotide differences at the consensus splice site between parental and *Sp/Sp* mutant DNA, and showed the same sequence (GTACTG...) found inserted in the *Pax-3*+I3 mRNA species detected by cDNA cloning (Fig. 2). On the other hand, analysis of the 3' extremity of intron 3 showed considerable alteration in the *Sp/Sp* mutant as compared to the wildtype sequence. Specifically, the wildtype sequence of CTTTTCTCCAG (position 749 -11 to -1) was found to be modified to a novel CTTTCGTGTG sequence, which included an A to T transversion at the normally invariant 3' AG splice signal. This mutated sequence was also found at the 3' extremity of the inserted fragment present in *Pax-3*+I3 mRNA species identified by cDNA cloning. These results establish that the 3' consensus splice site of intron 3 in the *Pax-3* gene of *Sp/Sp* mice is mutated, and strongly suggest that this mutation abrogates normal splicing of this intron, thus leading to the aberrantly spliced mRNA products detected by cDNA cloning, and eventually to the generation of nonfunctional Pax-3 polypeptides.

Discussion

The recent identification of genes and gene families which play crucial roles in determining the body plan of the developing mouse embryo has reinstated various mouse mutants as valuable tools for determining the mechanism of action of these genes. Once a phenotype is associated with the alteration of a particular gene, then the gene may be used as an entry point to search for other upstream regulatory or downstream target genes participating in the formation of a particular embryonic structure. In addition, characterizing mutant variants of these genes may provide important clues for the structure/function analysis of the corresponding protein. The identification of similar mutations in the human homologues of these mouse genes by synteny mapping and DNA cloning has also permitted the elucidation of the molecular basis of certain inherited disorders.

One such gene family is the group of sequence related *Pax* genes. Composed of eight members in mice, these genes code for transcription factors expressed almost exclusively in the developing mouse embryo (9,19). All *Pax* genes encode at least one DNA binding domain, the paired domain, which shows homology to the *prd* gene of *Drosophila* (10).The paired domain contains three predicted a helices, the first being necessary and sufficient for DNA binding (20). Some *Pax* genes (*Pax-3, 4, 6, 7*) code for an additional DNA binding domain, the homeodomain (19). The paired domain of Pax-1 and the paired and homeo domains of Pax-3 bind *in vitro* to distinct but overlapping sequences within a target promoter (11,21). In addition, *Pax-1, 2, 3, 7,* and *8* contain a conserved octapeptide motif of unknown function (19). Finally, the C-terminal half of Pax proteins is rich in Ser/Pro/Thr residues, a characteristic shared with trans-activating domains of other transcription factors (22).

Mutations in the *Pax-1* (23) and *Pax-6* (24) genes have been shown to be responsible for the defects in eye and vertebral column development caused by the *Sey* and *un* mouse mutants, respectively. Recently, we have demonstrated that a small 32 nucleotide deletion within the homeodomain of the *Pax-3* gene underlies the defects in neural tube closure characteristic of the radiation-induced Sp^{2H} allele of the *Sp* mutant (13). Interestingly, mutations in the human counterparts of *Pax-3* and *Pax-6* were subsequently detected in Waardenburg syndrome type I (25,26,27) and aniridia (28), two

human conditions sharing phenotypic similarities with the *Sp* and *Sey* mutants, respectively. These results clearly point to the importance of *Pax* genes in mammalian development. In order to gain further insight into the important structural and functional determinants of Pax proteins in general, and Pax-3 in particular, we have identified the molecular basis of the spontaneously arising *Sp* allele (14).

Complementary and genomic DNA cloning of *Pax-3* from *Sp/Sp* mutants identified a sequence variation in intron 3 involving at least five nucleotides, including a one nucleotide deletion and an A to T transversion at the invariant 3' consensus splice site (Figs. 2 and 3). Nucleotide sequencing of the wildtype *Pax-3* allele from a *Sp/+* heterozygote identified the same sequence that was seen in the DNA from the parental strains (C3H/HeJ and C57BL/6J), indicating that this sequence variation was not a strain specific polymorphism but rather a spontaneously arising mutation (data not shown). Proper splicing of intron 3 is completely impaired in *Sp/Sp* embryos resulting in four aberrantly spliced *Pax-3* mRNAs (Fig. 4). Two of these mRNA transcripts make use of cryptic 3' splice sites located 4 (*Pax-3*Δ4bp) and 13 (*Pax-3*Δ13bp) nucleotides into the downstream exon, while another uses the natural 3' splice site within intron 4, deleting intron 3 and all of exon 4 (*Pax-3*ΔE4). Finally, *Pax-3+I3* is an incompletely spliced mRNA retaining all of intron 3 (Fig. 4). The aberrant splicing in three of the four mRNAs (*Pax-3*Δ4bp, *Pax-3*Δ13bp, *Pax-3+I3*) introduces frameshift mutations leading to premature termination of translation due to the use of in-frame termination codons (Fig. 2). These proteins are predicted to lack an intact paired domain, octapeptide motif, homeodomain, as well as the entire carboxy terminal half of the protein, and are not expected to be functional. On the other hand, *Pax-3*ΔE4, the only in-frame *Pax-3* mRNA produced in *Sp/Sp* mutants, can encode an otherwise full length Pax-3 protein, lacking only the 45 amino acids corresponding to exon 4. It would appear then that the deletion of exon 4 is sufficient to abrogate normal Pax-3 function. The first 12 amino acids of exon 4 encode the C-terminal portion of the DNA binding paired domain which contains several residues precisely conserved in other *Pax* genes (29). Another highly conserved segment encoded by exon 4 is the octapeptide motif HSI(A/D)GIL(G/S) (amino acids 186 to 193) which is preserved in several members of the *Pax* and *prd* families (19,30). Although the function of these subdomains has not yet been established, the

preservation of their primary sequence during evolution may underlie preservation of important functional or structural determinants which are disrupted in the *Sp* mutant. Interestingly, deleting the terminal third region of the paired domain (including the third a helix) from the *Drosophila* prd protein did not abrogate DNA binding by the paired domain *in vitro* (20). Although our findings establish that the genetic alteration in *Pax-3* is sufficient to cause the neural tube defect observed in *Sp* mice, the mechanism by which the mutant phenotype is expressed, being either through a loss of function or through gain of a novel but deleterious function, remains unresolved. The observation that both the spontaneously arising *Sp* allele and the radiation-induced Sp^{2H} allele harbor different mutations in *Pax-3* yet present indistinguishable phenotypes, suggests that both mutations result in a comparable loss of Pax-3 function. A similar rationale has been previously proposed to account for the similar phenotypic expression of distinct *Pax-6* mutations underlying independent *Sey* alleles (24), as well as different *PAX-3* mutations affecting various families with Waardenburg syndrome type 1 (27).

The mechanism responsible for multiple nucleotide substitutions and deletion in the *Pax-3* mutation described is unknown but could involve an error in excision repair or base slippage during DNA replication (31). Mutations at the 3' splicing signal of introns from b-globin and *CFTR* genes have also been described in individuals with b-thalassemia (32) and cystic fibrosis (33). However, the unique *Pax-3* splicing mutation described here may provide interesting clues into the process of splice site selection. It has been proposed that normal splice site selection is determined by the local sequence context, based perhaps on the proximity of the AG dinucleotide to the branch site or polypyrimidine tract (34). A second proposal suggests that a simple scanning mechanism recognizes the first AG dinucleotide downstream of the branch point and polypyrimidine tract, irrespective of distance or local sequence context (35). While previous *in vitro* and *in vivo* studies were consistent with the scanning model (36,37,38), our analysis of *Pax-3* mRNAs from *Sp/Sp* mutants supports the former model. First, although the relative abundance of the various *Pax-3* mRNAs detected in *Sp/Sp* embryos is unknown, it is clear that the first AG dinucleotide downstream from the altered splice site is not the only alternative choice of the splicing machinery. Second, it appears that not all downstream AG

dinucleotides can serve as splice acceptor sites, since several are found in exon 4 but only the first two appear to be selected. It is interesting to note that a G nucleotide precedes the first cryptic AG splice site (position +753) since most wildtype acceptor splice sites are preceded by a C or T nucleotide (18). Given that the GAG splice site has been shown to be less efficient as a 3' acceptor (35), this may explain the alternate selection of other downstream 3' splice sites in *Sp* mice. Overall, our findings suggest that disrupting the 3' splice site of intron 3 of *Pax-3* in the *Sp* mutant leads to a competition between a limited number of less efficient downstream splice signals.

References

1. Edmonds L. D., and James, L. M. (1990) MMWR **39(SS-4)**, 19-23.

2. Copp, A. J., Brook, F. A., Estibeiro, J. P., Shum, A. S. W., and Cockfort, D. L. (1990) *Progress in Neurobiology* **35**, 363-403.

3. Moase, C.E., and Trasler, D.G. (1992) *J. Med. Genet.* **29**, 145-151.

4. Dickie M.M. (1964) *J. Hered.* **55**, 97-101.

5. Beechey, C.V., and Searle, A.G. (1986) *Mouse News Letter* **75**, 28.

6. Auerbach, R. (1954) *J. Exp. Zool.* **127**, 305-329.

7. Franz, T. (1990) *Acta Anat.* **138**, 246-253.

8. Franz, T. (1989) *Anat. Embryol.* **180**, 457-464.

9. Kessel, M., and Gruss, P. (1990) *Science* **249**, 374-379.

10. Bopp, D., Burri, M., Baumgartner, S., Frigerio, G., and Noll, M. (1986) *Cell* **47**, 1033-1040.

11. Goulding, M.D., Chalepakis, G., Deutsch, U., Erselius, J., and Gruss, P. (1991) *EMBO J.* **10**, 1135-1147.

12. Mancino, F., Vekemans, M., Trasler, D.G., and Gros, P. (1992) *Cytogen. Cell Genet.* (in press).

13. Epstein, D.J., Vekemans, M., and Gros, P. (1991) *Cell* **67**, 767-774.

14. Russell, W. L. (1947) *Genetics* **32**, 107.

15. Marchuk, D., Drumm, M., Saulino, A., and Collins, F.S. (1991) *Nucleic Acids Res.* **19**, 1154.

16. Sanger, F., Nicklen, S., and Coulson, A.R. (1977) *Proc. Natl. Acad. Sci. USA* **74,** 5463-5467.

17. Sambrook, J., Fritsch, E.F., and Maniatis, T. (1989) *Cold Spring Harbor Press*, Cold Spring Harbor, NY.

18. Mount, S.M. (1982) *Nucleic Acids Res.* **10,** 459-472.

19. Gruss, P., and Walther, C. (1992) *Cell* **69,** 719-722.

20. Treisman, J., Harris, E., and Desplan, C. (1991) *Genes and Dev.* **5,** 594-604.

21. Chalepakis, G., Fritsch, R., Fickenscher, H., Deutsch, U., Goulding, M., and Gruss, P. (1991) *Cell* **66,** 873-884.

22. Tanaka, M., and Herr, W. (1990) *Cell* **60,** 375-386.

23. Balling, R., Deutsch, U., and Gruss, P. (1988) *Cell* **55,** 531-555.

24. Hill, R.E., Favor, J., Hogan, B.L., Ton, C.C.T., Saunders, G.F., Hanson, I.M., Prosser, J., Jordan, T., Hastie, N.D., and van Heyningen, V. (1991) *Nature* **354,** 522-525.

25.Tassabehji, M., Read, A. P., Newton, V.E., Harris, R., Balling, R., Gruss, P., and Strachan, T. (1992) *Nature* **355,** 635-636.

26. Baldwin, C.T., Hoth, C.F., Amos, J.A., da-Silva, E.O., and Milunsky, A. (1992) *Nature* **355,** 637-638.

27. Morell, R., Friedman T.B., Moeljopawiro, S., Hartono, Soewito, and Asher J.H. (1992) *Hum. Mol. Genet.* **1,** 243-247.

28. Jordan, T., Hanson, I., Zaletayev, D., Hodgson, S., Prosser, J., Seawright, A., Hastie, N., and van Heyningen, V. (1992) *Nature Genetics* **1,** 328-332.

29. Walther, C., Guenet, J.-L., Simon, D., Deutsch, U., Jostes, B., Goulding, M., Plachov, D., Balling, R., and Gruss, P. (1991) *Genomics* **11**, 424-434.

30. Burri, M., Tromvoukis, Y., Bopp, D., Frigerio, G., and Noll, M. (1989) *EMBO J.* **8**, 1183-1190.

31. Levinson, G., and Gutman, G.A. (1987) *Mol. Biol. Evol.* **4**, 203-221.

32. Atweh, G.F., Anagnou, N.P., Shearin, J., Forget, B.G., and Kaufman, R.E. (1985) *Nucleic Acids Res.* **13**, 777-790.

33. Guillermit, H., Fanen, P., and Ferec, C. (1990) *Hum. Genet.* **85**, 450-453.

34. Green, M.R. (1991) *Ann. Rev. Cell. Biol.* **7**, 559-599.

35. Smith, C.W.J., Porro, E.B., Patton, J.G., and Nadal-Ginard, B. (1989) *Nature* **342**, 243-247.

36. Aeibi, M., Hornig, H., Padgett, R.A., Reiser, J. and Weissman, C. (1986) *Cell* **47**, 555-565.

37. Ruskin, B., and Green, M.R. (1985) *Nature* **317**, 732-734.

38. Reed, R., and Maniatis, T. (1985) *Cell* **41**, 95-105.

Acknowledgements

This work was supported by grants to PG from the Howard Hughes Medical Institute (HHMI) and to DGT from the Medical Research Council of Canada (MRC). PG is the recipient of a Scientist Award from the Fonds de Recherche en Santé du Québec; DJE and KJV are supported by studentships from the Fonds pour la formation de chercheurs et l'aide à la recherche and HHMI, respectively.

Figure 1

Analysis of *Pax-3* cDNA from wildtype and *Sp/Sp* embryos.

A) Schematic representation of *Pax-3* cDNA showing: untranslated sequences (solid lines), paired box (striped box), octapeptide motif (stippled box), homeobox (filled box), and oligonucleotide primers used for PCR amplification of the 5' (primers a and b) and 3' (primers c and d) halves of the cDNA.

B) Agarose gel electrophoresis of cDNA fragments corresponding to the 5' (lanes 1 and 2) and 3' (lanes 3 and 4) halves of *Pax-3* RNA from wildtype (lanes 1 and 3) and homozygous *Sp/Sp* embryos (lanes 2 and 4). Fragment sizes (left) are in base pairs.

A

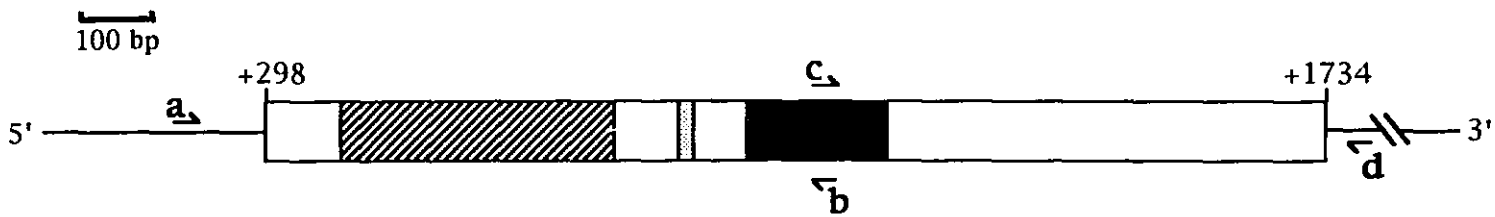

B

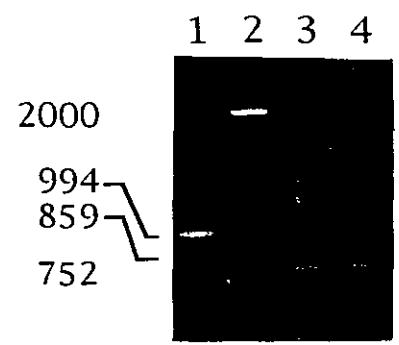

Figure 2

Sequence analysis of wildtype and aberrant *Pax-3* cDNAs from *Sp/Sp* embryos.

A) The nucleotide and predicted amino acid sequence of the 3' extremity of exon 3 (E3), the 5' and 3' extremities of intron 3 (I3) and exon 4 (E4) and the 5' extremity of exon 5 (E5) are shown. The dashed line within the *Pax-3*Δ4bp, *Pax-3*Δ13bp and *Pax-3*ΔE4 show deleted sequences. In-frame termination codons are identified (*). Functional domains in the cDNA are as described in Figure 1.

B) Autoradiograms of DNA sequences of *Pax-3* cDNAs from wildtype and *Sp/Sp*. The 3' end of exon 3 is indicated with an arrow.

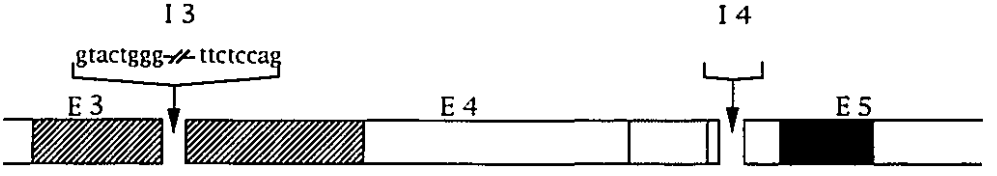

Pax 3 (+745) TCAG TGAGTTCTATCAGCCGCATCCTGAGG-//-GAGCGAG CCTCTGCACCTCAG (+897)
S V S S I S R I L R E R A S A P Q

Pax 3 Δ4bp TCAG- - - -TTCTATCAGCCGCATCCTGA
S V L S A A S *

Pax 3 Δ13bp TCAG- - - - - - - - - - - - - -CCGCATCCTGA
S A A S *

Pax 3 ΔE 4 TCAG- -//- - - - - - - - -CCTCTGCACCTCAG
S A S A P Q

Pax 3 +I 3 TCAGgtactggg -//- tag -//- cgtgtgTGAGTTCTA
S G T G *

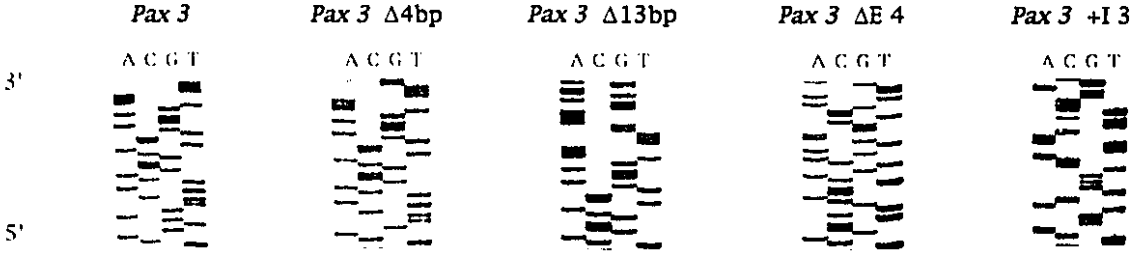

Figure 3

Sequence analysis of intron 3 of the *Pax-3* gene from wild type and *Sp/Sp* genomic DNA.

A) Partial nucleotide sequence of exons 3 and 4 (E3 and E4) and intron 3 (I3) of *Pax-3* from wildtype (C3H/HeJ) and homozygous *Sp/Sp* genomic DNA. Underlined sequence in *Sp/Sp* DNA identifies the altered 3' splice site.

B) Autoradiograms of DNA sequences showing the 3' splice site of intron 3 from wildtype and *Sp/Sp* DNA. The region of sequence divergence between wildtype and *Sp/Sp* is indicated with arrows.

A

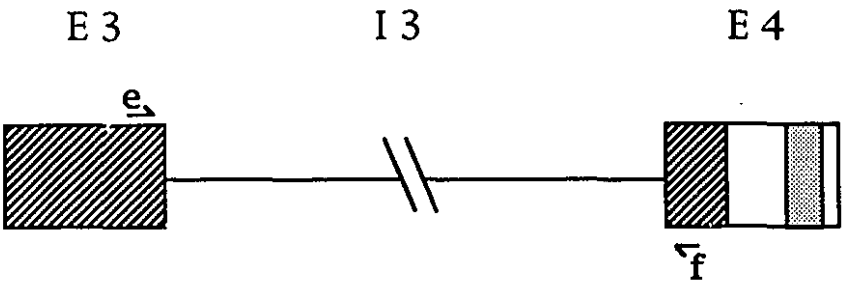

WT ...CCTCAG gtactgggtccatt...cctcttttctccag TGAGTT...

Sp/Sp ...CCTCAG gtactgggtccatt...cctcttt_cgtgtg TGAGTT...

B

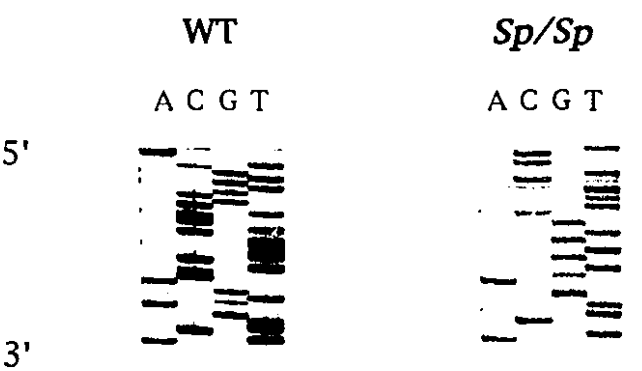

Figure 4

Schematic representation of normal and aberrant splicing of the *Pax-3* gene in wildtype and *Sp/Sp* mice. The five previously defined exons of *Pax-3* are boxed and numbered 1 to 5. Introns are represented by a solid line and splicing events involving exons 3, 4 and 5 are depicted for wildtype and *Sp/Sp* mRNAs. The unspliced intron 3 in the *Pax-3*+I3 splice form is represented as a dotted box. Nucleotide positions in the cDNA are according to Goulding *et al* (11). Functional domains within the *Pax-3* gene are as described in Figure 1.

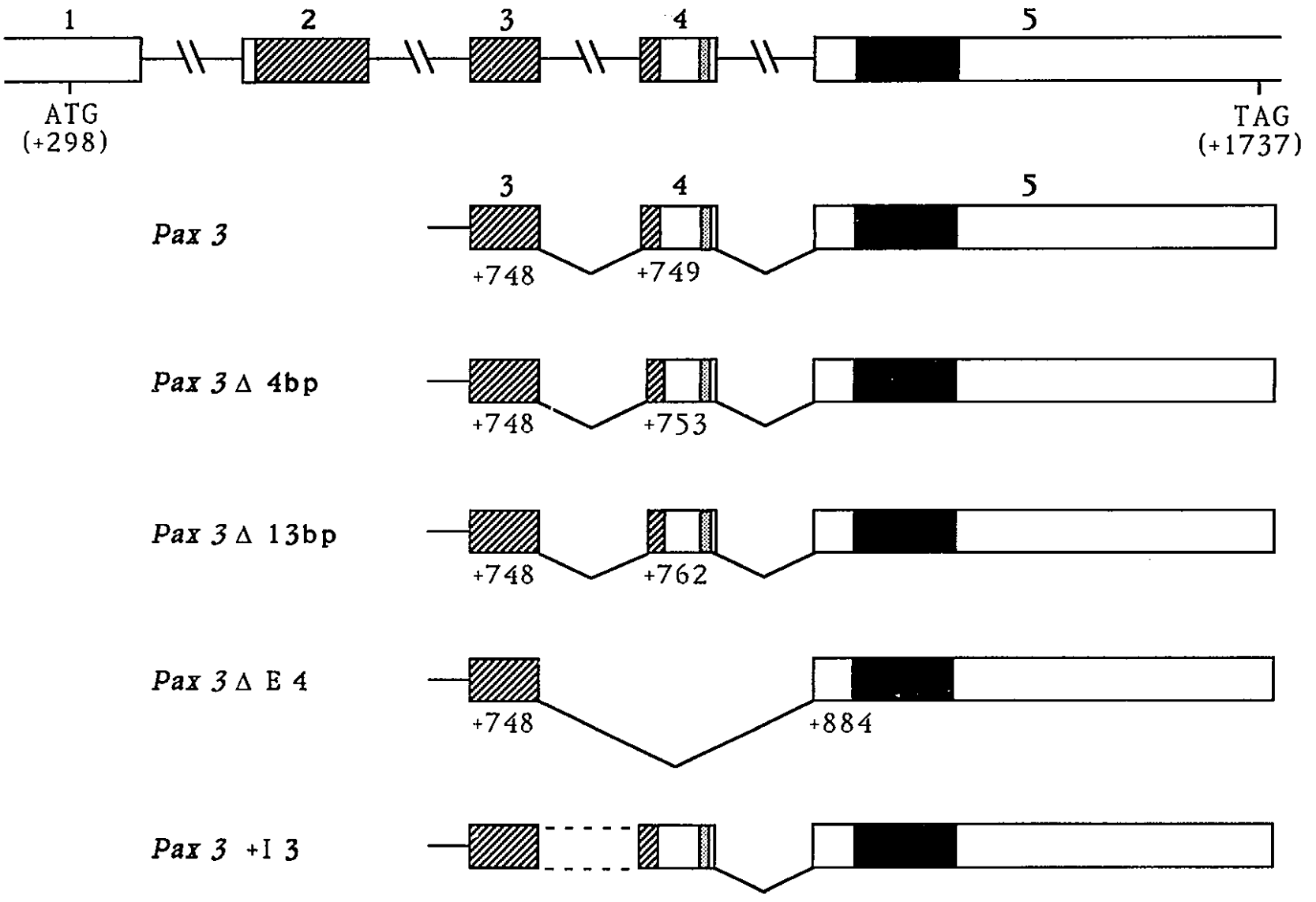
1
2
3
4
5
ATG
(+298)
TAG
(+1737)
3
4
5
Pax 3
+748
+749
Pax 3 Δ 4bp
+748
+753
Pax 3 Δ 13bp
+748
+762
Pax 3 Δ E 4
+748
+884
Pax 3 +I 3

Chapter 5

Characterization of a region specific library of microclones in the vicinity of the *Bcg* and *splotch* loci on mouse chromosome 1.

Abstract

The proximal portion of mouse chromosome 1 harbors a variety of mutant loci which have yet to be characterized at the molecular level. We have constructed a library of genomic DNA fragments from the proximal portion of mouse chromosome 1 by microdissection and microcloning techniques, with the aim of generating genetic markers in close proximity to some of these mutant loci. In order to facilitate the genetic mapping of 27 microclones from this library, we divided a 56 cM segment of chromosome 1 between the *Col3a1* and *Ren 1,2* genes into eight intervals defined by anchor loci. Restriction fragment length polymorphisms were determined for each of the microclones and their segregation with the anchor loci was followed in informative animals from a panel of 252 interspecific backcross mice (C57BL/6J x *Mus spretus*) x C57BL/6J. We were able to assign 26 of 27 (96%) randomly selected microclones to each of the defined chromosome 1 intervals. A total of eight microclones mapped within the large interstitial deletion found in the Sp^r mouse mutant. Two of these clones were found to be tightly linked to the host resistance locus *Bcg* and at least one to the neural tube defect mutant *splotch*. Other clones mapped to intervals containing several other mouse mutants. These novel DNA markers should aid in positional cloning strategies presently employed to identify these mutant loci. These clones should also be useful in the creation of both physical and YAC contiguous maps of the proximal portion of mouse chromosome 1.

Introduction

The cloning of a gene causing a hereditary disease based on its chromosomal localization (positional cloning) requires *a priori* that the disease be assigned to a particular chromosome by either genetic means (linkage analysis) or by the fortuitous finding of a chromosomal aberration (deletion, inversion, etc.) at or near the site of the disease locus. Once this is accomplished an array of molecular markers flanking the disease locus is required to help define the minimal genetic and physical limits of the region surrounding the gene. Only after the delineation of a candidate region can strategies involving yeast artificial chromosome (YAC) cloning and identification of transcription units be effectively applied towards the ultimate aim of isolating the disease gene of interest.

We have undertaken a positional cloning approach towards the identification of two mouse mutant genes mapping to the proximal portion of chromosome 1, namely the host resistance locus (*Bcg*) and *splotch* (*Sp*). Two alleles at the *Bcg* locus confer either resistance or susceptibility to infection with a variety of intracellular pathogens (Gros *et al.*, 1981). The *Sp* mouse is a neural tube closure mutant with additional defects in neural crest cell derivatives (Moase and Trasler, 1992). In order to define the proximal and distal limits of the *Bcg* and *Sp* candidate regions the proximal segment of mouse chromosome 1 had to be saturated with molecular markers. A highly efficient and rapid method for the generation of such markers involves the creation of genomic libraries from specific chromosomal regions using microdissection and microcloning techniques. These strategies have been successfully employed to generate band specific libraries from: *Drosophila* polytene chromosomes (Scalenghe *et al.*, 1981; Garza *et al.*, 1989; Johnson, 1990); mouse metaphase chromosomes in proximity to the *t* complex (Röhme et al., 1984), proximal region of the X chromosome (Fisher et al., 1985), germ line HSR (Weith et al., 1987), albino locus (Tönjes et al., 1991); as well as human chromosomes in the vicinity of various disease loci such as, Langer-Giedion syndrome (Lüdecke et al., 1989), neuroblastoma (Martinsson *et al.*, 1989), Prader-Willi syndrome (Buiting et al., 1990), Wilms tumor (Davis et al., 1990), fragile X region (MacKinnon et al., 1990), Neurofibromatosis-2 region (Fiedler et al., 1991), DiGeorge syndrome (Carey et al., 1992), and malignant

melanoma (Guan et al., 1992). Independent clones from these region specific libraries have been used for a multitude of purposes including, linkage analysis, physical mapping, identification of transcription units, as well as the identification of chromosomal rearrangements.

The evident advantages of creating a band specific genomic library using the microdissection and cloning techniques prompted us to generate such a library from the proximal portion of mouse chromosome 1 spanning cytogenetic bands C2-C5. This specific region was targeted because linkage analysis (Schurr et al., 1989a) and deletion studies (Epstein et al., 1991a) had previously assigned the *Bcg* and *Sp* loci to this region. In this report, we present the description and preliminary characterization of this library including the interval mapping data for 26 microclones to the proximal portion of mouse chromosome 1.

Materials and Methods

Mice

C57BL/6J mice were purchased from the Jackson Laboratory (Bar Harbor, ME). *Mus spretus* (Spain) mice were a generous gift of M. Potter (NIH, Bethesda, MD). Rb(1.18) 10Rma mice were kindly provided by H. Winking (Luebeck, FRG). The interspecific backcross progeny (C57BL/6J x *Mus spretus*) F1 x C57BL/6J were generated by mating F1 females with C57BL/6J males.

Microdissection and microcloning

Chromosome fragments of metaphase chromosomes were isolated and processed in an oil-chamber under microscopic inspection as described earlier (Weith *et al.*, 1987; Martinsson *et al.*, 1989). Eighty chromatin fragments corresponding to the 1C2-C5 chromosome region were microdissected from non-stained Rb(1.18)10Rma marker chromosomes using phase contrast optics and a deFonbrune micromanipulator. Subsequent molecular cloning of the DNA contained in the chromatin fragments was performed as described by Martinsson *et al.* (1989). Essentially, the DNA was extracted in 0.6 nl of DNA extraction buffer (10mM Tris-HCl, pH 7.6, 1mM EDTA, pH 8, 1% N-laurylsarcosine, 500 µg/µl Proteinase K). After phenolization, the DNA was digested with *Eco RI* at a final concentration of 380 U/µl in a 1.0 nl drop. The resulting restriction fragments were ligated into the *Eco RI* cloning site of the lambda vector NM 1149 (Murray 1983). The ligated material was then used for *in vitro* packaging and infection of C600*hfl* host bacteria (Murray 1983). Recombinant phages were recovered as single plaques after overnight incubation and stored individually in phage storage buffer (Sambrook *et al.*, 1989).

Isolation of microclone inserts

High titer plate lysates (1-5 x 10^{10} PFU/ml) were generated for each of the 296 plaque purified recombinant phages by infecting host strain *Escherichia coli* LE392. Two microliters of phage stock was used directly for amplification of DNA inserts from 172 of these clones by the polymerase chain reaction (PCR), using oligonucleotide primers of sequence (5')-

GCCTGGTTAAGTCCAAGC-(3') and (5')-GAGTATTTCTTCCAGGG-(3'), corresponding to vector sequences flanking the *EcoRI* cloning site (Kuziel and Tucker, 1987). The parameters for PCR were 1 min at 94°C, 1 min at 50°C, and 5 min at 72°C for 20 cycles, followed by a final extension period of 10 min at 72°C. High titer plate lysates from an additional 46 clones were used for the purification of vector DNA by the miniprep method (Sambrook *et al.*, 1989). Inserts were released by digestion with *EcoRI*. Microclone inserts were separated by electrophoresis onto 1% agarose gels containing TBE buffer (0.09 M Tris-borate, 0.002 M EDTA, pH 8) Southern blotted, and screened for the presence of highly repetitive sequences by hybridization with [α-^{32}P]dATP labeled total genomic mouse DNA. Microclone inserts free of highly repetitive sequences were purified by electrophoresis on 1% low-melting agarose gels and used as hybridization probes by labeling to high specific activity (6 x 10^8 cpm/μg) with [α-^{32}P]dATP, using the random primer labeling technique and the Klenow fragment of *Escherichia coli* DNA polymerase 1 (Feinberg and Vogelstein, 1983). Microclone probes containing mildly repetitive sequences were precompeted before hybridization by adding 100 μg of sonicated genomic mouse DNA to the labeled probe, boiling for 10 min, followed by an incubation at 65°C for 1 h.

Southern Hybridization

High molecular weight genomic DNA was isolated from spleens and livers according to a standard protocol (Sambrook *et al.*, 1989). Genomic DNA was digested to completion with a 10-fold excess (10 Units/μg DNA) of restriction endonucleases according to the conditions suggested by the supplier (Pharmacia, Bethesda Research Laboratories). Five micrograms of restricted genomic DNA was electrophoresed in 1% agarose gels containing TAE (40 mM Tris-acetate, 20 mM sodium acetate, and 20mM EDTA, pH 7.6) and transferred by capillary blotting onto nylon membranes (Hybond-N, Amersham). The membranes were prehybridized for 16 h at 65°C in 6x SSC, 0.5% SDS, 5x Denhardt's solution, and 0.2 mg/ml sonicated denatured herring sperm DNA. The membranes were first washed at room temperature in 2x SSC, 0.1% SDS for 20 min, followed by a second wash in 0.5x SSC, 0.1% SDS for 20 min at 65°C, and if necessary, a third wash in

0.1x SSC, 0.1% SDS for 20 min at 65°C. The membranes were exposed to XAR-film (Kodak) at -80°C with an intensifying screen for 16-72 h.

Statistical analysis

Genetic linkage was determined by segregation analysis. Gene order was deduced by minimizing the number of crossovers between the different loci within the linkage group (Green, 1981).

Results

Description of library

To facilitate the identification and dissection of the chromosomal region surrounding cytogenetic bands 1C2-C5, we used the Robertsonian chromosome Rb(1.18) 10 Rma containing a homogeneously staining region (HSR) located between bands 1C5 and D (Traut et al., 1984). This HSR on mouse chromosome 1 which had previously been microdissected (Weith *et al.*, 1989) acted as an excellent marker, lying immediately distal to our target region of interest. The 1C2-C5 region was excised from 80 unstained metaphase chromosomes. The chromosomal DNA was pooled, digested with the restriction enzyme *EcoRI*, and ligated into the dephosphorylated *EcoRI* site of the NM 1149 bacteriophage cloning vector (Murray 1983). A library of 296 clones was generated of which 77% contained detectable inserts. The microclone inserts were recovered by either PCR amplification or digesting the insert from the vector as described in the materials and methods. Table 1 summarizes various properties of this library. The insert size ranged from 0.1 kb to 7.2 kb with an average size of 1.9 kb. The inserts from 129 clones were run on 1% agarose gels, Southern blotted, and tested for the presence of repetitive sequences by their ability to hybridize to [α-^{32}P] dATP-labeled total genomic mouse DNA. Of the 129 inserts, 46 (36%) displayed a positive signal suggestive of the presence of repetitive sequences. From the pool of single copy or mildly repetitive inserts we randomly selected 27, in order to determine their map position. Six of these clones have previously been described (Vidal *et al.*, 1992).

Interval mapping of microclones

We have previously used linkage analysis to map 14 known genes to the proximal half of mouse chromosome 1 in a panel of 253 interspecific (C57BL/6J x *Mus spretus*) x C57BL/6J backcross animals (Schurr *et al.*, 1989a; Schurr *et al.*, 1989b; Schurr *et al.*, 1990., Malo *et al.*, 1991; Epstein *et al.*, 1991b). These DNA markers are dispersed over a genetic distance of approximately 56 cM. In order to facilitate the mapping of 27 recently isolated microclones we have divided the entire linkage group into eight intervals. The boundaries of the intervals were defined by seven of the previously mapped chromosome 1 loci (Table 2). In order to assign a

microclone insert to a particular interval, restriction fragment length polymorphisms (RFLPs) were identified for each of them. The inserts were radioactively labeled and used to probe Southern blots containing genomic DNA from both C57BL/6J and *Mus spretus* mouse strains which had been digested with a variety of restriction enzymes. Table 3 lists the informative restriction endonucleases and corresponding polymorphic genomic DNA fragments detected for each microclone probe.

The segregation of individual microclone inserts was followed in various subsets of the mapping panel shown in Figure 1. Several informative backcross animals with known single or double recombinational events between markers within each of the defined intervals were selected and typed for the strain specific allele of each insert. Each individual backcross animal exhibited either a homozygous C57BL/6J pattern or a heterozygous (*Mus spretus* x C57BL/6J) F1 pattern upon Southern blot hybridization with a particular insert. The segregation of the strain-specific polymorphism for each microclone insert in each backcross animal was compared with the segregation of the seven anchor loci used to define the particular intervals. By minimizing the number of crossovers between a particular insert and the proximal and distal boundary loci of a particular interval we were able to unambiguously assign 26 of the microclone inserts to their respective chromosome 1 intervals (Figure 2). Due to the fact that only subsets of our mapping panel were used for the typing of the various inserts, genetic distances between the markers were not determined. However, in some instances we were able to determine the gene order of these inserts upon the detection of a crossover between two markers within a given interval. To be certain that each insert was indeed segregating on mouse chromosome 1, at least 20 nonrecombinant animals were also typed. Only one insert was found not to segregate with any of the chromosome 1 markers (data not shown).

Discussion

We have undertaken a positional cloning approach towards the identification of two mouse mutant genes, *Bcg* and *Sp* , known to map to the proximal portion of chromosome 1 (Skamene et al., 1982; Snell, 1954). In order to satisfy the initial requirements of a positional cloning strategy, the saturation of the disease gene region with molecular markers, we generated a genomic library from the proximal portion of mouse chromosome 1 by the microdissection and microcloning techniques.

We mapped 26 microclones to eight chromosome 1 intervals by segregation analyses and found them to be spread out over a genetic distance of greater than 56 cM with no apparent bias in their distribution (Fig. 2a). The majority of the microclones (22/26) mapped between the *Col3a1* and *Ren 1,2* loci with an average spacing of 2.5 cM. The intervals between the *Cryg* and *Akp-3* loci (intervals 3, 4, and 5) were the primary targets for microdissection. These intervals correspond to cytogenetic bands C2-C5. Determination of the upper and lower limits for microdissection were based on previous studies which assigned the *Sp* locus to cytogenetic band C4-the chromosomal segment deleted in the Sp^r mouse mutant (Evans *et al.*, 1988)- and the finding that *Bcg* is tightly linked to *Vil* (Schurr *et al.*, 1989a). At the time of microdissection we did not know to which cytogenetic band *Vil* was assigned, therefore, the upper limit for microdissection was taken to be band C2-to which the *Cryg* locus had been assigned (Zneimer *et al.*, 1988) and which was known to map proximal to *Vil* (Schurr *et al.*, 1989a). The C5 band was designated the lower limit because the marker chromosome used for the microdissection procedure contained an HSR which was localized immediately distal to this band (Traut *et al.*, 1984). Slightly more than one third (9/26) of the microclones were found to map within intervals 3-5 (Fig. 2a), indicating that the chromosomal region of interest (bands C2-C5) was well represented in the microdissected library. Judging from the mapping of microclones to intervals proximal to *Cryg* and distal to *Akp-3*, it is apparent that chromosomal material was excised beyond the targeted region as well, during the microdissection process.

As previously stated, the closest known gene marker to *Bcg* is *Vil* (Schurr *et al.*, 1989a). We identified two microclones, *D1McG165*and *D1McG136*, which did not recombine with *Vil* in our panel of 252 backcross

animals (Fig2a). Additional genetic analyses have now shown that *D1McG165* does not recombine with *Bcg* in a total of 1424 meioses tested and that *D1McG136* is located 0.2 cM distal to *Bcg* (Malo *et al.*, 1993a). In addition to their tight genetic linkage *D1McG165* and *D1McG136* have aided in the generation of a physical map surrounding the *Bcg* locus (Malo *et al.*,1993b). The *D1McG165* microclone was positioned 190 kb proximal to *Vil*, while *D1McG136* was found to map at a maximal distance of 800 kb distal to *Vil*. The *D1McG136* microclone has thus defined both the genetic and physical limits immediately distal to the location of the *Bcg* gene. These microclones should assist in the eventual cloning of the *Bcg* gene.

The *Sp* locus has been assigned to the chromosomal segment deleted in the Sp^r mouse mutant (Evans et al., 1988). The *Vil*, *Des*, *Inha*, and *Akp-3* loci are also included in this deletion (Epstein *et al.*, 1991a). Our efforts therefore focused on saturating intervals 4 and 5 (*Vil* to *Akp-3*)with molecular markers in order to further define the genetic and physical region encompassing the *Sp* locus. During the course of this work a candidate gene, *Pax-3*, was described (Goulding *et al.*, 1991) and subsequently determined to be mutated in several alleles of *Sp* (Epstein et al., 1991b, 1993; Vogan et al., 1993). Nonetheless, the description of microclones in the vicinity of *Sp/Pax-3* remains of interest as a strategical approach for positional cloning in general. Six microclones mapped on either side of the *Pax-3* gene, two to interval 4 and four to interval 5 (Fig. 2). One of these microclones, *D1McG156* was found to map 1.2 cM proximal to *Pax-3* (Vidal *et al.*, 1992).

In addition to *Sp* and *Bcg*, the proximal portion of mouse chromosome 1 harbors a variety of mutant loci some of which have yet to be characterized at the molecular level (Fig. 2b). These mutations affect such diverse features as limb development (doublefoot, *dbf*; dominant hemimelia, *dh*), lens development (eye lens obsolescence, *elo*), gait (tumbler, *tb*), as well as pigmentation and texture of the coat (dilute suppressor, *dsu*; leaden, *ln*; fuzzy, *fz*) (Lyon and Searle, 1989). These mouse mutants have been mapped to positions on mouse chromosome 1 which correspond to the same intervals which we have used to assign the various microclones (Seldin *et al.*, 1991) (Fig. 2b). Once again, the microclones isolated from the 1C2-C5 microdissected library should help define the

minimal genetic and physical limits of the regions surrounding the various mutant loci.

As a result of their wide distribution on the proximal portion of mouse chromosome 1, the microclones should also prove useful in the creation of long range physical maps spanning the dissected region. An average spacing between microclones of 2.5 cM (for the 56 cM region separating the *Col3a1* and *Ren1,2* loci) was obtained with the mapping of only a portion of the available single copy inserts found in the microdissected library. We estimate that an additional 118 single copy inserts are readily available for mapping purposes. The remaining clones contain repetitive sequences and make up 36% of the library (Table 1). Microclones containing repetitive sequences may also be used for mapping purposes by either digesting out the repetitive sequence or competing it out with total genomic mouse DNA. When considering the 118 unique sequence inserts, in addition to the 22 we have already mapped (between *Col3a1* and *Ren1,2*) an average spacing of 0.4 cM between microclones should be obtained. Although our panels of backcross animals may not contain enough informative crossovers to order each of the microclones, the interval mapping strategy will allow for the positioning of microclones to distinct segments of chromosome 1. Once the interval mapping of the microclones is accomplished it will be feasible to initiate the ordering of the microclones within their respective intervals by pulse field gel electrophoresis. The eventual goal will be to generate a long range physical map of the entire proximal portion of mouse chromosome 1. Concomitantly, the microclones may easily be converted to sequence tagged sites (STSs) so that they may be employed in screening strategies of YAC libraries (Green and Olson, 1990; Bentley *et al.*, 1992) with the eventual goal of obtaining contiguous YAC clones overlapping the proximal portion of mouse chromosome 1.

Acknowledgements

We are grateful to H. Winking (Luebeck, FRG) for providing Rb(1.18) 10Rma mice. This work was supported by a grant to P.G. from the Howard Hughes Medical Institute. P.G. is a Chercheur Boursier from the Fonds de Recherches en Santé. D.J.E. holds the David Stewart Memorial Fellowship from McGill University.

References

Bentley, D.R., Todd, C., Collins J., Holland, J., Dunham, I., Hassock, S., Bankier, A., and Giannelli, F. (1992). The development and application of automated gridding for efficient screening of yeast and bacterial ordered libraries. Genomics **12:** 534-541.

Buiting, K., Neumann, M., Lüdecke, H.J., Senger, G., Claussen, U., Antich, J., Passarge, E., and Horsthemke, B. (1990). Microdissection of the Prader-Willi syndrome chromosome region and identification of potential gene sequences. Genomics **6:** 521-527.

Carey, A.H., Claussen, U., Lüdecke, H.J., Horsthemke, B., Ellis, D., Oakey, H., Wilson, D., Burn, J., Williamson, R., and Scambler, P.J. (1992). Interstitial deletions in DiGeorge syndrome detected with microclones from 22q11. Mamm. Genome **3:** 101-105.

Davis, L.M., Senger, G., Lüdecke, H.J., Claussen, U., Horsthemke, B., Zhang, S.S., Metzroth, B., Hohenfellner, K., Zabel, B., and Shows, T.B. (1990). Proc. Natl. Acad. Sci. USA **87:** 7005-7009.

Epstein, D.J., Malo, D., Vekemans, M., and Gros, P. (1991a). Molecular characterization of a deletion encompassing the *splotch* mutation on mouse chromosome 1. Genomics **10:**89-93.

Epstein, D.J., Vekemans, M., and Gros, P. (1991b). *splotch* (Sp^{2H}), a mutation affecting development of the mouse neural tube shows a deletion within the paired homeodomain of *Pax-3*. Cell **67:** 767-774.

Epstein, D.J., Vogan, K.J., Trasler, D.G., and Gros, P. (1993). A mutation within intron 3 of the *Pax-3* gene produces aberrantly spliced mRNA transcripts in the splotch (*Sp*) mouse mutant. Proc. Natl. Acad. Sci. USA **90:** 532-536.

Evans, E.P., Burtenshaw, M., Beechey, C.V., and Searle, A. (1988). A *splotch* locus deletion visible by Giemsa banding. Mouse News Lett. **81:** 66.

Feinberg, A.P., and Vogelstein, B. (1983). A technique for radiolabeling DNA restriction endonuclease fragments to a high specific activity. Anal. Biochem. **132:** 6-13.

Fisher, E.M.C., Cavanna, J.S., and Brown, S.D.M. (1985). Microdissection and microcloning of the mouse X chromosome. Proc. Natl. Acad. Sci. USA **82:** 5846-5849.

Fiedler, W., Claussen, U., Lüdecke, H.-J., Senger, G., Horsthemke, B., Van Kessel, A.G., Goertzen, W., and Fahsold, R. (1991). New markers for the Neurofibromatosis-2 region generated by microdissection of chromosome 22. Genomics **10:** 786-791.

Garza, D., Ajioka, J.W., Carulli, J.P., Jones, R.W., Johnson, D.H., and Hartl, D.L. (1989). Physical mapping of complex genomes. Nature **340:**577-578.

Goulding, M.D., Chalepakis, G., Deutsch, U., Erselius, J., and Gruss, P. (1991). *Pax-3*, a novel murine DNA binding protein expressed during early neurogenesis. EMBO J. **10:**1135-1147.

Green, E.D., and Olson, M.V. (1990). Systematic screening of yeast artificial-chromosome libraries using the polymerase chain reaction. Proc. Natl. Acad. Sci. USA **87:** 1213-1217.

Green, E.L. (1981). Breeding systems. *In* "The Mouse in Biomedical Research" (H.L. Foster, J.D. Small, and J.G. Fox, Eds.), p.91, Academic Press, New York.

Gros, P., Skamene, E., and Forget, A. (1981). Genetic control of natural resistance to *Mycobacterium bovis* (BCG) in mice. J. Immunol. `2417-2421.

Guan, X.-Y., Meltzer, P.S., Cao, J., and Trent, J.M. (1992). Rapid generation of region-specific genomic clones by chromosome microdissection: Isolation of DNA from a region frequently deleted in malignant melanoma. Genomics **14:** 680-684.

Johnson, D.H. (1990). Molecular cloning of DNA from specific chromosomal regions by microdissection and sequence-independent amplification of DNA. Genomics **6:** 243-251.

Kuziel, W.A, and Tucker, P.W. (1987). Determination of vector:insert junctions in λgt10 cDNAs that do not recut with *EcoRI*. Nucleotide sequence of the *λimm*434 *HindIII-EcoRI* DNA fragment encoding part of the cI protein. Nucleic Acids Res. **15:** 3181.

Lüdecke, H.J., Senger, G., Claussen, U., and Horsthemke, B. (1989). Cloning defined regions of the human genome by microdissection of banded chromosomes and enzymatic amplification. Nature **338:** 348-350.

Lyon, M.F., and Searle, A.G. (1989). "Genetic variants and strains of the laboratory mouse", 2nd ed., Oxford Univ. Press. London/New York.

MacKinnon, R.N., Hirst, M.C., Bell, M.V., Watson, J.E.V., Claussen, U., Lüdecke, H.J., Senger, G., Horsthemke, B., and Davies, K.E. (1990). Microdissection of the fragile X region. Am. J. Hum. Genet. **47:** 181-187.

Malo, D., Schurr, E., Epstein, D.J., Vekemans, M., Skamene, E., and Gros, P. (1991). The host resistance locus Bcg is tightly linked to a group of cytoskeleton-associated protein genes that include villin and desmin. Genomics **10:** 356-364.

Malo, D., Vidal, S.M., Hu, J., Skamene, E., and Gros, P. (1993a). High resolution linkage map in the vicinity of the host resistance locus *Bcg*. Genomics (Submitted)

Malo, D., Vidal, S.M., Lieman, J.H., Ward, D.C., and Gros, P. (1993b). Physical delineation of the minimal chromosomal segment encompassing the murine host resistance locus Bcg. Genomics (Submitted)

Martinsson, T., Weith, A., Cziepluch, C., and Schwab, M. (1989). Chromosome 1 deletions in human neuroblastoma: generation and fine mapping of microclones from the distal 1p region. Genes, Chromosomes and Cancer **1:** 67-78.

Moase, C.E., and Trasler, D.G. (1992). Splotch locus mouse mutants: models for neural tube defects and Waardenburg syndrome type I in humans. J. Med. Genet. **29:** 145-151.

Murray, N.E. (1983). Phage lambda and molecular cloning. *In* "lambda II" (R.W. Hendrick, J.W., Roberts, F.W., Stahl, and R.A. Weisberg, Eds. pp 395-432. Cold Spring Harbor Press, Cold Spring Harbor, N.Y.

Röhme, D., Fox, H., Herrmann, B., Frischauf, A.-M., Edström, J.-E., Mains, P., Silver, L.M., and Lehrach, H. (1984). Molcecular clones of the mouse *t* complex derived from microdissected metaphase chromosomes. Cell **36:** 783-788.

Sambrook, J., Fritsch, E.F., and Maniatis, T. (1989). "Molecular cloning: A laboratory manual". 2nd edition. Cold Spring Harbor Press, Cold Spring Harbor, NY.

Scalenghe, F., Turco, E., Edström, J.E., Pirotta, V., and Melli, M. (1981). Microdissection and cloning of DNA from a specific region of *Drosophila melanogaster* polytene chromosomes. Chromosoma **82:** 205-216.

Schurr, E., Skamene, E., Forget, A., and Gros, P. (1989a). Linkage analysis of the *Bcg* gene on mouse chromosome 1: identification of a tightly linked marker. J. Immunol. **142:** 4507-4513.

Schurr, E., Henthorn, P.S., Harris, H., Skamene, E., and Gros, P. (1989b). Localization of two alkaline phosphatase genes to the proximal region of mouse chromosome 1. Cytogenet. Cell Genet. **52:** 65-67.

Schurr, E., Skamene, E., Morgan, K., Chu, M.-L., and Gros, P. (1990). Mapping of Col3a1 and Col6a3 to proximal murine chromosome 1 identifies conserved linkage of structural protein genes between murine chromosome 1 and human chromosome 2q. Genomics **8:** 477-486.

Seldin, M.F., Roderick, T.H., and Paigen, B. (1991). Mouse Chromosome 1. Mamm. Genome **1:** S1-S17.

Skamene, E., Gros, P., Forget, A., Kongshavn, P.A.L., St-Charles, C., and Taylor, B.A. (1982). Genetic regulation of resistance to intracellular pathogens. Nature **297:** 506-509.

Snell, G.D., Dickie, M.M., Smith, P., and Kelton, D.E. (1954). Linkage of loop-tail, leaden, splotch, and fuzzy in the mouse. Heredity **8:** 271-273.

Tönjes, R.R., Weith, A., Rinchik, E.M., Winking, H., Carnwath, J.W., Kaliner, B., Paui, D. (1991). Microclones derived from the mouse chromosome 7 D-E bands map within the proximal region of the c^{14coS} deletion in albino mutant mice. Genomics **10:** 686-691.

Traut, W., Winking, H., and Adolph, S. (1984). An extra segment in chromosome 1 of wild *Mus musculus*: a C-band positive homogeneously staining region. Cytogenet. Cell Genet. **38:** 290-297.

Vidal, S.M., Epstein, D.J., Malo, D., Weith, A., Vekemans, M., and Gros, P. (1992). Identification and mapping of six microdissected genomic DNA probes to the proximal region of mouse chromosome 1. Genomics **14:** 32-37.

Vogan, K.J., Epstein, D.J., Trasler, D.G., and Gros, P. (1993). The splotch-delayed (Sp^d) mouse mutant carries a point mutation within the paired box of the *Pax-3* gene. Genomics (Submitted)

Weith, A., Winking, H., Brackman, B., Boldyreff, B., and Traut, W. (1987). Microclones from a mouse germ line HSR detect amplification and complex rearrangements of DNA sequences. EMBO J. **6:**1295-1300.

Zneimer, S.M., and Womack, J.E. (1988). Regional localization of the fibronectin and gamma crystallin genes to mouse chromosome 1 by in situ hybridization. Cytogenet. Cell Genet. **48:** 238-241.

Table 1

Properties of the 1C2-C5 library.

Dissected region	1C2-C5
Number of chromosomes dissected	80
Number of independent clones	296
Proportion of clones with inserts	196/253 (77%)
Average size of clones	1.9 kb (0.1 kb - 7.2 kb)
Proportion of repetitive clones	46/129 (36%)
Clones used for mapping	27
Proportion of clones mapping to the proximal segment of mouse chromosome 1	26/27 (96%)

Table 2

List of markers used to define eight chromosome 1 intervals. (r) number of recombinants; (n) number of interspecific backcross animals typed for the boundary loci defining the interval. Size of interval is given in centimorgans (cM) with the standard error.

Interval	r	n	Size of interval (cM)
1. - *Col3a1*	-	-	-
2. *Col3a1* - *Cryg*	17	131	13.0 ± 2.94
3. *Cryg* - *Vil*	12	253	4.7 ± 1.33
4. *Vil* - *Pax 3*	17	253	6.7 ± 1.57
5. *Pax 3* - *Akp-3*	13	253	5.1 ± 1.38
6. *Akp-3* - *Col6a3*	7	192	3.6 ± 1.34
7. *Col6a3* - *Ren-1,2*	23	98	23.4 ± 4.27
8. *Ren-1,2* -	-	-	-

Table 3

List of DNA restriction fragment length polymorphisms identified by each of the chromosome 1 specific microclones.

Locus	Insert size (kb)	Enzyme	Fragment size in C57BL/6J DNA (kb)	Fragment size in *M. spretus* DNA (kb)
D1McG26	2.2	*BamH* I	9.4	6.0
D1McG85	1.3	*Taq* I	4.3	5.0
D1McG96	2.1	*Msp* I	3.8	0.8
D1McG98	0.6	*Taq* I	4.3	3.8
D1McG103	2.8	*Msp* I	8.0	2.8
D1McG105	3.0	*Msp* I	11.0	12.0
D1McG107	0.4	*Msp* I	0.8	2.2
D1McG111	0.7	*Msp* I	1.7	2.0
D1McG136	1.1	*Taq* I	12.0	2.5
D1McG154	2.5	*Pvu* II	3.9	3.7
D1McG178	0.6	*Msp* I	8.6	8.4
D1McG182	0.6	*Hind* III	7.8	2.1
D1McG198	0.7	*Taq* I	6.2	5.0
D1McG199	1.6	*Taq* I	12.5	4.3, 6.3
D1McG203	2.1	*Taq* I	1.5	1.6
D1McG206	2.1	*Pvu* II	7.3	7.2
D1McG207	2.2	*Msp* I	2.3	1.7
D1McG208	2.0	*Msp* I	13.5	11.0
D1McG214	0.4	*Hind* III	7.1	8.6
D1McG217	2.0	*Taq* I	1.7	2.0
D1McG240	3.3	*Msp* I	4.2	6.2
D1McG242	1.4	*Msp* I	8.4	8.6

Figure 1

Haplotype analysis of 252 (C57BL/6J x *Mus spretus*) F1 X C57BL/6J backcross progeny for 7 loci on chromosome 1. Each locus tested is listed at the left. Each column represents a chromosomal haplotype identified in the backcross progeny (C57BL/6J x *Mus spretus*) F1 X C57BL/6J. Closed boxes: *Mus spretus* alleles; open boxes: C57BL/6J alleles. The number of backcross mice for each haplotype is listed at the bottom of each column. Haplotypes listed at the far right correspond to proposed double crossovers.

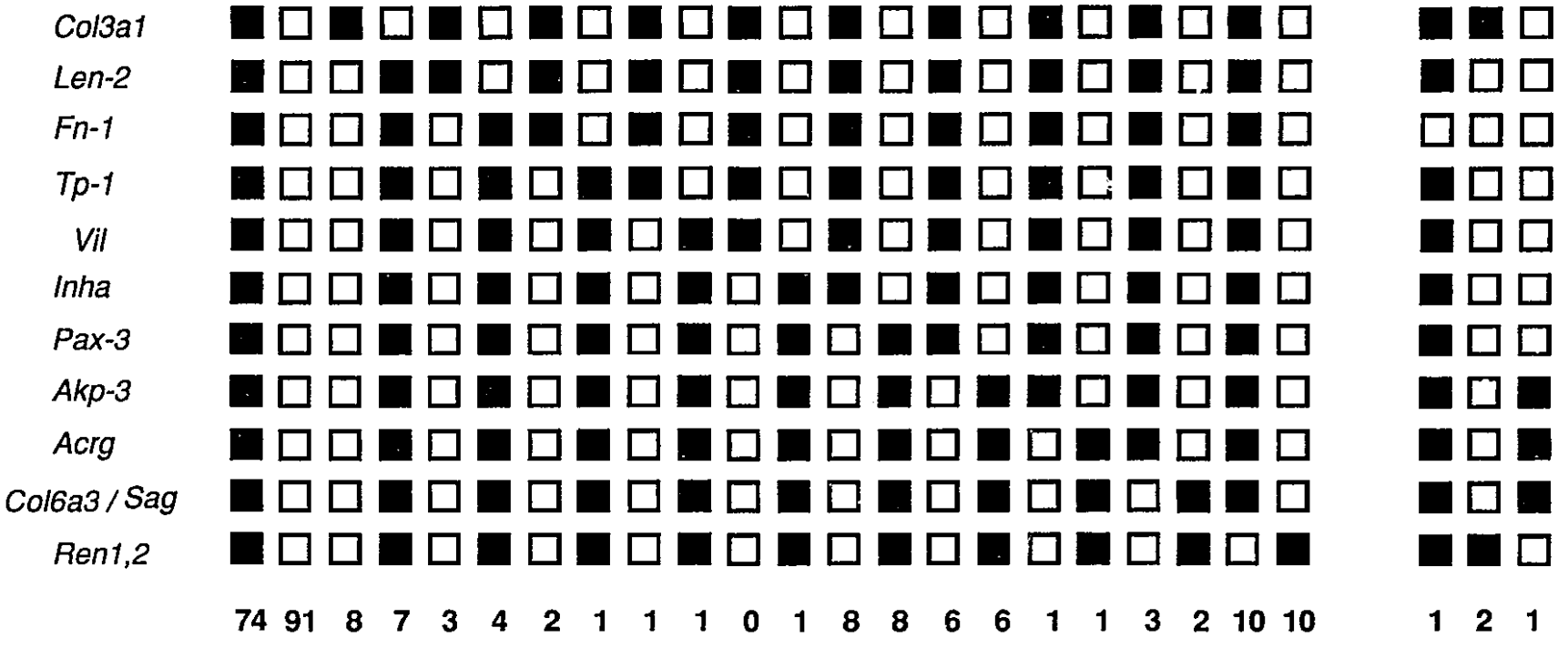
Col3a1
Len-2
Fn-1
Tp-1
Vil
Inha
Pax-3
Akp-3
Acrg
Col6a3 / Sag
Ren1,2
74 91 8 7 3 4 2 1 1 1 0 1 8 8 6 6 1 1 3 2 10 10
1 2 1

Figure 2

A) Interval mapping of 26 microclones on mouse chromosome 1. Eight intervals are defined by the seven marker loci at the right. Each of the microclones listed at the left were positioned by linkage analysis. The * indicates that the microclone could only be mapped between the *Akp-3* and *Akp-4* loci. Genetic distances are in cM.

B) Interval map location of various mouse mutants mapping to the proximal portion of chromosome 1.

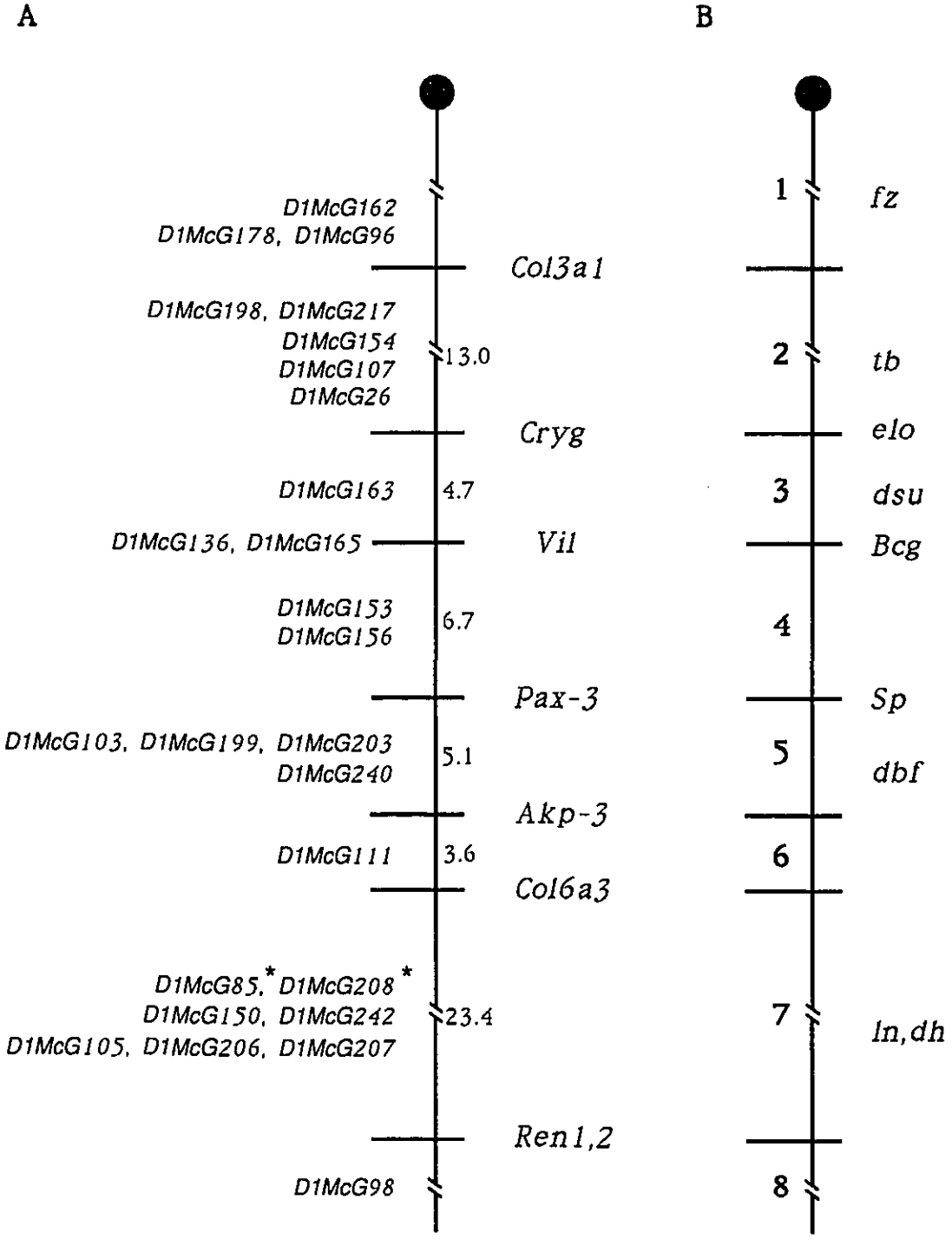
A
B
D1McG162
D1McG178, D1McG96
Col3a1
D1McG198, D1McG217
D1McG154
D1McG107
D1McG26
13.0
Cryg
D1McG163
4.7
D1McG136, D1McG165
Vil
D1McG153
D1McG156
6.7
Pax-3
D1McG103, D1McG199, D1McG203
D1McG240
5.1
Akp-3
D1McG111
3.6
Col6a3
D1McG85,* D1McG208 *
D1McG150, D1McG242
D1McG105, D1McG206, D1McG207
23.4
Ren1,2
D1McG98
1
fz
2
tb
elo
3
dsu
Bcg
4
Sp
5
dbf
6
7
ln,dh
8

Chapter 6

General Discussion

We initiated a positional cloning strategy in order to identify the molecular basis underlying the defects observed in the *Sp* mouse mutant. Armed with a large interstitial deletion on mouse chromosome 1 encompassing several genetic loci including *Sp* (Evans *et al.*, 1988; Epstein *et al.*, 1991a), a region specific library of microdissected clones spanning this chromosomal segment, and a panel of intraspecific backcross animals segregating the *Sp* phenotype (in collaboration with F. Mancino and D.G. Trasler, Department of Biology, McGill University) we set out to define a minimal candidate interval within which the *Sp* gene would be contained (Epstein *et al.*, 1993b). Once a reasonably small genetic and physical interval flanking the *Sp* locus had been delineated, often considered to be 1 cM or the physical equivalent of about 1 million base pairs (Collins 1992), we were prepared to search this candidate region for transcribed sequences. The likelihood of these transcripts being equivalent to the *Sp* gene product would then have been assessed by comparing their individual expression patterns with that of the tissues affected in homozygous *Sp* embryos, in addition to examining the integrity of the candidate transcripts in the various *Sp* alleles.

During the course of this work a candidate gene, *Pax-3*, was described (Goulding *et al.*, 1991) and subsequently determined to be mutated in several alleles of *Sp* (Epstein *et al.*, 1991b, 1993a; Vogan *et al.*, 1993). The spectrum of mutations in the *Pax-3* gene that have been identified in the various *Sp* alleles confirms that *Pax-3* and *Sp* are allelic but more significantly it implicates *Pax-3* as an important regulator of the cascade of events required during the formation of the mouse neural tube. In order to assess the significance of the mutations present in the various *Sp* alleles with respect to important structural and functional determinants of the Pax-3 protein, we attempted to correlate the genetic lesion with the severity of the *Sp* phenotype in a variety of *Sp* alleles.

The severity of the phenotypes of the homozygous *Sp* alleles correlates well with the genetic lesions identified in each of them. The homozygous Sp^r mutant being a preimplantation lethal displays the most severe phenotype of the *Sp* alleles (Beachey and Searle 1986). This phenotype is consistent with the fact that an approximated 30 megabase (the equivalent of 15 cM) segment of mouse chromosome 1 spanning the *Tp-1* to *Acrg* loci (which includes *Pax-3*) is deleted in the Sp^r allele (Epstein

et al., 1991a,b). It is somewhat surprising that such a large deletion is compatible with survival in the heterozygous state given the early embryonic lethality of monosomic mouse embryos; however, other mouse mutants with large deletions have been reported to be viable as heterozygotes (Cattanach *et al.*, 1993).

Phenotypically, the range of defects seen in homozygous *Sp* and Sp^{2H} alleles are virtually identical even though their molecular lesions in *Pax-3* are completely different. Both alleles display exencephaly and spina bifida to varying degrees, show agenic or dysgenic neural crest cell (NCC) derived structures (absence of Schwann cells, persistent truncus arteriosus, and limb musculature defects have yet to be confirmed in the *Sp* allele), and die at approximately day 13 of gestation (Auerbach 1954; Franz 1989, 1990, 1993). At the molecular level the *Sp* allele is characterized by an A to T transversion at position -2 in the third intron of *Pax-3* which abrogates the normal splicing of this intron due to the loss of its natural 3' splice acceptor (Epstein et al., 1993a). Consequently, four aberrantly spliced *Pax-3* mRNA transcripts are generated, three of which result in drastically truncated proteins while the fourth produces an intact protein which lacks the 45 amino acids corresponding to exon 4 (coding for the carboxy terminus of the paired domain and the octapeptide motif). Because the levels of the four aberrantly spliced *Pax-3* mRNA transcripts in the *Sp* allele have yet to be quantified it remains to be determined whether the Pax-3 protein that lacks the carboxy terminus of the paired domain and octapeptide motif retains any function.

The *Pax-3* gene of the Sp^{2H} allele has a 32 nucleotide deletion within the paired-type homeobox. This deletion causes a shift in the reading frame of the *Pax-3* mRNA transcript which results in a premature termination of translation and hence, the production of a Pax-3 protein missing the majority of its homeodomain and putative transcriptional activation domain (Epstein *et al.*, 1991b). Surprisingly, the *Pax-3* gene from the Sp^{1H} allele contains the same 32 nucleotide deletion as that from the Sp^{2H} allele suggesting that the Sp^{1H} and Sp^{2H} mouse mutants are in fact, one and the same (Epstein *et al.*, unpublished results). This finding is comprehendible given that these two alleles arose in successive litters sired by the same male progenitor after being subjected to X-irradiation (Beachey and Searle 1986). Presumably, the mutation occured in a primordial germ cell from which an

abundance of gametes arose and subsequently went on to fertilize eggs upon successive matings.

The fact that the different *Pax-3* mutations detected in homozygous *Sp* and Sp^{2H} embryos produce indistinguishable phenotypes suggests that both mutations result in a comparable loss of Pax-3 function. However, because neither of the *Pax-3* mutations in the *Sp* or Sp^{2H} alleles disturb the first α-helix of the paired domain, which is known to exhibit DNA binding properties (Treisman et al., 1991)(see section 3 of the Literature review), it cannot be ruled out that the homozygous phenotype displayed by these mutants is due, in part, to dominant negative effects exhibited by the truncated Pax-3 proteins. The white belly spot, the semi-dominant feature portrayed in all heterozygous *Sp* alleles, is most likely the result of a gene dosage effect rather than a dominant negative effect because the heterozygous phenotype is the same whether the altered allele is completely deleted (as in the $Sp^{r}/+$ heterozygote) or present in mutant form (as in the *Sp*/+, $Sp^{2H}/+$ and $Sp^{d}/+$ heterozygotes).

Splotch-delayed (Sp^{d}) is the least severe of the *Sp* alleles exhibiting only posterior neural tube defects (although on some genetic backgrounds exencephaly is occassionaly observed, Moase and Trasler 1992), reduced rather than completely absent NCC derived structures, and compared to other *Sp* alleles a delayed death, usually around the time of birth (Dickie 1964; Moase and Trasler 1989). We have recently characterized the molecular defect in *Pax-3* which is responsible for the Sp^{d} phenotype (Vogan *et al.*, 1993). A guanine to cytosine transversion was identified at nucleotide position 421 in *Pax-3* mRNA transcripts (according to the published sequence of Goulding *et al.*, 1991) isolated from homozygous Sp^{d} embryos, resulting in a nonconservative, Gly to Arg, amino acid substitution at position 42 (starting from the initiator Met) which falls within the paired domain. The significance of this amino acid substitution is better understood in context of its location within the Pax-3 protein. Of the 14 amino acids between positions 39 and 52 of the paired domain (N-terminal to the first α-helix), 11 are precisely conserved, including the glycine at position 42, in all paired domain containing proteins of mouse, Drosophila and human (Walther *et al.*, 1991). Treisman *et al* (1991) have proposed that this conserved region might be important for proper folding of the paired domain, while the less conserved α-helical region is required for

DNA binding. Point mutations resulting in amino acid substitutions in this highly conserved region have also been identified in other *Pax* genes, most notably *Pax-1* (Gly to Ser at position 48) and PAX3 (Pro to Leu at position 50; Asn to His at position 47) and are responsible for the phenotypes observed in *undulated* (Balling *et al.*, 1988) Waardenburg syndrome type 1 (WSI) (Baldwin *et al.*, 1992) and Waardenburg syndrome type III (WSIII) (Hoth *et al.*, 1993), respectively. With the aid of secondary structure prediction algorithms it was found that three of the four amino acid substitutions identified in the aforementioned mutants (*Spd/Pax-3*, *un/Pax-1*, WSI/PAX3) would disrupt the formation of predicted β-turns, thus altering the proteins' structures and corresponding functions (Treisman *et al.*, 1991; Hoth *et al.*, 1993; Vogan *et al.*, 1993).

DNAse I protection experiments have shown that a mutant Drosophila paired protein containing the same amino acid substitution as was described for *un* is incapable of footprinting the e5 element of the *eve* promoter (Treisman *et al.*, 1991). Furthermore, the un/Pax-1 mutant protein was shown to have reduced affinity for the e5 sequence compared to wildtype protein in gel shift assays and actually exhibited an altered DNA binding specificity in being able to bind to modified e5 sequences that were only weakly bound by wildtype Pax-1 (Chalepakis *et al.*, 1991). Given the similarities in the *Pax-1* and *Pax-3* mutations in *un* and Sp^d, respectively and their common disruptions of protein structure, it is likely that the Sp^d/Pax-3 mutant protein would also exhibit alterations in its DNA binding properties. The possibility that the Sp^d/Pax-3 protein would retain some of its normal DNA binding properties may explain the less severe phenotype that has been described for this mouse mutant.

Having met the primary objectives set forth at the start of this project, the identification of the *Sp* gene product, attempts were initiated to satisfy the second objective, identification of *Pax-3* mutations in a human disease comparable to that of *Sp*. The proximal portion of mouse chromosome 1 spanning two collagen genes, *Col3a1* and *Col6a3*, represents an approximated 32 cM linkage group syntenic to the distal portion of human chromosome 2q (Schurr *et al.*, 1990). The mapping of *Sp/Pax3* to this region on mouse chromosome 1 suggested that if *PAX3* mutations were causal of a human disease, its phenotype should be segregating with human chromosome 2q markers.

Waardenburg Syndrome type I (WSI) is a dominant disorder characterized by varying degrees of cochlear deafness, pigmentary disturbances of the skin, hair, iris, and the ocular fundus, as well as a lateral displacement of the inner canthi (dystopia canthorum), the presence of which distinguishes WSI from WSII (McKusick 1990). Prompted by the finding of a *de novo* paracentric inversion (2) (q35q37.3) in a child with WSI (Ishikiriyama *et al.*, 1989), several studies showed that some but not all WSI loci were linked to *Fn* and *ALPP*, two genes which map to the distal portion of human chromosome 2q (Foy *et al.*, 1990; Asher *et al.*, 1991; Farrer *et al.*, 1992). The similarities in some of the phenotypic features between *Sp* and WSI (primarily the pigmentary disturbances because *Sp*/+ mice are not deaf (Steel and Smith 1992)), their homologous chromosomal assignments, and our prior knowledge that *Pax-3* was disrupted in all *Sp* mutants, made WSI an excellent candidate for the human homologue of *Sp* and prompted us to investigate whether *PAX3* was altered in these individuals. DNA samples were collected from affected and unaffected members of 25 different families known to be segregating WSI and assessment of the integrity of the *PAX3* gene by single strand conformational polymorphism (SSCP) analysis was carried out. Unfortunately, we were unsuccessful in identifying *PAX3* mutations in individuals with WSI before several such reports appeared in the literature (Tassabehji *et al.*, 1992, 1993; Baldwin *et al.*, 1992; Morell *et al.*, 1992; Tsukomoto *et al.*, 1992; Hoth *et al.*, 1993).

Explanations for our lack of success are as follows. First, recent studies have shown WSI to be a heterogeneous disorder, with only 50% of cases mapping to chromosome 2q (Farrer *et al.*, 1992). It is possible that the WSI families that we screened did not map to chromosome 2q and therefore would not be expected to show mutations in *PAX3*. Second, SSCP analysis is optimal for small (approximately 300 bp) fragments of DNA; accomodating for the size of a typical exon. To amplify the exons of a gene for SSCP analysis, primers are designed to intron sequences flanking the individual exons. At the time when SSCP analysis was being conducted the genomic structure of *PAX3* had not been entirely worked out, making it possible to screen only a portion of the gene (the paired box and a portion of the homeobox) for mutations. It is therefore possible, that mutations may be residing in the unscreened portions of the *PAX3* gene. The third

explanation for our lack of success in identifying PAX3 mutations may have been due to limitations in the technique itself, although this possibility is less likely given the high sensitivity of SSCP (Michaud *et al.*, 1992).

At present, five papers have reported PAX3 mutations in six different pedigrees in which WSI is segregating (Tassabehji *et al.*, 1992, 1993; Baldwin *et al.*, 1992; Morell *et al.*, 1992; Hoth *et al.*, 1993). Each of the affected individuals is heterozygous for the PAX3 mutation, however, no correlation has been made between the severity of the defect (presence or absence of deafness) and the type of mutation. Of the six different PAX3 mutations that have been described in WSI individuals, five have been found in the paired box (Figure 1). Two of these mutations are frameshifts resulting from small deletions (Figure 1)(Morell *et al.*, 1992; Tassabehji *et al.*, 1993). Two of the other mutations, an in-frame 18 bp deletion within the first α-helix of the paired domain and an Arg to Leu amino acid substitution at codon 56 of the paired domain (invariant among all *Pax* genes), are presumed to interfere directly with the paired domain's DNA binding properties (Tassabehji *et al.*, 1992; Hoth *et al.*, 1993). The remaining paired domain mutation causes an amino acid substitution in a highly conserved region N-terminal to the first α-helix, where the *Sp^d* mutation is situated (Figure 1)(Baldwin *et al.*, 1992; Vogan *et al.*, 1993). The last of the defined PAX3 mutations in individuals with WSI also results in a frameshift due to a 2 bp deletion within the conserved octapeptide sequence (Tassabehji *et al.*, 1993).

Of notable interest was the report that some individuals with WSII and WSIII also harbor PAX3 mutations (Figure 1) (Tassabehji *et al.*, 1993; Hoth *et al.*, 1993). Both WSII and WSIII share phenotypic features with WSI, the differences being that dystopia canthorum is absent from WSII and musculoskeletal abnormalities are present in WSIII. Although clinically these syndromes have been defined as distinct, their molecular basis, at least in some cases, appears to be the same. These findings are not inconsistent with the diverse expression profile of *Pax-3* in the mouse. In addition to the dorsal aspect of the neuroepithelium, craniofacial and other NCC derived structures, *Pax-3* is also expressed in dermomyotome cells of the somites as well as the limb bud mesenchyme, two known sources of myogenic precursors (Goulding *et al.*, 1991). It is thus likely that the muscle defects in individuals with WSIII also stem from disturbances in the

Figure 1

Compilation of *PAX3* mutations in individuals with WSI, II, and III and the mouse mutant Sp^d. Numbered arrows point to discrete regions of the PAX3 cDNA which correlate to the described mutation. Codon numbering follows that of the published full length mouse cDNA (Chalepakis et al., 1991) and starts at the initiator ATG. PB, paired box; OP, octapeptide; HB, homeobox. Black boxes within the PB and HB represent predicted α-helices. All mutations have been described elsewhere: 1 (Baldwin *et al.*, 1992); 2 and 8 (Hoth *et al.*, 1993); 3 (Tassabehji *et al.*, 1992); 4 (Morrell *et al.*, 1992); 5, 6, and 7 (Tassabehji *et al.*, 1993); 9 (Vogan *et al.*, 1993).

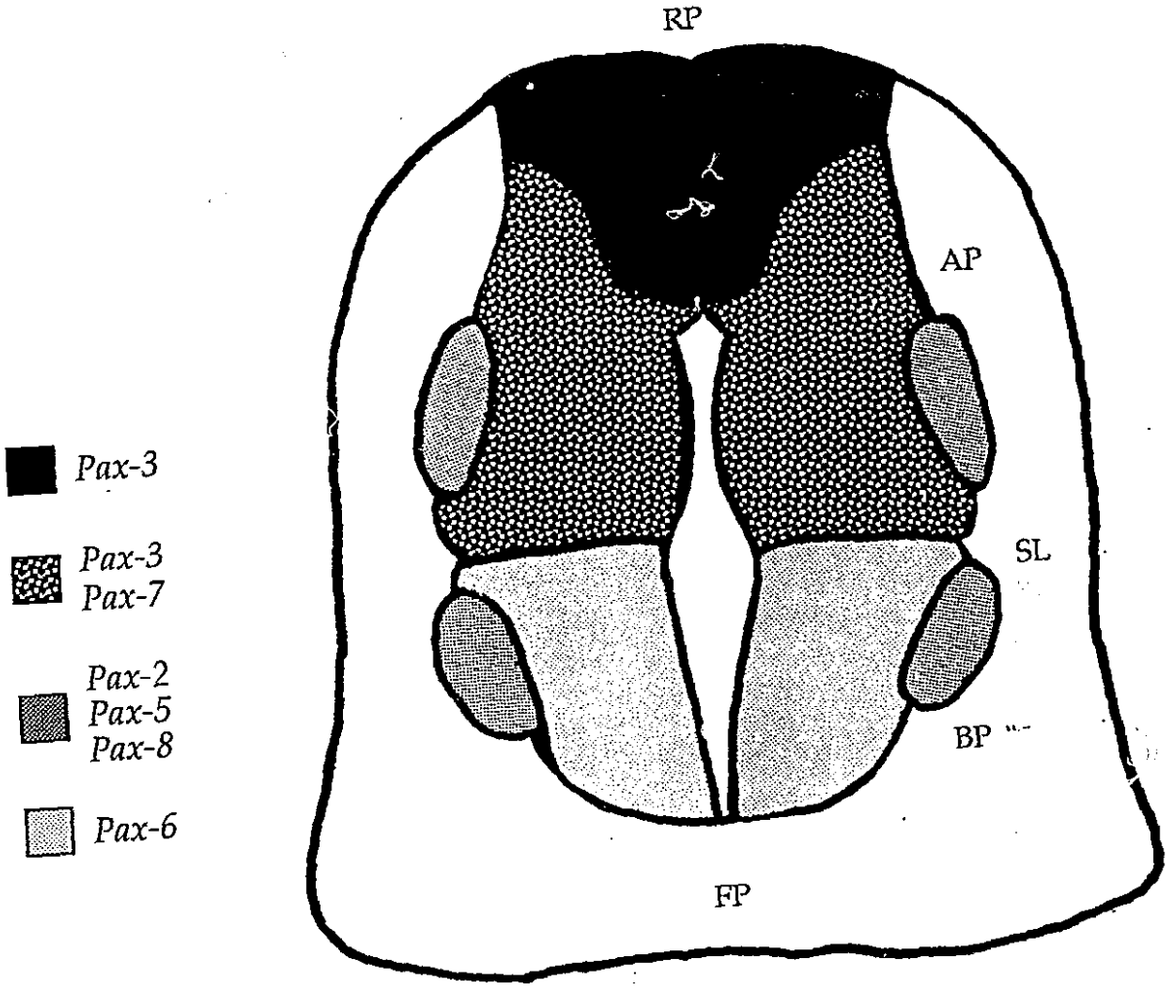
RP
AP
SL
BP
FP
Pax-3
Pax-3
Pax-7
Pax-2
Pax-5
Pax-8
Pax-6

function of Pax-3 during myogenesis. Furthermore, some *Sp* alleles have also been shown to exhibit limb musculature defects (Franz *et al.*, 1993). Why *PAX3* mutations cause defects to these structures in some but not all individuals may eventually be explained by the type of mutation present, but perhaps more likely by the genetic background of the individual, which may act to modify the expression of the phenotype in a tissue specific manner. The role of PAX3 in myogenesis has taken on an additional twist given that chromosomal translocations interrupting the *PAX3* gene and an uncharacterized locus on chromosome 13 have been identified in three cases of alveolar rhabdomyosarcoma, a solid tumour of striated muscle (Barr *et al.*, 1993).

As previously stated, one of the purposes in identifying the *Sp* gene was to determine whether mutations in its human homologue would result in a comparable phenotype. Having established that WSI is the human homologue of the mouse *Sp* locus and that both WSI and *Sp* heterozygotes display similar disturbances in NCC derived structures, it remains to be determined whether homozygous WSI individuals are afflicted with defects in neural tube closure as are their mouse counterparts. Given the low frequency of WSI in the general population (1/42000), its low mutation rate (1/270000) (Waardenburg 1951) and the likelihood of its early embryonic lethality, it is not surprising that homozygous cases of WSI have not been reported in the literature. Nevertheless, we have encountered a severely malformed abortus with anencephaly conceived from a brother-sister mating in which both parents are affected with WSI (unpublished observations). The couple had previously conceived two other children also affected with WSI. Screening for *PAX3* mutations in members of this family, including the abortus, is presently being conducted in order to determine whether this case of anencephaly is a fortuitous finding, or is pathogenetically related to a homozygous *PAX3* mutation.

It is particularly interesting that at least six individuals from separate families heterozygous for WSI have been reported with spina bifida (Pantke and Cohen 1971; de Saxe *et al.*, 1984; Carezani-Gavin *et al.*, 1992; Begleiter and Harris 1992; Chatkupt *et al.*, 1993). The frequency of NTDs in individuals with WSI has yet to be compared with that of the general population so it remains unknown whether these reported cases are simply representative of fortuitous findings (due to ascertainment bias). However,

since 9% of *Sp* heterozygotes exhibit NTDs, in addition to the fact that certain environmental agents cause NTDs more often in *Sp* heterozygotes than wildtype controls (Moase and Trasler 1992), it is compelling to speculate that at least some of the cases of NTDs seen in WSI individuals are related to their mutant genotypes.

The importance of *Pax-3* in mammalian development has clearly been demonstrated through the study of its phenotypic effects when in mutant form as displayed by the *Sp* mouse and individuals with WSI, II, and III. What remains to be understood however, is the actual biochemical function that *Pax-3* has in the process of neurogenesis and limb muscle development. Several lines of evidence have suggested that members of the *Pax* gene family serve to regulate the transcriptional activity of target genes during the development of various embryonic structures. First, all Pax proteins possess the DNA binding paired domain, while certain others (Pax-3, 4, 6, and 7) contain a second DNA binding element, the paired-type homeodomain (reviewed in Gruss and Walther 1992). Second, Pax-2, in addition to two Drosophila orthologues of the *Pax* gene family, Pox meso and Pox neuro, have been localized to the nucleus (Dressler and Douglass 1992; Bopp *et al.*, 1989). Third, Pax-1 and Pax-3 proteins have been shown to bind the e5 sequence of the Drosophila *even-skipped* promoter *in vitro* (Chalepakis *et al.*, 1991; Goulding *et al.*, 1991) while Pax-5 and Pax-8 have each demonstrated the ability to activate transcription from biologically relevant target promoters (Kozmik *et al.*, 1992; Zannini *et al.*, 1992).

Presently, no downstream targets of *Pax-3* have been identified. Close examination of expression profiles of genes either disrupted in *Sp* embryos or overlapping wildtype Pax-3 expression during normal development may suggest candidate genes for regulation by Pax-3 during neurogenesis. Before predicting candidate genes which may be modulated by Pax-3 a brief review of its own expression pattern is warranted.

Pax-3 expression initiates at day 8.5 p.c. and is restricted to dorsal aspects of the neural tube including the roof plate (Goulding *et al.*, 1991). Within this domain, *Pax-3* is expressed specifically in the mitotically active cells of the ventricular zone (Figure 2). The sulcus limitans demarcates the ventral boundary of *Pax-3* expression and coincides with the [illegible]neation between the alar and basal plates. This dorsal restriction in *Pax-3* expression appears to be regulated by signals secreted from the notochord

and floor plate which are also responsible for regulating *Pax-6* (Goulding et al., 1993). *Pax-3* expression extends almost continuously from the prosencephalon to the anterior margin of the posterior neuropore (Goulding *et al.*, 1991). Temporal variations in *Pax-3* expression exist between rostral and caudal portions of the neural tube with expression in the caudal neural tube occurring later than rostral expression; thus coinciding with the rostro/caudal pattern in which the neural tube develops. *Pax-3* expression is also observed in dermomyotome cells of the somites and also follows the rostro/caudal gradient of development. By day 14 p.c., *Pax-3* expression has subsided in all but the caudal portion of the neural tube. In addition to the neural tube, *Pax-3* expression was also found in a variety of NCC derived structures but it remains unclear whether it is expressed in the NCCs themselves (Goulding *et al.*, 1991). Finally, *Pax-3* was also detected in the undifferentiated mesenchyme of both the forelimb and hindlimb.

The functional significance of the *Pax-3* expression profile has yet to be elucidated. It is particularly interesting however, that like members of the Drosophila *prd* gene set, *Pax-3* is expressed, in part, within a segmented structure, the dermomyotome cells of the somites (Goulding *et al.*, 1991). In fact, several members of the murine *Pax* gene family are expressed in segmented structures. *Pax-1* is expressed in the sclerotome and *Pax-7* in the myotome of the somites which gives rise to the intervertebral disks and skeletal muscles of the trunk, respectively (Deutsch *et al.*, 1988; Jostes *et al.*, 1991). *Pax-2* and *Pax-8* are expressed in the segmentally arranged mesonephric tubules (Dressler *et al.*, 1990; Plachov *et al.*, 1990). It should not be considered a mere coincidence then, that a group of highly conserved structurally and functionally related proteins should have similar roles in establishing pattern formation within segmentally arranged structures in both Drosophila and mice.

The members of the Drosophila *prd* gene set have a dual role. In addition to being expressed in the segmented embryo, they are also expressed during neurogenesis where they serve to regulate neuronal identity of differentiating neuroblasts (Bopp *et al.*, 1989; Nottebohm *et al.*, 1992; Dambly-Chaudière *et al.*, 1992). The expression of *Pax-3* within the neural tube suggests that it too may have a role in the patterning of the nervous system. In fact, many members of the *Pax* gene family are expressed in defined regions along the length of the antero/posterior axis of the

developing neural tube, suggesting that these genes serve to compartmentalize the spinal cord along its longitudinal axis (Gruss and Walther 1992). The significance of regionalizing the spinal cord is understood when examining the development of the various neuronal structures. At the time of neural tube closure and up until approximately day 11 p.c., the neural tube is comprised of a single cell layer, the ventricular zone (Altman and Bayer 1984). The ventricular zone consists of mitotically active cells which act as the source of stem cell populations for the entire central nervous system. Commencing on day 11 p.c., ventricular zone cells in the ventral portion of the neural tube stop dividing and migrate radially to form two new zones, the intermediate and marginal zones (Altman and Bayer 1984). The progression of this neural differentiation occurs ventral to dorsal and by day 14 p.c. the ventricular zone cells have stopped mitosis (coinciding with the down regulation of *Pax-3* and *Pax-6* expression in this tissue (Goulding *et al.*, 1991; Walther and Gruss 1991)) and form the ependyma which lines the central lumen (Altman and Bayer 1984). The intermediate and marginal zones have expanded considerably during neural development and go on to form the grey and white matter of the central nervous system, respectively. At this point the neural tube can be divided into five epithelial plates, they are, from dorsal to ventral, the roof, alar, intermediate, basal, and floor plates (Figure 2)(Altman and Bayer 1984). The roof and floor plates give rise to neuroglial rather than neuronal cell types, while the alar, intermediate and basal plates give rise to sensory, relay and motor neurons, respectively (Altman and Bayer 1984). The expression of *Pax-3* in the alar and roof plates; *Pax-7* in the alar plate (overlapping *Pax-3* expression); *Pax-6* in the basal plate; and *Pax-2*, *5*, and *8* in subsets of the alar and basal plates suggests that the *Pax* gene family may serve to pattern the neural tube in a dorsal/ventral fashion in order to specify neuronal cell types (Figure 2)(Gruss and Walther 1992). So far, however, a strict correlation of *Pax* gene expression and differentiation of specific neuronal cell types has yet to be established. Thus, like members of the Drosophila *prd* gene set, the *Pax* gene family appears to serve a dual purpose in that they establish or maintain antero/posterior polarity within segmented structures, as well as participate in the dorso/ventral patterning of the neural tube for the possible purpose of specifying neuronal cell types.

Figure 2

Diagrammatic representation of *Pax* gene expression in a transverse section of a day 11 embryonic mouse neural tube. Shaded areas are limited to the ventricular zone with the exception of *Pax-2, 5* and 8 expression which extends into the intermediate zone. RP, roof plate; FP, floor plate; AP, alar plate; BP, basal plate; and SL, sulcus limitans (Modified from Gruss and Walther 1992).

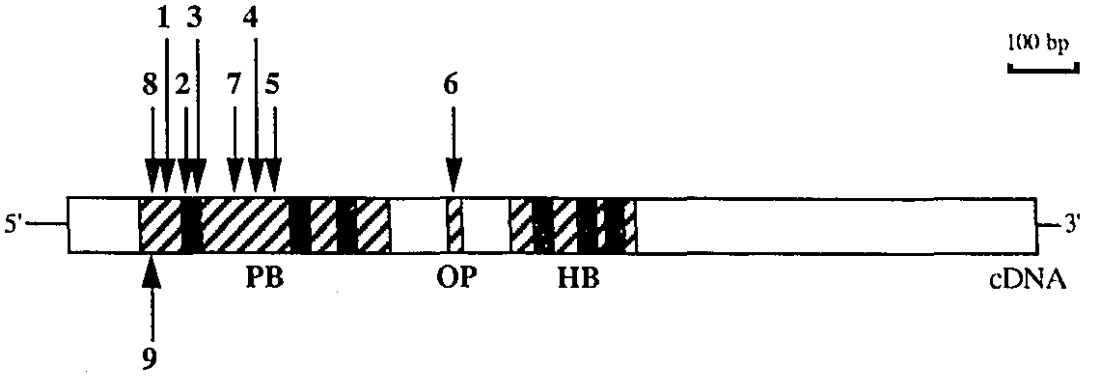

Mutation	Altered Codon	Effect on Protein
WSI		
1. C to T transition (BU-26)	codon 50	Pro to Leu substitution
2. G to T transversion (BU-35)	codon 56	Arg to Leu substitution
3. 18 bp deletion (WS.05)	codon 62-67	Six amino acid deletion
4. 14 bp deletion (Mich-1)	codon 89-93	Frameshift causing premature termination of translation downstream of Pro^{112}.
5. One bp deletion (WS.06)	codon 96	Frameshift causing premature termination of translation downstream of Val^{109}.
6. Two bp deletion (WS.11)	codon 186-187	Frameshift causing premature termination of translation presumably within the homeodomain.
WSII		
7. G to C transversion (WS.15)	codon 81	Gly to Ala substitution
WSIII		
8. A to C transversion (BU47)	codon 47	Asn to His substitution
Sp ^{d}		
9. G to C transversion	codon 42	Gly to Arg substitution

It is particularly interesting that expression of *Pax-2* in the developing kidney is restricted to undifferentiated renal structures and that its expression is repressed during the terminal differentiation of the renal tubule epithelium (Dressler and Douglass 1992). The failure of *Pax-2* to be down-regulated in Wilms tumour and the detection of severe kidney abnormalities in transgenic mice continuously expressing *Pax-2* suggests that *Pax-2* shut-off is required for the proper terminal differentiation of kidney epithelial structures (Dressler and Douglass 1992; Dressler *et al.*, 1993). A similar role may be envisioned for *Pax-3* during neural development. Down-regulation of *Pax-3* may be required for the differentiation of particular neuronal structures which form in the dorsal portion of the neural tube. The creation of transgenic mice persistently expressing *Pax-3* should help to address this hypothesis.

The candidacy of target genes for regulation by *Pax-3* can be evaluated on the basis of their overlapping temporal and spatial expression domains, as well as by the disruption of their normal expression in homozygous *Sp* embryos. Although many developmentally regulated genes including homeobox genes, oncogenes, growth factors and their receptors, extracellular matrix proteins and their receptors and others, may share some overlap with *Pax-3* expression, only a few of these show developmental regulation of a type that suggests a role in the formation of the neural tube.

The expression patterns, as determined by *in situ* hybridization, were assessed for several members of the *wnt* gene family of putative cell signalling molecules in wildtype and homozygous *Sp* mouse embryos at day 9.5 of gestation (A. McMahon, personal communication). Targeted disruption of the *Wnt-1* gene in the mouse has shown that its primary role is in regulating central nervous system development (McMahon and Bradley 1990; Thomas and Capecchi 1990). *Wnt-1* and *wnt-3a* are each expressed in overlapping temporal and spatial domains with *Pax-3*; primarily in the roof plate of the neural tube (reviewed in Nusse and Varmus 1992). Neither of these genes were found to be abnormally expressed in the homozygous *Sp* embryos suggesting that their expression is not directly regulated by *Pax-3* at this time. Recently however, a control element responsible for *wingless* (*wg*-the Drosophila orthologue of *wnt-1*)-dependent maintenance of *gsb-BSH9* (a Drosophila orthologue of *Pax* genes) expression was identified (Li

et al., 1993). Although it is unlikely that *Pax-3* is misexpressed in embryos homozygous for the *wnt-1* null allele given that the spinal cord appears to be unaffected in these animals (McMahon and Bradley 1990; Thomas and Capecchi 1990), it will be worthwhile to investigate whether other *Pax* genes are under the influence of the *Wnt-1* signalling pathway. Interestingly, *Pax-5* shows a sharp rostral boundary that overlaps both *Wnt-1* and *engrailed-1* genes at the midbrain/hindbrain boundary (Asano and Gruss 1992). Furthermore, the injection of antibodies against what may be the Pax-5 equivalent in zebrafish, Zf pax[b], leads to malformations at the midbrain/hindbrain boundary (similar to those seen in the targeted disruption of *Wnt-1* in the mouse) and alterations of *wnt-1* and *engrailed-2* expression in this area (Krauss *et al.*, 1992). Taken together, these findings suggest that *Pax-5* may be regulating or regulated by *wnt-1* and/or *engrailed* loci.

Another gene which has been implicated in neural development, shows some overlap in its expression with *Pax-3* in a temporal and spatial fashion and appears to be abnormally expressed in the *Sp* mouse is the neural cell-adhesion-molecule, *N-CAM* (see Section 2.3. of the Literature review). *N-CAM* expression in the neuroepithelium shows regional specificity along the cranio/caudal and dorsal/ventral axes, being expressed throughout the spinal cord between day 8 and 8.75 p.c. and eventually becoming restricted to lateral and ventral aspects at day 11.5-12.5 p.c. in primarily caudal portions of the neural tube, coinciding with the peak of *Pax-3* expression (Bally-Cuif *et al.*, 1993; Goulding *et al.*, 1991). Although highly speculative at this point, it is conceivable that Pax-3 serves to repress *N-CAM* expression in the dorsal aspects of the neuroepithelium and regions of the brain. The functional relevance of this restriction may possibly be for the emigration of NCCs from the dorsal portion of the neuroepithelium. A tightly bound neuroepithelium would not be conducive for NCC emigration and could possibly be responsible for the delay in neural tube closure in *Sp* animals by preventing the neural folds from coming together due to the increase in intercellular adhesion (Thiery *et al.*, 1985). Initial experiments to test whether this hypothesized interaction is direct could be performed by determining whether *Pax-3* can bind to the *N-CAM* promoter and inhibit its transcription in cotransfection assays. These types of experiments were previously performed with two members of the Xenopus *Hox 2* cluster and

showed that *Hox 2.5* can activate and *Hox 2.4* inhibit the activation of a reporter gene driven by the *N*-CAM promoter (Jones *et al.*, 1992).

Though any number of genes may be tested to see if they are misexpressed in *Sp* mice, these studies are limited in that they can only be performed with known genes. Our laboratory is presently taking a less biased approach in our search for genes acting downstream of *Pax-3*. Utilizing techniques such as differential cDNA screening and PCR based differential display (Liang and Pardee 1992), we hope to identify transcripts which are differentially expressed in wildtype versus *Sp* mutant embryos. These approaches should help to identify downstream targets of *Pax-3* with the eventual aim of dissecting the cascade of events required in the formation of the mammalian neural tube.

References

Akam, M. (1987). The molecular basis for metameric pattern in the Drosophila embryo. Development *101*, 1-22.

Altman, J., and Bayer, S. (1984). The development of the rat spinal cord. Adv. Anat. Embryol. Cell Biol. *85*, 1-164.

Asano, M., and Gruss, P. (1992). *Pax-5* is expressed at the midbrain-hindbrain boundary during mouse development. Mech. Dev. *39*, 29-39.

Asher, J. H. Jr., and Friedman, T. B. (1990). Mouse and hamster mutants as models for Waardenburg syndromes in humans. J. Med. Genet. *27*, 618-626.

Asher, J. H. Jr., Morell, R., and Friedman, T. B. (1991). Waardenburg syndrome (WS): The analysis of a single family with a WSI mutation showing linkage to RFLP markers on human chromosome 2q. Am. J. Hum. Genet. *48*, 43-52.

Auerbach, R. (1954). Analysis of the developmental effects of a lethal mutation in the house mouse. J. Exp. Zool. *127*, 305-329.

Albertini, D.F., Fawcett, D.W., and Olds, P.J. (1975). Morphological variations in gap junctions of ovarian granulosa cells. Tiss. and Cell. *7*, 389-405.

Baird, P.A. (1983). Neural tube defects in the Sikhs. Am. J. Med. Genet. *16*, 49-56.

Baldwin, C.T., Hoth, C.F., Amos, J.A., da-Silva, E.O., and Milunsky, A. (1992). An exonic mutation in the HuP2 paired domain gene causes Waardenburg's syndrome. Nature *355*, 637-638.

Ballabio, A. (1993). The rise and fall of positional cloning? Nature Genet. *3*, 277-279.

Balling, R., Deutsch, U., and Gruss, P. (1988). *undulated*, a mutation affecting the development of the mouse skeleton, has a point mutation in the paired box of *Pax 1*. Cell 55, 531-555.

Bally-Cuif, L., Goridis, C., and Santoni, M-J. (1993). The mouse NCAM gene displays a biphasic expression pattern during neural tube development. Development *117*, 543-552.

Baraitser, M., and Burn, J. (1984). Brief clinical report: Neural tube defects as an X-linked condition. Am. J. Med. Genet. *17*, 383-385.

Barr, F.G., Galili, N., Holick, J., Biegel, J.A., Rovera, G., and Emanuel, B.S. (1993). Rearrangement of the PAX3 paired box gene in the paediatric solid tumour alveolar rhabdomyosarcoma. Nature Genet. *3*, 113-117.

Baumgartner, S., Bopp, D., Burri, M., and Noll, M. (1987). Structure of two genes at the *gooseberry* locus related to the *paired gene* and their spatial expression during *Drosophila* embryogenesis. Genes Dev. *1*, 1247-1267.

Baumgartner, S., and Noll, M. (1991). Network of interactions among pair-rule genes regulating *paired* expression during primordial segmentation of *Drosophila*. Mech. Dev. 33, 1-18.

Beechey, C. V., and Searle, A. G. (1986). Mutations at the *Sp* locus. Mouse News Letter 75, 28.

Begleiter, M.L., and Harris, D.J. (1992). Waardenburg syndrome and meningocele. Am. J. Med. Genet. *44*, 541.

Bender, W., Akam, M., Karch, F., Beachy, P.A., Peofer, M., Spierer, P., Lewis, E.B., Hogness, D.S. (1983). Molecular genetics of the Bithorax complex in *Drosophila melanogaster*. Science *221*, 23-29.

Bergsma, D. (1979). "Birth defects compendium" second edition. Alan R. Liss, Inc. Ney York.

Bittles, A.H., Mason, W.M., Greene, J., and Rao, N.A. (1991). Reproductive behavior and health in consanguineous marriages. Science *252*, 789-794.

Bopp, D., Burri, M., Baumgartner, S., Frigerio, G., and Noll, M. (1986). Conservation of a large protein domain in the segmentation gene *paired* and in functionally related genes of Drosophila. Cell *47*, 1033-1040.

Bopp, D., Jamet, E., Baumgartner, S., Burri, M., and Noll, M. (1989). Isolation of two tissue-specific *Drosophila* paired box genes, *Pox meso* and *Pox neuro*. EMBO J. *8*, 3447-3457.

Botstein, D., White, R.L., Skolnick, M., and Davis, R.W. (1980). Construction of a genetic linkage map in man using restriction fragment length polymorphisms. Am. J. Hum. Genet. *32*, 314-331.

Brook, F.A., Shum, A.S.W., Van Stratten, H.W.M., and Copp, A.J. (1991). Development *113*, 671-678.

Brock, D.J.H. (1983). Ultrasound in detection of neural tube defects. Lancet *2*, 1251-1252.

Bultman, S.J., Michaud, E.J., and Woychik, R.P. (1992). Molecular characterization of the mouse *agouti* locus. Cell *71*, 1195-1203.

Burri, M., Tromvoukis, Y., Bopp, D., Frigerio, G., and Noll, M. (1989). Conservation of the paired domain in metazoans and its structure in three isolated human genes. EMBO J. *8*, 1183-1190.

Bush, K.T., Lynch, F.J., DeNittis, A.S., Steinberg, A.B., Lee, H-Y., and Nagele, R. (1990). Neural tube formation in the mouse: a morphometric and computerized three-dimensional reconstruction study of the relationship between apical constriction of neuroepithelial cells and the shape of the neuroepithelium. Anat. Embryol. *181*, 49-58.

Byrne, J. and Warburton, D. (1986). Neural tube defects in spontaneous abortions. Am. J. Med. Genet. *25*, 327-333.

Campbell, L.R., Dayton, D.H., and Sohal, G.S. (1986). Neural tube defects: a review of human and animal studies on the etiology of neural tube defects. Teratology *34*, 171-187.

Carezani-Gavin, M., Clarren, S.K., and Steege, T. (1992). Waardenburg syndrome associated with meningomelocele. Am. J. Med. Genet. *42*, 135.

Carter, C.O., David, P.A., and Laurence, K.M. (1968). A family study of major central nervous system malformations in South Wales. J. Med. Genet. *5*, 81-105.

Carter, C.O., and Evans, K. (1973). Spina bifida and anencephalus in Greater London. J. Med. Genet. *10*, 209-234.

Carter, C.O. (1974). Clues to the aetiology of neural tube malformations. Develop. Med. Child. Neurol. *16 [Suppl. 32]*, 3-15.

Carter, C.O. (1976). Genetics of common single malformations. Br. Med. Bull. *32*, 21-26.

Cattanach, B.M., Burtenshaw, M.D., Rasberry, C., and Evans, E.P. (1993). Large deletions and other gross forms of chromosome imbalance compatible with viability and fertility in the mouse. Nature Genet. *3*, 56-61.

Chalepakis, G., Fritsch, R., Fickenscher, H., Deutsch, U., Goulding, M., and Gruss, P. (1991). The molecular basis of the *undulated/Pax-1* mutation. Cell 66, 873-884.

Chatkupt, S., Chatkupt, S., and Johnson, W.G. (1993). Waardenburg syndrome and myelomeningocele in a family. J. Med. Genet. *30*, 83-84.

Chung, C.S., and Myrianthopoulos, N.C. (1968). Racial and prenatal factors in major congenital malformations. Am. J. Hum. Genet. *20*, 44-59.

Collins, F.S. (1992). Positional cloning: Let's not call it reverse anymore. Nature Genet. *1*, 3-6.

Copp, A.J. (1985). Relationship between timing of posterior neuropore closure and development of spinal neural tube defects in mutant (curly tail) and normal mouse embryos in culture. J. Embryol. exp. Morph. 88, 39-54.

Copp, A.J., Brook, F.A., and Roberts, H.J. (1988). A cell-type-specific abnormality of cell proliferation in mutant (curly tail) mouse embryos developing spinal neural tube defects. Development *104*, 285-295.

Copp, A. J., Brook, F. A., Estibeiro, J. P., Shum, A. S. W., and Cockfort, D. L. (1990). The embryonic development of mammalian neural tube defects. Progress in Neurobiology *35*, 363-403.

Dambly-Chaudière, C., Jamet, E., Burri, M., Bopp, D., Basler, K., Hafen, E., Dumont, N., Spielmann, P., Ghysen, A., and Noll, M. (1992). The paired box gene *pox neuro*: A determinant of poly-innervated sense organs in Drosophila. Cell 69, 159-172.

de Saxe, M., Kromberg, J.G.R., and Jenkins, T. (1984). Waardenburg syndrome in South Africa. Part I. An evaluation of the clinical findings in 11 families. S. Afr. Med. J. 66, 256-261.

Demenais, F., Le Merrer, M., Briard, M.L., and Elston, R.C. (1982). Neural tube defects in France: Segregation analysis. Am. J. Med. Genet. *11*, 287-298.

Dempsey, E.E., and Trasler, D.G. (1983). Early morphological abnormalities in splotch mouse embryos and predisposition to gene-and retinoic acid-induced neural tube defects. Teratology 28, 461-472.

Deol, M.S. (1966). Influence of the neural tube on the differentiation of the inner ear in the mammalian embryo. Nature *209*, 219-220.

Deutsch, U., Dressler, G.R., and Gruss, P. (1988). Pax-1, a member of a paired box homologous murine gene family is expressed in segmenting structures during development. Cell 53, 617-625.

DiNardo, S., and O'Farrell, P.H. (1987). Establishment and refinement of segmental pattern in the *Drosophila* embryo: spatial control of *engrailed* expression by pair-rule genes. Genes Dev. *1*, 1212-1225.

Dickie, M. M. (1964). New splotch alleles in the mouse. J. Hered. 55, 97-101.

Dressler, G. R., Deutsch, U., Chowdhury, K., Nornes, H. O., and Gruss, P. (1990). *Pax2*, a new murine paired-box-containing gene and its expression in the developing excretory system. Development *109*, 787-795.

Dressler, G.R., and Douglass, E.C. (1992). Pax-2 is a DNA-binding protein expressed in embryonic kidney and Wilms tumor. Proc. Natl. Acad. Sci. 89, 1179-1183.

Dressler, G.R., Wilkinson, J.E., Rothenpieler, U.W., Patterson, L.T., Williams-Simons, L., and Westphal, H. (1993). Deregulation of Pax-2 expression in transgenic mice generates severe kidney abnormalities. Nature 362, 65-67.

Edelman, G. M. (1986). Cell adhesion molecules in the regulation of animal form and tissue pattern. Ann. Rev. Cell Biol. 2, 81-116.

Edmonds L. D., and James, L. M. (1990). Temporal trends in the prevalence of congenital malformations at birth based on the Birth Defects Monitoring Program, United States, 1979-1987. MMWR *39(SS-4)*, 19-23.

Elwood, J.M., and Elwood, J.H. (1980). Epidemiology of anencephalus and spina bifida. Oxford, Oxford University Press.

Embury, S., Seller, M.J., Adinolfi, M, and Polani, P.E. (1979). Neural tube defects in curly-tail mice. I. Incidence, expression and similarity to human condition. Proc. R. Soc. Lond. B. 206, 85-94.

Epstein, D.J., and Vekemans, M. (1990). Genetic control of the survival of murine trisomy 16 fetuses. Teratology *42*, 571-580.

Epstein, D.J., Malo, D., Vekemans, M., and Gros, P. (1991a). Molecular characterization of a deletion encompassing the splotch mutation on mouse chromosome 1. Genomics *10*, 89-93.

Epstein, D. J., Vekemans, M., and Gros, P. (1991b). *Splotch* (Sp^{2H}), a mutation affecting development of the mouse neural tube, shows a deletion within the paired homeodomain of *Pax-3*. Cell 67, 767-774.

Epstein, D.J., Vogan, K.J., Trasler, D.G., and Gros, P. (1993a). A mutation within intron 3 of the *Pax-3* gene produces aberrantly spliced mRNA transcripts in the splotch (*Sp*) mouse mutant. Proc. Natl. Acad. Sci. USA *90*, 532-536.

Epstein, D.J., Bardeesy, N., Vidal, S., Malo, D., Weith, A., Vekemans, M., and Gros, P. (1993b). Characterization of a region-specific library of microclones in the vicinity of the *Bcg* and *splotch* loci on mouse chromosome 1. Genomics (Submitted)

Espey, L.L., and Stutts, R.H. (1972). Exchange of cytoplasm between cells of the membrane granulosa in rabbit ovarian follicles. Biol. Reprod. 6, 168-175.

Essien, F.B., Haviland, M.B., and Naidoff, A.E. (1990). Expression of a new mutation (*Axd*) causing axial defects in mice correlates with maternal phenotype and age. Teratology *42*, 183-194.

Evans, E.P., Burtenshaw, M., Beechey, C.V., and Searle, A. (1988). A *splotch* locus deletion visible by Giemsa banding. Mouse News Lett. *81*, 66.

Farag, T.I., Teebi, A.S., and Al-Awadi, S. (1986). Brief Clinical Report: Nonsyndromal anencephaly: Possible autosomal recessive variant. Am. J. Med. Genet. *24*, 461-464.

Farrer, L.A., Grundfast, K.M., Amos, J., *et al.* (1992). Waardenburg Syndrome (WS) Type I is caused by defects at multiple loci, one of which is near ALPP on chromosome 2: First report of the WS consortium. Am. J. Hum. Genet. *50*, 902-913.

Fellous, M., Boué, J., Malbrunot, C., Wollman, E., Sasportes, M., Van Cong, N., Marcelli, A., Rebourcet, R., and Hubert, Ch. (1982). A five-generation family with sacral agenesis and spina bifida: Possible similarities with the mouse T-locus. Am. J. Med. Genet. *12*, 465-487.

Fineman, R.M., Jorde, L.B., Martin, R.A., Hasstedt, S.J., Wing, S.D., and Walker, M.L. (1982). Am. J. Med. Genet. *12*, 457-464.

Foy, C., Newton, V., Wellesely, D., Harris, R., and Read, A. (1990). Assignment of the locus for Waardenburg syndrome type I to human chromosome 2q37 and possible homology to the splotch mouse. Am. J. Hum. Genet. 46, 1017-1023.

Franz, T. (1989). Persistent truncus arteriosus in the splotch mutant mouse. Anat. Embryol. *180*, 457-464.

Franz, T. (1990). Defective ensheathment of motoric nerves in the splotch mutant mouse. Acta Anat. *138*, 246-253.

Franz, T. (1992). Neural tube defects without neural crest defects in Splotch mice. Teratology 46, 599-604.

Franz, T.. Kothary, R., Surani, M.A.H., Halata, Z., and Grim, M. (1993). The splotch mutation interferes with muscle development in the limbs. Anat. Embryol. In press.

Fraser, F.C. (1976). The multifactorial/threshold concept-uses and misuses. Teratology *14*, 267-280.

Frigerio, G., Burri, M., Bopp, D., Baumgartner, S. and Noll, M. (1986). Structure of the segmentation gene *paired* and the Drosophila PRD gene set as part of a gene network. Cell *47*, 735-746.

Furmann, W., Seeger, W., Bohm, R. (1971). Apparently monogenic inheritance of anencephaly and spina bifida in a kindred. Humangenetik *13*, 241-243.

Geelan, J.A.G., and Langman, J. (1979). Ultrastructural observations on closure of the neural tube in the mouse. Anat. Embryol. 156, 73-88.

Gehring, W.J. (1992). The homeobox in perspective. TIBS *17*, 277-280.

Goldbard, S.B., and Warner, C.M. (1982). Genes affecting the timing of early mouse embryo development. Biol. Reprod. *27*, 419-424.

Goulding, M.D., Chalepakis, G., Deutsch, U., Erselius, J., and Gruss, P. (1991). *Pax-3*, a novel murine DNA binding protein expressed during early neurogenesis. EMBO J. *10*, 1135-1147.

Goulding, M.D., Lumsden, A., and Gruss, P. (1993). Signals from the notochord and floor plate regulate the region-specific expression of two Pax genes in the developing spinal cord. Development *117*, 1001-1016.

Gruneberg, H. and Truslove, G.M. (1960). Genet. Res. *1*, 69-90.

Gruss, P., and Walther, C. (1992). Pax in Development. Cell 69, 719-722.

Gutjahr, T., Frei, E., and Noll, M. (1993). Complex regulation of early *paired* expression: initial acrivation by gap genes and pattern modulation by pair-rule genes. Development *117*, 609-623.

Hall, B.K. (1988). The neural crest. Oxford University Press, England.

Hall, J.G., Friedman, J.M., Kenna, B.A., Popkin, J., Jawanda, M., and Arnold, W. (1988). Clinical, genetic, and epidemiological factors in neural tube defects. Am. J. Hum. Genet. *43*, 827-837.

Heldin, C-H. (1992). Structural and functional studies on platelet-derived growth factor. Embo J. *11*, 4251-4259.

Hoey, T., and Levine, M. (1988). Divergent homeo box proteins recognize similar DNA sequences in *Drosophila*. Nature *332*, 858-861.

Hogan, B., Costantini, F., and Lacy, E. (1986). Manipulating the mouse embryo. A laboratory manual. Cold Spring Harbor Laboratory.

Holmes, L.B., Driscoll, S.G., and Atkins, L. (1976). Etiologic heterogeneity of neural tube defects. N. Engl. J. Med. *294*, 365-369.

Hoth, C.F., Milunsky, A., Lipsky, N., Sheffer, R., Clarren, S.K., and Baldwin, C.T. (1993). Mutations in the paired domain of the human PAX3 gene cause Klein-Waardenburg Syndrome (WS-III) as well as Waardenburg Syndrom Type I (WS-I). Am. J. Med. Genet. *52*, 455-462.

Hsu, C.Y., Van Dyke, J.H. (1948). An analysis of growth rates in neural epithelium of normal and spina bifidous (myeloschisis) mouse embryos. Anat. Rec. *100*, 745.

Hui, C-C., and Joyner, A. (1992). A mouse model of Greig cephalopolysyndactyly syndrome: The *extra-toes*^{J} mutation contains an intragenic deletion of the *Gli3* gene. Nature Genet. *3*, 241-246.

Ingham, P.W. (1988). The molecular genetics of embryonic pattern formation in Drosophila. Nature *335*, 25-34.

Ingham, P.W., and Martinez Arias, A. (1992). Boundaries and fields in early embryos. Cell 68, 221-235.

Ishikiriyama, S., Tonoki, H., Shibuya, Y., Chin, C., Harado, N., Abe, K., and Niikawa, N. (1989). Waardenburg syndrome type I in a child with de novo inversion (2)(q35q37.3). Am. J. Med. Genet. *33*, 505-507.

Jacobson, A.G., and Gordon, R. (1976). Changes in the shape of the developing vertebrate nervous system analyzed experimentally, mathematically and by computer simulation. J. exp. Zool. *197*, 191-246.

James, W.H. (1988). Anomalous X chromosome inactivation: the link between female zygotes, monozygotic twinning, and neural tube defects? J. Med. Genet. *25*, 213-216.

Jensson, O., Arnason, A., Gunnarsdottir, H., Petursdottir, I., Fossdal, R., and Hreidarsson, S. (1988). A family showing apparent X-linked inheritance of both anencephaly and spina bifida. J. Med. Genet. *25*, 227-229.

Johnson, D.R. (1967). *Extra-toes*: a new mutant gene causing multiple abnormalities in the mouse. J. Embryol. exp. Morph. *17*, 543-581.

Jones, F.S., Prediger, E., Bittner, D.A., De Robertis, E.M., and Edelman, G.M. (1992). Cell adhesion molecules as targets for *Hox* genes: Neural cell adhesion molecule promoter activity is modulated by cotransfection with *Hox-2.5* and *-2.4*. Proc. Natl. Acad. Sci. USA *89*, 2086-2090.

Jostes, B., Walther, C., and Gruss, P. (1991). The murine paired box gene, *Pax7*, is expressed specifically during the development of the nervous and muscular system. Mech. Dev. *33*, 27-38.

Juriloff, D.M., MacDonald, K.B., and Harris, M.J. (1989). Genetic analysis of the cause of exencephaly in the SELH/Bc mouse stock. Teratology *40*, 395-405.

Kapron-Bras, C., and Trasler, D.G. (1988). Histological comparison of the effects of the splotch gene and retinoic acid on the closure of the mouse neural tube. Teratology *37*, 389-399.

Kaufman, M.H. (1979). Cephalic neurulation and optic vesicle formation in the early mouse embryo. Am. J. Anat. *155*, 425-444.

Kaufman, T.C., Seeger, M.A., and Olsen, G. (1990). Molecular and genetic organization of the Antennapedia gene complex of *Drosophila melanogaster*. Adv. Genet. *27*, 309-362.

Kessel, M., and Gruss, P. (1990). Murine developmental control genes. Science *249*, 374-379.

Kilchherr, F., Baumgartner, S., Bopp, D., Frei, E., and Noll, M. (1986). Isolation of the *paired* gene of *Drosophila* and its spatial expression during early embryogenesis. Nature *321*, 493-499.

Kirby, M.L., Gale, T.F., Stewart, D.E. (1983). Neural crest cells contribute to normal aorticopulmonary septation. Nature *220*, 1059-1061.

Kissinger, C. R., Liu, B., Martin-Blanco, E., Kornberg, T., and Pabo, C. O. (1990) Crystal structure of an engrailed homeodomain-DNA complex at 2.8 Å resolution: A framework for understanding homeodomain-DNA interactions. Cell 63, 579-590.

Knox, P., and Wells, P. (1979). Cell adhesions and proteoglycans. 1. The effects of exogenous proteoglycans on the attachment of chick embryo fibroblasts to tissue culture plastic and collagen. J. Cell. Sci. *40*, 77-88.

Kozmik, Z., Wang, S., Dörfler, P., Adams, B., and Busslinger, M. (1992). The promoter of the CD19 gene is a target for the B-cell-specific transcription factor BSAP. Mol. Cell. Biol. *12*, 2662-2672.

Krauss, S., Maden, M., Holder, N., and Wilson, S.W. (1992). Zebrafish pax[b] is involved in the formation of the midbrain-hindbrain boundary. Nature *360*, 87-89.

Lalouel, J.M., Morton, N.E., and Jackson, J. (1979). Neural tube malformations: complex segregation analysis and calculation of recurrence risks. J. Med. Genet. *16*, 8-13.

Laughon, A., and Scott, M.P. (1984). Sequence of *Drosophila* segmentation gene: protein structure homology with DNA binding proteins. Nature *310*, 25-31.

Leck, I. (1972). The etiology of human malformations: Insights from epidemiology. Teratology *5*, 303-314.

Leck, I. (1974). Causation of neural tube defects: Clues from epidemiology. Br. Med. Bull. *30*, 158-163.

Le Douarin, N. (1982). The neural crest. Cambridge University Press, Cambridge, U.K.

Lee, H.-Y., Sheffield, J.B., Nagele, R.G. Jr., and Kalmus, G.W. (1976). The role of extracellular material in chick neurulation. I. Effects of concanavalin A. J. Exp. Zool. *198*, 261-266.

Lemire, R.J. (1988). Neural tube defects. JAMA *259*, 558-562.

Lewis, E.B. (1978). A gene complex controlling segmentation in Drosophila. Nature *276*, 565-570.

Li, X., Gutjahr, T., and Noll, M. (1993). Separable regulatory elements mediate the establishment and maintenance of cell states by the *Drosophila* segment-polarity gene *gooseberry*. EMBO J. *12*, 1427-1436.

Liang, P., and Pardee, A.B. (1992). Differential display of eukaryotic messenger RNA by means of the polymerase chain reaction. Science *257*, 967-971.

Linnemann, D. and Bock, E. (1989). Cell adhesion molecules in neural development. Dev. Neurosci. *11*, 149-173.

Lyon, M.F., and Searle, A.G. (1989). Genetic variants and strains of the laboratory mouse. 2nd ed., Oxford Univ. Press. London/New York.

MacDonald, K.B., Juriloff, D.M., and Harris, M.J. (1989). Developmental study of neural tube closure in a mouse stock with a high incidence of exencephaly. Teratology 39, 195-213.

Mariman, E.C.M., and Hamel, B.C.J. (1992). Sex ratios of affected and transmitting members of multiple case families with neural tube defects. J. Med. Genet. 29, 695-698.

McGinnis, W., Levine, M., Hafen, E., Kuroiwa, A., and Gehring, W. (1984). A conserved DNA sequence in homeotic genes of the *Drosophila Antennapedia* and *bithorax* complexes. Nature 308, 428-433.

McGinnis, W., and Krumlauf, R. (1992). Homeobox genes and axial patterning. Cell 68, 283-302.

McKusick, V., A. (1990). Mendelian inheritance in man, ninth ed. Johns Hopkins University Press, Baltimore.

McMahon, A.P., and Bradley, A. (1990). The *Wnt-1* (*int-1*) proto-oncogene is required for development of a large region of the mouse brain. Cell 62, 1073-1085.

Michaud, J., Brody, L.C., Steel, G., Fontaine, G., Martin, L.S., Valle, D., and Mitchell, G. (1992). Strand-separating conformational polymorphism analysis: Efficacy of detection of point mutations in the human ornithine δ-aminotransferase gene. Genomics *13*, 389-394.

Milunsky, A., Jick, H., Jick, S.S, *et al.*, (1989). Multivitamin/folic acid supplementation in early pregnancy reduces the prevalence of neural tube defects. JAMA 262, 2847-2852.

Milunsky, A., Ulcickas, M., Rothman, K.J., Willett, W., Jick, S.S., and Jick, H. (1992). Maternal heat exposure and neural tube defects. JAMA *268*, 882-885.

Mills, J.L., Rhoads, G.G., Simpson, J.L., *et al.*, (1989). The absence of a relation between the periconceptional use of vitamins and neural-tube defects. N. Engl. J. Med. *321*, 430-435.

Moase, C. E., and Trasler, D. G. (1989). Spinal ganglia reduction in the splotch-delayed mouse neural tube defect mutant. Teratology *40*, 67-75.

Moase, C. E., and Trasler, D. G. (1990). Delayed neural crest cell emigration from *Sp* and Sp^d mouse neural tube explants. Teratology *42*, 171-182.

Moase, C. E., and Trasler, D. G. (1991). N-CAM alterations in splotch neural tube defect mouse embryos. Development *113*, 1049-1058.

Moase, C.E., and Trasler, D.G. (1992). Splotch locus mutants: models for neural tube defects and Waardenburg syndrome type I in humans. J. Med. Genet. *29*, 145-151.

Morell, R., Friedman, T.B., Moeljopawiro, S., Hartono, Soewito, and Asher, J.H. (1992). Hum. Molec. Genet. *1*, 243-247.

Morris, G.L., and O'Shea, K.S. (1983). Anomalies of neuroepithelial cell associations in the splotch mutant embryo. Dev. Brain Res. 9, 408-410.

Morrison-Graham, K., and Weston, J.A. (1989). Mouse mutants provide new insights into the role of extracellular matrix in cell migration and differentiation. Trends in Genetics 5, 116-121.

Morriss, G.M., and New, D.A.T. (1979). Effect of oxygen concentration on morphogenesis of cranial neural folds and neural crest in cultured rat embryos. J. Embryol. exp. Morphol. *54*, 17-35.

Morrissey, D., Askew, D., Raj, L., and Weir, M. (1991). Functional dissection of the *paired* segmentation gene in *Drosophila* embryos. Genes and Dev. 5, 1684-1696.

Morriss-Kay, G.M., and Crutch, G. (1982). Culture of rat embryos with β-D-xyloside: evidence of a role for proteoglycans in neurulation. J. Anat. *134*, 491-506.

Morriss-Kay, G.M., and Putz, B. (1986). Abnormal neural fold developmentin mouse trisomy 12 and trisomy 14. II. LM and TEM. Brain Res. Bull. *16*, 825-832.

Morriss-Kay, G.M., and Tuckett, F. (1985). The role of microfilaments in cranial neurulation in rat embryos: effects of short-term exposure to cytochalasin D. J. Embryol. exp. Morphol. 88, 333-348.

MRC Vitamin Research Group (1991). Lancet 338, 131-137.

Mulinare, J., Cordero, J.F., Erickson, J.D., and Berry, R.J. (1988). Periconceptual use of multivitamins and the occurrence of neural tube defects. JAMA 260, 3141-3145.

Muller, F., and O'Rahilly, R. (1987). The development of the human brain, the closure of the caudal neuropore, and the beginning of secondary neurulation at stage 12. Anat. Embryol. *176*, 413-430.

Murray, S.A., Larsen, W.J., O'Donnell, S. (1978). Gap junctional endocytosis and loss of cell cohesion in cultured human adenocarcinoma of adrenal cortex. Anat. Rec. *190*, 489.

Nance, W.E. (1969). Anencephaly and spina bifida: A possible example of cytoplasmic inheritance in man. Nature *224*, 373-375.

Newgreen, D., and Gibbons I. (1982). Factors controlling the time of onset of the migration of neural crest cells in the fowl embryo. Cell Tiss. Res. *224*, 145-160.

Nichols, D.H. (1981). Neural crest formation in the head of the mouse embryo as observed using a new histological technique. J. Embryol. exp. Morphol. 64, 105-120.

Nottebohm, E., Dambly-Chaudière, C. and Ghysen, A. (1992). Connectivity of chemosensory neurons is controlled by the gene *poxn* in *Drosophila*. Nature 359, 829-832.

Nusse, R., and Varmus, H.E. (1992). *Wnt* genes. Cell 69, 1073-1087.

Nüsslein-Volhard, C., and Wieschaus, E. (1980). Mutations affecting segment number and polarity in *Drosophila*. Nature 287, 795-801.

Office of Population Census and Surveys (1985). Mortality Statistics. Series DH3 no. 18. Her Majesty's Stationary Office: London.

Opitz, J.M., and Gilbert, E.F. (1982). Editorial comment: CNS anomalies and the midline as a "developmental field". Am. J. Med. Genet. *12*, 443-455.

O'Shea, K.S. (1987). Gene and teratogen induced defects of early central nervous system development. Scanning Electron Microscopy 3, 1195-1213.

O'Shea, K.S., and Liu, L.-H. (1987). Basal lamina and extracellular matrix alterations in the caudal neural tube of the delayed splotch embryo. Dev. Brain Res. 37, 11-26.

O'Shea, K.S., Rheinheimer, J.S.T., and O'Shea, J.M. (1987). Morphometric analysis of the forebrain anomalies in the delayed Splotch mutant embryo. J. Craniofac. genet. dev. Biol. 7, 357-369.

Otting, G., Qian, Y.Q., Billeter, M., Müller, M., Affolter, M., Gehring, W.J., and Wüthrich, K. (1990). Potein-DNA contacts in the structure of a homeodomain-DNA complex determined by nuclear magnetic resonance spectroscopy in solution. EMBO J. 9, 3085-3092.

Pantke, O., and Cohen, M. (1992). Waardenburg syndrome associated with meningomyelocele. Am. J. Med. Genet. *42*, 135-136.

Penrose, L.S. (1957). Genetics of anencephaly. J. Ment. Defic. Res. *1*, 4-15.

Perris, R., and Johansson, S. (1987). Amphibian neural crest cell migration on purified extracellular matrix components: a chondroitin sulphate proteoglycan inhibits locomotion on fibronectin substrates. J. Cell Biol. 2511-2521.

Phillips, M.T., Kirby, M.L., Forbes, G. (1987). Analysis of cranial neural crest distribution in the developing heart using quail-chick chimeras. Circ. Res. 60, 27-30.

Pietrzyk, J. (1980). Neural tube malformations: Complex segregation analysis and recurrence risk. Am. J. Med. Genet. *7*, 293-300.

Plachov, D., Chowdhury, K., Walther, C., Simon, D., Guenet, J-L., and Gruss, P. (1990). *Pax8*, a murine paired box gene expressed in the developing excretory system and thyroid gland. Development *110*, 643-651.

Polman, A. (1951). Anencephaly, spina bifida and hydrocephaly. Genetica *25*, 29-78.

Putz, B., and Morris-Kay, G.M. (1981). Abnormal neural fold development in trisomy 12 and trisomy 14 mouse embryos. I. Scanning electron microscopy. J. Embryol. exp. Morphol. 66, 141-158.

Reith, A.D., and Bernstein, A. (1991). Molecular basis of mouse developmental mutants. Genes and Dev. 5, 1115-1123.

Roberts, C.J., and Lloyd, S. (1973). Area differences in spontaneous abortion rates in South Wales and their relation to neural tube defects incidence. Br. Med. J. *1*, 20-22.

Ruppert, J.M. Kinzler, K.W., Wong, A.J., Bigner, S.H., Kao, F.-T., Law, M.L., Seuanez, H.N., O'Brien, S.J., and Vogelstein, B. (1988). The *GLI*-Kruppel family of human genes. Mol. Cell. Biol. 8, 3104-3113.

Ruppert, J.M., Vogelstein, B., Arheden, K., and Kinzler, K.W. (1990). *GLI3* encodes a 190-kilodalton protein with multiple regions of GLi similarity. Mol Cell. Biol. *10*, 5408-5415.

Rutishauser, U., Acheson, A., Hall, A.K., Mann, D.M., and Sunshine, J. (1988). The neural cell adhesion molecule as a regulator of cell-cell interactions. Science *240*, 53-57.

Rutishauser, U., and Jessel, T.M. (1988). Cell adhesion molecules in vertebrate neural development. Physiol. Rev. 68, 819-857.

Sadler, T.W. (1978). Distribution of surface coat material on fusing neural folds of mouse embryos during neurulation. Anat. Rec. *191*, 345-350.

Sadler, T.W., Greenberg, D., Coughlin, P., and Lessard, J.L. (1982). Actin distribution patterns in the mouse neural tube during neurulation. Science *215*, 172-174.

Sakai, Y. (1989). Neurulation in the mouse: manner and timing of neural tube closure. Anat. Rec. 223, 194-203.

Schimmang, T., Lemaistre, M., Vortkamp, A., and Rüther, U. (1992). Expression of the zinc finger gene *Gli3* is affected in the morphogenetic mouse mutant *extra-toes* (Xt). Development *116*, 799-804.

Schoenwolf, G.C., and Nichols, D.H. (1984). Histological and ultrastructural studies on the origin of caudal neural crest cells in mouse embryos. J. comp. Neurol. *222*, 496-505.

Schoenwolf, G.C., and Smith, J.L. (1990). Mechanisms of neurulation: traditional viewpoint and recent advances. Development *109*, 243-270.

Schurr, E., Skamene, E., Morgan, K., Chu, M.-L., and Gros, P. (1990). Mapping of Col3a1 and Col6a3 to proximal murine chromosome 1 identifies conserved linkage of structural protein genes between murine chromosome 1 and human chromosome 2q. Genomics 8, 477-486.

Scott, M., and Weiner, A. (1984). Structural relationships among genes that control development: sequence homology between the *Antennapedia*, *Ultrabithorax* and *fushi tarazu* loci of *Drosophila*. Proc. Nat. Acad. Sci. USA *81*, 4115-4119.

Scott, M., and O'Farrell, P.H. (1986). Spatial programming of gene expression in early *Drosophila* embryogenesis. Ann. Rev. Cell Biol. *2*, 49-80.

Scott, M.P., Tamkun, J.W., and Hartzell, G.W., III (1989). The structure and function of the homeodomain. Biochim. Biophys. Acta 989, 25-48.

Searle, A.G. (1959). The incidence of anencephaly in a polytypic population. Ann. Hum. Genet. *23*, 279-288.

Seller, M.J. (1987a). Unanswered questions on neural tube defects. Br. Med. J. *294*, 1-2.

Seller, M.J. (1987b). Neural tube defects and sex ratios. Am. J. Med. Genet. *26*, 699-707.

Seller, M.J., and Perkins-Cole, K.J. (1987). Sex difference in mouse embryonic development at neurulation. J. Reprod. Fert. *79*, 159-161.

Shaffer, L.G., Marazita, M.L., Bodurtha, J., Newlin, A., and Nance, W.E. (1990). Evidence for a major gene in familial anencephaly. Am. J. Med. Genet. 36, 97-101.

Smith, L.J. and Stein, K.F. (1962). Axial elongation in the mouse and its retardation in homozygous loop-tail mice. J. Embryol. exp. Morphol. *10*, 73-87.

Smithells, R.W., Nevin, N.C., Seller, M.J. *et al.*, (1983). Further experience of vitamin supplementation for prevention of neural tube defect recurrences. Lancet *1*, 1027-1031.

Snell, G. D., Dickie, M. M., Smith, P., and Kelton, D. E. (1954). Linkage of loop-tail, leaden, splotch, and fuzzy in the mouse. Heredity 8, 271-273.

Solursh, M., and Morriss, G.M. (1977). Glycosaminoglycan synthesis in rat embryos during the formation of the primary mesenchyme and neural folds. Dev.Biol. *57*, 75-86.

St Johnston, D., and Nüsslein-Volhard, C. (1992). The origin of pattern and polarity in the Drosophila embryo. Cell 68, 201-219.

Steel, K.P., and Smith., R.J.H. (1992). Normal hearing in *Splotch* (*Sp/+*), the mouse homologue of Waardenburg syndrome type 1. Nature Genet. *2*, 75-79.

Stephenson, D.A., Mercola, M., Anderson, E., Wang, C., Stiles, C.D., Bowen-Pope, D.F., and Chapman, V.M. (1990). Platelet-derived growth factor receptor α subunit gene (*Pdgfra*) is deleted in the mouse patch (*Ph*) mutation. Proc. Natl. Acad. Sci. 88, 6-10.

Stevenson, A.C., Johnston, H.A., Stewart, M.I.P., and Golding, D.R. (1966). Congenital malformations: a report of a study of series of consecutive births in 24 centres. Bull. WHO *34 [Suppl.]*, 25-34.

Strong, L.C., and Hollander, W.F. (1949). Hereditary Looptail in the house mouse. J. Hered. *40*, 329-334.

Tassabehji, M., Read, A. P., Newton, V.E., Harris, R., Balling, R., Gruss, P., and Strachan, T. (1992). Waardenburg syndrome patients have mutations in the human homologue of the *Pax-3* paired box gene. Nature 355, 635-636.

Tassabehji, M., Read, A. P., Newton, V.E., Patton, M., Gruss, P., Harris, R., and Strachan, T. (1993). Mutations in the PAX3 gene causing Waardenburg syndrome type 1 and type 2. Nature Genet. *3*, 26-30.

Theiler, K., and Stevens, L.C. (1960). The development of rib fusions, a mutation in the house mouse. Am. J. Anat. *106*, 171-183.

Thiery, J.-P., Duband, J.-L., and Tucker, G.C. (1985). Cell migration in the vertebrate embryo: Role of cell adhesion and tissue environment in pattern formation. Ann. Rev. Cell Biol. *1*, 91-113.

Thomas, K.R., and Capecchi, M.R. (1990). Targeted disruption of the murine *int-1* proto-oncogene resulting in severe abnormalities in midbrain and cerebellar development. Nature *346*, 847-850.

Todd, J.A. (1992). La carte des microsatellites est arrivée! Hum. Molec. Genet. *1*, 663-666.

Toriello, H.V., Warren, S.T., Lindstrom, J.A. (1980). Brief communication: Possible X-linked anencephaly and spina bifida-report of a kindred. Am. J. Med. Genet. 6, 119-121.

Toriello, H.V. (1984). Report of a third kindred with X-linked anencephaly/spina bifida. (Letter) Am. J. Med. Genet. *19*, 411-412.

Toriello, H.V., and Higgins, J.V. (1985). Possible causal heterogeneity in spina bifida cystics. Am. J. Med. Genet. *21*, 13-20.

Treisman, J., Gönczy, P., Vashishtha, M., Harris, E., and Desplan, C. (1989). A single amino acid can determine the DNA binding specificity of homeodomain proteins. Cell 59, 553-562.

Treisman, J., Harris, E., and Desplan, C. (1991). The paired box encodes a second DNA-binding domain in the paired homeo domain protein. Genes and Dev. 5, 594-604.

Tsukamoto, K., Tohma, T., Ohta, T., Yamakawa, K., Fukushima, Nakamura, Y., and Niikawa, N. (1992). Cloning and characterization of the inversion breakpoint at chromosome 2q35 in a patient with Waardenburg syndrome type I. Hum. Molec. Genet. *1*, 315-317.

Tsunoda, Y., Tokunaga, T., Sugie, T. (1985). Altered sex ratio of live young after transfer of fast-and slow-developing mouse embryos. Gamete Res. *12*, 301-304.

Vidal, S.M., Malo, D., Vogan, K., Skamene, E., and Gros, P. (1993). Natural resistance to infection with intracellular parasites: Isolation of a candidate for *Bcg*. Cell *73*, 469-485.

Vekemans, M., and Trasler, T. (1987). Animal model: Genetic control of the survival of trisomic fetuses in mice: A preliminary report. Am. J. Med. Genet. *26*, 763-771.

Verma, I.C. (1978). High frequency of neural tube defects in north India. Lancet *1*, 879-880.

Vogan, K., Epstein, D.J., Trasler, D.G., and Gros, P. (1993). The *splotch-delayed* (Sp^d) mouse mutant carries a point mutation within the paired box of the *Pax-3* gene. Genomics (In press)

Vortkamp, A., Gessler, M., and Grzeschik, K.H. (1991). GLI3 zinc-finger gene interrupted by translocations in Greig syndrome families. Nature 352, 539-540.

Waardenburg, P.J. (1951). A new syndrome combining developmental anomalies of the eyelids, eyebrows, and nose root with pigmentary defects of the iris and head hair and with congenital deafness. Am. J. Hum. Genet. 3, 195-253.

Wald, N.J., and Cuckle, H.S. (1977). Maternal serum alpha-fetoprotein measurement in antenatal screening for anencephaly and spina bifida in

early pregnancy: Report of U.K. collaborative study on alpha-fetoprotein in relation to neural-tube defects. Lancet *1*, 1323-1332.

Walther, C., Guenet, J.-L., Simon, D., Deutsch, U., Jostes, B., Goulding, M.D., Plachov, D., Balling, R., and Gruss, P. (1991). Pax: A murine multigene family of paired box-containing genes. Genomics *11*, 424-434.

Walther, C., and Gruss, P. (1991). Pax-6, a murine paired box gene is expressed in the developing CNS. Development *113*, 1435-1449.

Waterman, R.E. (1976). Topographical changes along the neural fold associated with neurulation in the hamster and mouse. Am. J. Anat. *146*, 151-171.

Wilson, D.B. (1974). Proliferation in the neural tube of the splotch (Sp) mutant mouse. J. comp. Neurol. *154*, 249-256.

Wilson, D.B., and Finta, L.A. (1979). Gap junctional vesicles in the neural tube of the splotch (*Sp*) mutant mouse. Teratology *19*, 337-340.

Wilson, D.B., and Wyatt, D.P. (1986). Pathogenesis of neural dysraphism in the mouse mutant Vacuolated Lens (*vl*). J. Neuropathol. Exp. Neurol. *45*, 43-55.

Wilson, D.B., and Wyatt, D.P. (1988a). Closure of the posterior neuropore in the *vl* mutant mouse. Anat. Embryol. *178*, 559-563.

Wilson, D.B., and Wyatt, D.P. (1988b). Cytochemical analysis of neural dysraphism in the *vl* mutant mouse. J. Neuropathol. Exp. Neurol. *47*, 609-617.

Wilson, D.B., and Wyatt, D.P. (1992). Abnormal elevation of the neural folds in the Loop-Tail mutant mouse. Acta Anat. *143*, 89-95.

Windham, G.C., and Sever, L.E. (1982). Neural tube defects among twin births. Am. J. Hum. Genet. *34*, 988-998.

Winter, R.M. (1988). Malformation syndromes: a review of mouse/human homology. J. Med. Genet. *25*, 480-487.

Winter, R.M. and Huson, S.M. (1988). Greig cephalopolysyndactyly syndrome: A possible mouse homologue (Xt-Extra toes). Am J. Med. Gen. *31*, 793-798.

Yen, S. and MacMahon, B. (1968). Genetics of anencephaly and spina bifida. Lancet *2*, 623-626.

Yang, X-M., and Trasler, D.G. (1991). Abnormalities of neural tube formation in pre-spina bifida splotch-delayed mouse embryos. Teratology *43*, 643-657.

Zannini, M., Francis-Lang, H., Plachov, D., and Di Lauro, R. (1992). Pax-8, a paired domain-containing protein, binds to a sequence overlapping the recognition site of a homeodomain and activates transcription from two thyroid-specific promoters. Mol. Cell. Biol. *12*, 4230-4241.

Claims to originality

This thesis contains the following original results.

1. The determination that *splotch* and *Pax-3* are allelic.

2. The identification of a deletion in the paired-type homeodomain of *Pax-3* in homozygous Sp^{2H} mouse embryos.

3. The identification of a mutation in the third intron of the *Pax-3* gene from *Sp* mice which abrogates its proper splicing.

4. The determination that *Pax-3* is entirely deleted in the Sp^{r} mouse mutant.

5. The delineation of the chromosomal segment deleted in the Sp^{r} mouse mutant.

6. The generation and mapping of a large number of anonymous probes spanning the proximal portion of mouse chromosome 1.